NONLINEAR SIGNAL PROCESSING OF ELECTROENCEPHALOGRAM :
APPLICATION IN THE STUDY OF NEURODYNAMICS

P. INDIC

THESIS SUBMITTED TO
THE COCHIN UNIVERSITY OF SCIENCE AND TECHNOLOGY
IN PARTIAL FULFILLMENT OF THE REQUIREMENTS FOR
THE AWARD OF THE DEGREE OF **DOCTOR OF PHILOSOPHY**
IN THE FACULTY OF TECHNOLOGY

INTERNATIONAL SCHOOL OF PHOTONICS
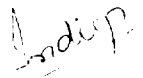COCHIN UNIVERSITY OF SCIENCE AND TECHNOLOGY
COCHIN - 682022, INDIA
November 2000

The shaping force of " *Nonlinear Signal Processing of*

Electroencephalogram : Application in the Study of Neurodynamics." is

Prof. R. Pratap whose farsightedness, advice, love and affection made

this work possible and I am most grateful to him. Prof. Pratap opened a

new epoch in theoretical neurophysics by blending profound physical

intuition with formidable mathematical formulation. This work is due to

the spectacular theoretical foundation and is dedicated to Prof. Pratap-

my *friend, philosopher and guide.*

P. Indic

DECLARATION

I hereby declare that the work presented in the thesis entitled *Nonlinear Signal Processing of Electroencephalogram : Application in the Study of Neurodynamics* is based on the original work done by me under the guidance of Dr.V P N Nampoori, Professor, International School of Photonics, Cochin University of Science and Technology, and has not been included in any other thesis submitted previously for the award of any degree.

P. Indic

Cochin 22

November 1, 2000

CERTIFICATE

Certified that the research work presented in the thesis entitled *Nonlinear Signal Processing of Electroencephalogram : Application in the Study of Neurodynamics* is the report of the original work carried out by Mr. P. Indic in the International School of Photonics, Cochin University of Science and Technology, Cochin 682022 under my guidance and supervision and has not been included in any other thesis submitted previously for the award of any degree.

Prof. V. P. N. Nampoori

Cochin 22

November 1, 2000

ACKNOWLEDGEMENT

I would like to thank Ms. Pravitha Ramanand who helped inordinately during the research.

Dr. R Sreenivasan and Dr M.P Joy of NIMHANS, helped with their tits and bits of research. Their support was of great assistance and I am thankful to them.

I would also like to thank Dr. Tessamma Thomas, Dept. of Electronics for being generous to me.

I thank all my colleagues at International School of Photonics and School of Engineering, particularly Mr. Roy V Paul, Mr. Nibu A George, Ms Bindu V and Mr. B. Aneeshkumar for making my research joyful.

And thanks to Ms. R Mridhu, my comrade, who filled my days with much contentment and humor.

P.Indic

PREFACE

Interfacings of various subjects generate new field of study and research that help in advancing human knowledge. One of the latest of such fields is Neurotechnology, which is an effective amalgamation of neuroscience, physics, biomedical engineering and computational methods. Neurotechnology provides a platform to interact physicist; neurologist and engineers to break methodology and terminology related barriers. Advancements in Computational capability, wider scope of applications in nonlinear dynamics and chaos in complex systems enhanced study of neurodynamics. However there is a need for an effective dialogue among physicists, neurologists and engineers.

Application of computer based technology in the field of medicine through signal and image processing, creation of clinical databases for helping clinicians etc are widely acknowledged. Such synergic effects between widely separated disciplines may help in enhancing the effectiveness of existing diagnostic methods. One of the recent methods in this direction is analysis of electroencephalogram with the help of methods in nonlinear dynamics. This thesis is an effort to understand the functional aspects of human brain by studying electroencephalogram. The algorithms and other related methods developed in the present work can be interfaced with a digital EEG machine to unfold the information hidden in the signal. Ultimately this can be used as a diagnostic tool.

In the human anatomy, while most parts of human body are fairly understood, both functionally and constitutionally, it is increasingly getting realized that the human brain, which has a volume of approximately 10 cm^3, plays the most

significant role and is least understood. The earliest effort in understanding the human brain started with the working of the nervous system and the cells that exist in brain viz. neurons. Researchers later tried to chart the emotion centers in the human brain and gave a broad classification of these centers, thereby tried to establish that the emotion centers and the capacity to think and analyze problems are all localized in skull space. However this conclusion is questioned and there exists a school who supported the idea of collective effect in any thought process as well as higher functions of brain such as recognition, association, recollection etc. Probably *the truth lies somewhere in between and is still in an inconclusive state.*

It is known that the human brain consists of about 10^{10} neurons, of which about 4 to 5% are operative while the rest are in a dormant state. Even this itself is an enormously large number. Recent studies however have shown that new neurons are being created when the old ones get destroyed. When the death rate is larger than the birth rate, brain experiences a slow degeneration. Probably one can constantly activate these newly generated neurons and thereby bridge this gap and stem down the degeneration. Previous investigations were invasive in nature. However recent development in nonlinear mathematics and deterministic chaos has opened new vistas in many fields of science - brain in particular. The nonlinear dynamical studies of human brain using electroencephalograms and magnetoencephalograms considered as a time series started recently have opened the possibilities of better understanding of brain. However these efforts are yet to make roads in realm of clinical applications and this is the motivation of this work

RESEARCH PUBLICATONS

A. JOURNALS.

1. _P.Indic_, "Time scale dependance of human brain dynamics" _International J. Neuroscience_, vol. 99, pp. 195, 1999

2. _P.Indic_, R. Pratap, V P N Nampoori and N. Pradhan, " Significance of time scales in nonlinear dynamical analysis of Electroencephalogram signals" _International J. Neuroscience_, vol. 99, pp181, 1999

3. V.P.N. Nampoori, _P.Indic_, N. Pradhan, R. Pratap, R. Sreenivasan. "Cortical dynamics and phase synchronisation during meditation"- special issue on _Nonlinear Phenomenon - Indian National Science Academy_, pp.395, 2000.

B. CONFERENCE PROCEEDINGS

1. _P. Indic_, V P N Nampoori, R. Pratap and N. Pradhan," Dynamics of brain during meditation as revealed from EEG analysis," _Proc. of First National conference on Scientific and philosophical basis of Consciousness, organised by National Institute of Advanced studies, held on Feb 8-13, 1999,Bangalore, pp 137,1999_

C. SEMINAR / CONFERENCE / SCIENCE CONGRESS.

1. *P. Indic*, " Cortical dynamics and coordination during meditation", *International Conference on Complex Systems, Nashua, USA, May 21-26, 2000.*

2. *P. Indic*, V P N Nampoori, R. Pratap and N. Pradhan," Dynamics of brain during meditation as revealed from EEG analysis," *First National conference on Scientific and philosophical basis of Consciousness, organised by National Institute of Advanced studies, Feb 8-13, 1999, Bangalore.*

CONTENTS

The study of dynamics is essentially a study of motion or the evaluation of the system as a function of time. This helps one to predict the future of the system when the state of the system is known at present. The present study is an effort towards this direction where the dynamical system is human brain and the state evolution is specified by the changes in the process going on in the brain. In the parlance of modern brain research, the evolution is the changes in cognitive process in human brain. The most significant aspect is brain as a dynamical system is nonlinear, complex in which all processes are collective and is thermodynamically open. In brain the feedback-feedforward features play a significant and at times the most dominant role. This results in the system being in a nonequilibrium and non Marcoffian state and hence the present known techniques of dynamics as applied to the study of brain become inadequate. In this work therefore some new concepts have been developed and these are indicated in the chapters as follows.

In classical point of view linearity is always assumed in a system. The time evolution of a system is studied by considering the system as linear and the solution obtained has to satisfy the condition of superposition. Thus superposability of solutions, Fourier-Laplace or Orthogonal functional expansion of solution of dynamical system are all usual techniques one uses in the study of dynamics. However most of these become either inadequate or irrelevant when one considers nonlinear system far removed from equilibrium. Poincare was probably the first to

realize this difficulty and therefore attempted to device new analytical and computational techniques to represent the state of a nonlinear dynamical system.

Human brain as has already been mentioned, is a nonlinear, complex and "living" system. Recent observations (Gould et al, 1999) indicated that the number of neurons, which constitute the elementary units of an active brain, is ever being generated in millions or billions in adult primates. This is quite against the belief till now that the brain development is completed during the first five years. Again a further observation is that neurons generated at basal ganglia do migrate both laterally and upwards in the brain. Though this is a slow process, the observations are significant from dynamical point of view, in that, the total number of neurons are not conserved at any space-time point and that if one tries to activate these constantly one can control the degeneration of brain.

Neurons form the elementary constituents of human brain. The individual neurons are studied by observing the signal propagation characteristics. Hodgkin and Huxley (1952) were the pioneers who carried out a systematic study of signal propagation in neuron. In this however, they considered the problem as one of signal propagation in a coaxial cable. However the signal transduction along a nerve has very different features as compared to the passage of electric current in a cable. In a coaxial cable there are transmission losses whereas there is no signal attenuation in a nerve. Furthermore when a signal is given at a point in a neuron, it excites the neighboring ones, which in turn would again excite more neurons, thereby generate a cascade process without any attenuation in its strength. For this energy is derived

from the physico-chemical process. This signal would generate a "pattern" in the brain, and is retained and recalled in the higher function of brain such as recollection, association etc. Also there are excitator and inhibitor neurons and their dynamics depend on thresholds in activation. Hence in developing a general theory of the cognitive process in the brain one has to take all the above factors and more significantly the nonequilibrium dynamical nature of the system.

Statistical mechanics is a branch of dynamics which, enables one to understand the macroscopic dynamics having known the microscopic dynamics of a large number of constituents. This is exactly the procedure developed by Brusell School. In other words how does one obtain a fluid description given by Navier-Stoke's equation staring from the Hamiltonian representation of atoms and molecules. In the usual statistical mechanics one starts from Boltzmann equation and averaging them over the ensemble one obtains equations such as Eulers or Navier-Stokes. There still exists a gap between the Hamiltonian representation and Boltzmann description. This is brought out very clearly in the Brusell description of Nonequilibrium statistical mechanics. The first step in this scheme is to break up dynamics in terms of time scale and Hamiltonian description of a dynamical system contains all time scales. If one develops the dynamics in terms of interaction time scales, one gets a self-consistent field approximation or a mean field theory. The averaging of any dynamical quantity using the distribution function obtained from the above equation results in an Euler description. On the other hand a description based on a relaxation time scale, would give rise to a Boltzmann description or Focker-Planck equation. Averaging a physical variable with this distribution function

would result in Navier-Stokes equation or an evolutionary equation with macroscopic time scales. All these are very adequately described in the classic treatise by Balescu (1975).

This thesis has been arranged in the following manner. The chapters 2-8 deal with the theoretical basis for the analysis of Electroencephalogram data. Data has been collected from persons under various conditions such as eyes closed, eyes open, epilepsy and those from 'Vipassana' meditation state. The results are presented from each sample of the above categories. It should however be stressed that one cannot get identical results from a group of identical subjects in any category, since each member of the group do have different psychological history which affects the brain function. Hence even a group of five or ten subjects who are clinically normal will show different behaviour since their psychological make up is distinctly different from one another.

In this work the various aspects that go into the dynamics have been developed *ab-initio*. The salient features of nonlinearity that are relevant to the present problem have been discussed in chapter 2. In particular the linear stability and the inadequacy when one considers nonlinear system and some of the current research in limit cycles, bifurcation of solutions and the aspects of chaos and how one should deal when there exists noise especially when the interactions are nonlinear in nature. It should be stressed here that this chapter is only a bird's eye view. Chapter 3 gives an account of the present methods adopted in the study of time series. In most of the time series analysis one adopts a linear analysis and it has been

shown how this approach becomes inadequate in a nonlinear time series. The discussions are based on signal processing point of view both linear and nonlinear. A detailed account is given of the various algorithms developed in the study of nonlinear time series. The case of nonstationary of the time series, which is very peculiar to real world data series and which do not appear in data generated from nonlinear equations or set of equations are also discussed. The invariant parameters such as dimensions, entropy etc. are discussed in this chapter. In the light of these, in chapter 4 the Electroencephalogram (EEG) has been considered as a time series. Different waves such as alpha, beta, theta and delta are the macroscopic characteristics as one can infer from the signal. A Fourier decomposition would also give this information. However whether these waves are real intrinsic waves or whether these are the end product of a nonlinear process resulting in a synergic effect is to be understood. Besides these there is a very significant component in the form of chaos.

Chapter 5 gives an account of the various existing neural models such as those of Anderson- Cooper, Parikh- Pratap, neural network models and the current work that is going on in generating a model based on Nonequilibrium statistical mechanics. Chapter 6 gives a discussion on the phenomenon of synchronisation. The various subsystems can exhibit phase and amplitude synchronisation and a new characterizing parameter namely coherence index is defined in this chapter. The Coherence index is the harmonic ratio between the phase and amplitude synchronization indices and this gives the degree of coherence. In a dynamical system, if the phase and amplitude are synchronized (i.e. each is equal to unity), then

the coherence index is unity. This index would be positive and has a value between 0 and 1. This forms another parameter to characterize an attractor along with parameters such as attractor basin, embedding dimension, generalized dimension, generalized entropy and Lyapunov exponent/function. Incidentally, a new characterizing parameter would give a more accurate specification of the attractor.

The chapter 7 gives a method of evaluating plausible time scales that could exist in a biological system and the significance of this is that there could exist a wide variety of time scales which are physically relevant for the various processes. These time scales can overlap. Hence it is significant to understand the genesis of nonlinearity in a dynamical system due to interaction of time scales. Very often in systems such as plasma, the time scales are widely separated and hence one can isolate dynamics corresponding to a particular time scale from the various other time scales. This obviously becomes impossible if the time scales are close by or even overlap. A power spectrum analysis cannot separate these time scales as is well known Fourier decomposition becomes impossible in a nonlinear system.

Chapter 8 gives an indication of the general formulation of Nonequilibrium statistical mechanics. This is a self contained chapter and for the sake of completeness an account of the various attempts previously carried out in formulating Nonequilibrium statistical mechanics in neural systems is also presented. A general framework of Nonequilibrium statistical mechanics adopted by Pratap (2000) is presented and in this formulation instead of taking the actual neurons as the constituting elements, an equivalent system of attractors which is a map onto a space

6

spanned by the invariant parameters is considered. To get a measure of potential a singular value decomposition (SVD) of the EEG data obtained from a particular channel is evaluated and the calculation gives a set of eigen values/eigen functions, which are functions of the invariant parameters. The eigen functions are a set of orthogonal functions and using these functions along with eigen values one can obtain an effective potential at the point from which the data was collected. An account of the verification of different methods employed in this work is presented in Chapter 9. These include Average mutual information criteria, Global false nearest neighbor, Fixed mass approach etc. A critical approach of the different methods of phase evaluation is also discussed. The algorithms developed have been tested on various standard nonlinear equations such as logistic equation, Henon map, Rossler equation, coupled Rossler equation and the standard sets such as, mixed sine waves and random numbers. An account of the EEG electrode location sites (International 10-20 system) and a description of EEG data used for analysis are also included in this chapter.

The results obtained are presented in chapter 10 and this chapter is probably the most crucial one. The results are described in three different sections. Part I gives the physical aspects of brain dynamics and in this section the significance of time scales in nonlinear dynamical analysis of EEG has been discussed. It has been shown that the nonstationary nature of EEG is due to the interaction of various time scales. An investigation is also carried out to understand the dynamics of brain during meditation. The degree of coordination of different brain regions during meditation is evaluated and the results are presented in Part II. This is measured by finding an

index based on Shannon entropy. Part III deals with the dynamical aspect of the neocortex. A method to evaluate phase and amplitude from Poincare map is also presented. A new index, Coherence index, is evaluated for eyes closed and meditation data. This section contains a summary of the effective potential as seen by a specified attractor at a given instant and at a particular location in the scalp. Results and discussion is included in Chapter 11 In general, the work focuses on deriving the wealth of information contained in the EEG to get a deeper understanding of the brain functioning.

Further, an effort has been made to develop an interface between the highly sophisticated mathematical analysis and the clinical operations to alleviate human sufferings.

Chapter 2

NONLINEAR OSCILLATIONS

The general mathematical theory of nonlinear oscillations has been discussed in this chapter. The limitation of stability analysis and the need for new methods of understanding the nonlinear system has been presented.

2.1 Stability Analysis

Consider a nonlinear autonomous two dimensional system

$$\dot{x}_1 = f_1(x_1, x_2)$$

$$\dot{x}_2 = f_2(x_1, x_2) \tag{2.1}$$

where, f_1 and f_2 are C^1 defined on R^2. The system defines a vector field $F=(f_1(x_1,x_2),f_2(x_1,x_2))$ from R^2 to R^2. Eq. (2.1) takes the form

$$\dot{X} = F(X) \tag{2.2}$$

where, $X=(x_1, x_2)$

The Jacobian of the system at a point X is the matrix

9

$$DF(X) = \begin{pmatrix} \dfrac{\partial f_1}{\partial x_1} & \dfrac{\partial f_1}{\partial x_2} \\ \dfrac{\partial f_2}{\partial x_1} & \dfrac{\partial f_2}{\partial x_2} \end{pmatrix} \tag{2.3}$$

In the case of linear homogeneous system where $F(X) = AX$, $DF(X)$ is just A, the Jacobian with constant elements. In the case of linear systems the equilibrium point for this system in a plane is the origin for nonzero A whereas nonlinear systems can have multiple equilibrium. This is one of the major differences between a linear and a nonlinear system. If $\overline{X}$ is an equilibrium solution of the nonlinear set of equations one can determine the linear stability about $\overline{X}$ by linearising the equation in the neighborhood of $\overline{x}$ and write the linearised equation as

$$\dot{X} = DF(\overline{X})X \tag{2.4}$$

where, X is the perturbation part and $DF(\overline{X})$ is the Jacobian evaluated at $\overline{X}$. It may be realized that the linearisation implies $|X| \ll |\overline{X}|$. The dynamical behaviour of the system in the neighborhood of $\overline{X}$ is determined by assuming a solution

$$X(t) = C_1 e^{\lambda_1 t}\psi_1 + C_2 e^{\lambda_2 t}\psi_2 \tag{2.5}$$

for the two dimensional system where C_1, C_2 are constants, λ_1, λ_2 are two eigen values and ψ_1, ψ_2 are the eigen functions of the matrix $DF(\overline{X})$. The stability is inferred if the two eigen values are

10

Real, negative	$\bar{x}$ is a stable node-a point attractor
Real, positive	$\bar{x}$ is an unstable node
Any one is real, positive	$\bar{x}$ is an unstable node

If λ_1, λ_2 are complex conjugates, then if the real parts are

Both negative	$\bar{x}$ is a stable node asymptotically. The trajectories spiral inwards and converge to a node.
Both positive	$\bar{x}$ is an unstable node asymptotically. The trajectories spiral outwards and diverge.
If $\lambda_1 < 0 < \lambda_2$	$\bar{x}$ is unstable asymptotically. One component spirals inside while the other diverges outwards.
Zero	The system goes over to a limit cycle.
Zero and $|\lambda_1| < |\lambda_2|$	It results in a limit cycle

In fact all these inferences are true only if the nonlinear system of equation can be linearised in the neighborhood of the equilibrium state. In other words the linear system of equation represents the nonlinear system of equation in the vicinity of the equilibrium points. It should however be realized that linearization of a nonlinear differential equation is valid only in the small neighborhood around the point over which the linearization has been effective both in space and time. Evolution of a nonlinear system beyond this neighborhood would introduce nonlinear effects giving erroneous results. The global stability of linear homogeneous system represents the local stability of nonlinear autonomous system. Thus by evaluating the eigen values one can infer the stability of the system. However this method of analysis is valid for those system of equations for which the Taylor series expansion is possible. A linear

or nonlinear system $\dot{x} = F(x)$ is called *hyperbolic* if and only if all eigen values of the Jacobian evaluated at the equilibrium point $\bar{x}$ have nonzero real parts. This conclusion is a result of Hartman-Grobman Theorem.

According to Hartman-Grobman theorem if $\overline{X}$ is a hyperbolic equilibrium of $\dot{X} = F(X)$, then there is a neighborhood of X in which F is topologically equivalent to the linear vector field $\dot{x} = DF(\overline{X})X$. where $X = \overline{X} + x$

The two dynamical systems are topologically equivalent if there is a homeomorphism h: U $\rightarrow$ V mapping the orbits of one system on to the other, preserving direction in time. This method of linearised stability analysis of nonlinear system is found useful in several applications. Essentially this gives a local stability criterion for hyperbolic equilibrium of nonlinear systems and by evaluating the eigen values of the Jacobian for each equilibrium and classifying them as equivalent to linear systems at the origin.

There are cases however when the linearisation fails. Consider the set of equations

$$\dot{x}_1 = x_2 + ax_1\left(x_1^2 + x_2^2\right)$$
$$\dot{x}_2 = -x_1 + ax_2\left(x_1^2 + x_2^2\right)$$

$$(2.6)$$

By inspection $X=(x_1, x_2)$ is an equilibrium solution say $\bar{x}$ and the Jacobian at this point results in

12

$$DF(\bar{x}) = \begin{pmatrix} 0 & 1 \\ -1 & 0 \end{pmatrix} \tag{2.7}$$

The characteristic polynomial is

$$\lambda^2 + 1 = 0 \tag{2.8}$$

and the eigen values of the Jacobian are $\pm i$. Since the eigen values have zero real parts they are nonhyperbolic and as per Linear stability analysis the equilibrium is a center as the eigen values are imaginary. However converting the system of equation into polar co-ordinates, the equation becomes

$$\begin{aligned} \dot{\theta} &= -1 \\ \dot{r} &= ar^3 \end{aligned} \tag{2.9}$$

with equilibrium $\bar{r} = 0$. Whereas $\bar{r}$ is globally asymptotically stable if a<0, neutrally stable if a =0 and unstable if a>0. Thus there exists different solutions depending on the value of a. This inference is not obtained in the previous case in which it has been concluded a neutral stability. Thus linearization is not reliable for nonhyperbolic case. However the Poincare theorem gives an indication for the stability of a nonhyperbolic system

According to Poincare a center equilibrium of the linearised system is either a center or a focus of the original nonlinear system.

In Eq. (2.9) θ increases in a counter clockwise manner. However $\dot{\theta} = -1$ implies that the trajectory is directed in a clockwise manner. In the equation $\dot{r} = ar^3$, if $a < 0$ then the trajectory winds in a clockwise manner to the equilibrium point $r=0$. If $a=0$ the trajectory are circles with the origin as the center, while for $a>0$, the trajectory spirals out starting from the origin. Thus for the case $a<0$, $\bar{r}$ is globally asymptotically stable and this is called a focus, while for the $a>0$, it is asymptotically unstable. For $a=0$ is the case of neutral stability and $\bar{x}$ is called the center. This is however not always possible.

Another method of finding the equilibrium is by applying Lyapunov's Direct Method. According to Lyapunov theorem, let $\bar{x}$ be a fixed point of $\dot{x} = f(x), x \in R^2$ and let V, the Lyapunov function be differentiable on some neighborhood W of $\bar{x}$ and satisfy:

(i) $V(\bar{x}) = 0$;

(ii) $V(x) > 0$ if $x \neq \bar{x}$;

(iii) $\dot{V}(x) \leq 0$ on $W - \{\bar{x}\}$;

Then $\bar{x}$ is stable. If $\dot{V} < 0$ as in (iii), then $\bar{x}$ is asymptotically stable and hence can be a focus. While for (1), it would correspond to neutral stability.

To justify the above mentioned statement, let V be taken as

$$V = x_1^2 + x_2^2 \qquad\qquad (2.10)$$

14

Then

$$\dot{V} = \frac{\partial V}{\partial x_1} \dot{x}_1 + \frac{\partial V}{\partial x_2} \dot{x}_2 \qquad (2.11)$$

Substituting for $\dot{x}_1$ and $\dot{x}_2$ from Eq.(2.6) and using Eq. (2.10) Eq. (2.11) takes the form

$$\dot{V} = 2ar^4 \qquad (2.12)$$

in polar co-ordinates. This clearly indicates that $\bar{r}$ is a globally asymptotic attractor for a<0, a center for a=0 and a repeller for a>0. The method of Lyapunov is very powerful. However defining a proper Lyapunov function is a difficult task and there does not exist a prescription to write this function. It is rather an art than a science. However the advantage of Lyapunov direct method is that one can determine the stability of equilibrium directly without solving the system of equations.

Another significance of Lyapunov direct method is that it establishes a general property of the systems. Let $U(x)$ be a real valued differentiable function on R^n and let the equation of motion be written as $\dot{x} = -\nabla U(x)$ where $U(x)$ can be interpreted as a potential and hence the system is conserved. It can be proved that a gradient system is asymptotically stable at $\bar{x}$ if $U(x)$ has an isolated local minimum there (Epstein, 1997).

Next consider a potential $V = U(x) - U(\bar{x})$ such that $V(\bar{x}) \equiv 0$. For all

points in the neighborhood W around $\bar{x}$, V>0. It can be proved that V is a Lyapunov

function and that $V(x)$ in W is greater than zero. It can also be proved that $\dot{V} < 0$ on

$W - \bar{x}$.

From the equations of motion

$$\frac{dV}{dt} = \frac{\partial U}{\partial x_i} \frac{dx_i}{dt} = \frac{\partial U}{\partial x_i} \left(-\frac{\partial U}{\partial x_i} \right)$$

$$= -\left(\frac{\partial U}{\partial x_i} \right)^2 = -\|\nabla U(x)\|^2 \tag{2.13}$$

on $W - \bar{x}$.

The Eq.(2.1) takes the form

$$\dot{X} = F = 1_2 \times \nabla H \tag{2.14}$$

in the phase space spanned by (x_1, x_2) and that 1_2 is a unit vector in the z direction in

which x_1, x_2 are the x, y co-ordinates respectively and H is the Hamiltonian.

This further shows that the motion is confined to equi Hamiltonian surfaces

in the phase space. Since the scalar product of the equations of motion with ∇H is

identically zero, this further shows that

$$\dot{H} = \nabla H . F = \nabla H . 1_2 \times \nabla H \equiv 0 \tag{2.15}$$

16

and this implies that H is a conserved quantity and H is a constant of motion. This further shows that a gradient field dissipative as against a conserved Hamiltonian field. Again

$$\nabla \bullet F = \nabla \bullet \left[1_2 \times \nabla H \right] = \nabla \bullet \left[\nabla \times 1_2 H \right] \equiv 0 \qquad (2.16)$$

since divergence of Curl is identically zero. Hence there are no sources or sinks in a conservative system.

Thus Hamiltonian flows are volume preserving. This is known as Liouville Theorem. Hamiltonian flows therefore cannot have sinks or sources, for the existence of sources or sinks would violate the constancy along trajectories.

If a system has a Hamiltonian representation and has equilibrium, where the eigen values are purely imaginary, the equilibrium is nonhyperbolic. Hence the linearisation fails. However it can be concluded from Poincare theorem that the center or focus is the equilibrium point. Since the system being Hamiltonian, the equilibrium point is the center or saddle. Thus inferring from above two conditions, the equilibrium point is a center. This indicates that *Nonlinear systems exhibit quite different behaviour.*

2.2 Limit Cycles

The behaviour of nonlinear system is quite different from the linearised form of the same nonlinear equation. From nonlinear dynamical point of view the principal endeavor in the study of nonlinear systems had been the existence of limit cycles. Poincare showed that a set of differential equation

$$\dot{x} = f(x, y)$$
$$\dot{y} = g(x, y) \tag{2.17}$$

occasionally admit a solution represented by a closed curve in the phase plane, which is called the limit cycles. A limit cycle is defined, as a closed trajectory such that no trajectory sufficiently near to it is also closed i.e. a limit cycle is an isolated trajectory. Every trajectory starting from nearby points will wind itself on to this curve as $t \rightarrow \infty$ or unwinds itself as $t \rightarrow -\infty$. If all nearby trajectories approach a limit cycle as $t \rightarrow \infty$ one can consider this as a stable limit cycle. If they approach the limit cycle as $t \rightarrow -\infty$, it is called unstable. However with the advent of theory of chaotic dynamics this perception has changed. Nevertheless the theory of limit cycle plays a crucial role in the study of the dynamics of nonlinear system. Consider the following system of equation

$$\dot{x}_1 = x_2 + x_1\left(\lambda - x_1^2 - x_2^2\right)$$
$$\dot{x}_2 = -x_1 + x_2\left(\lambda - x_1^2 - x_2^2\right) \tag{2.18}$$

In polar co ordinates this has the form

$$\dot{\theta} = -1$$
$$\dot{r} = r(\lambda - r^2)$$

<div align="right">(2.19)</div>

Here again the first part of Eq.(2.19) indicates that the trajectory moves in the clockwise direction.

For $\lambda \leq 0$, $\dot{r} < 0$, the solutions spiral to the origin as $t \to \infty$. For $\lambda > 0$, there are three cases:

1. $r^2 > \lambda$, $\dot{r} < 0$

2. $r^2 < \lambda$, $\dot{r} > 0$

3. $r^2 = \lambda$, $\dot{r} = 0$

This indicates that the trajectories beginning outside the circle, $r^2 = \lambda$, wind inward while the trajectories beginning inside the circle wind outward and that as $t \to \infty$ these entire trajectories spiral towards the circle $r^2 = \lambda$. It is an attractor which as $t \to \infty$ the orbits converge on to a circle of $r = \sqrt{\lambda}$. This is called a stable limit cycle. For the time reversed system the same object is an unstable limit cycle. The stable limit cycle is a basic model for all self-sustained oscillators, i.e.; those that return or recover to some fundamental periodic orbit when perturbed from it.

The main theoretical tool in search for limit cycles is the Poincare-Bendixson Theorem, whose contemporary statement requires the definition of ω limit and α

<div align="right">19</div>

limit points. The basic idea of ω and α limit points are: any point to which a trajectory converges in forward time is an ω limit point, and any point to which the time-reversed trajectory converges is an α limit point. A limit cycle is then defined as a periodic orbit that is ω or α limits set of other orbits.

The Poincare Bendixson theorem states that if

$$\Gamma = \left(x(t), y(t)\right)$$ be a trajectory of motion specified by

$$\dot{x} = f(x, y)$$
$$\dot{y} = g(x, y); f, g \in C^1$$

(2.20)

such that, for $t \geq t_0$, remains in a closed and bounded region of the plane containing no equilibrium points. Then Γ is a limit cycle or $\omega(t)$ is a periodic point.

The main difficulty in applying this theorem lies in establishing equilibrium free closed and bounded "trapping" regions. The other limitation is that the Poincare Bendixson theorem cannot be applied to autonomous systems of dimension greater than two. For higher dimension, the phenomenon of bifurcation leading to chaos sets in - an important concept in nonlinear dynamics.

2.3 Bifurcation

Consider the equation

$$\dot{x} = f(x, \mu), x \in R^n, \mu \in R^k$$

(2.21)

μ is a single real valued parameter. The values of μ at which the dynamics of the system changes qualitatively are called bifurcation points. This is often referred as change in the topological structures of the phase portrait (Epstein, 1997). The field $f(x, \mu)$ is structurally unstable if nearby fields $f(x, \mu + \varepsilon)$ have different topological structures. In other words phase portrait at μ is not topologically equivalent to the phase portrait at $\mu + \varepsilon$.

The field f is said to be structurally stable if and only if there is a neighborhood of f such that all fields in the neighborhood are topologically equivalent to f i.e. a mapping from one function to another in this neighborhood must be one to one, continuos and has an inverse. Such trajectory mapping is called homeomorphism and if this exists in the neighborhood, then these functions are called topologically equivalent. In short, there should not be any qualitative change in the dynamics of the system. The critical value μ^* for which the flow of $\dot{x} = f(x, \mu), x \in R^n, \mu \in R^k$ changes from structurally stable to structurally unstable is called a bifurcation value.

Hopf Bifurcation Theorem in R^2 states that suppose the parameterized system $\dot{x} = f(x, \mu), x \in R^n, \mu \in R^k$ has a fixed point at the origin for all values of the real parameter μ and if the eigen values $\lambda_1(\mu)$ and $\lambda_2(\mu)$ (λ_1 and λ_2 are complex conjugates since the dynamics is in R^2) of the Jacobian of f, at 0, are purely imaginary, then for $\mu = \mu^*$. the real parts of the eigen values, $Re\lambda_1(\mu)$ and $Re \lambda_2(\mu)$ are equal, since $\lambda_1 = \overline{\lambda_2}$, it now satisfies the condition

$$\frac{d}{d\mu}\left(\text{Re }\lambda_1(\mu)\right)\bigg|_{\mu = \mu^*} > 0$$

and hence the dynamics undergo noticeable changes.

Then

(a) $\mu = \mu^*$ is a bifurcation point of the system.

(b) For $\mu \in \left(\mu_1, \mu^*\right)$, for some $\mu_1 < \mu^*$, the origin is a stable focus

(c) For $\mu \in \left(\mu_2, \mu^*\right)$, for some $\mu_2 > \mu^*$, the origin is an unstable focus

surrounded by a stable limit cycle whose size increases with μ.

First the theorem deals with complex conjugate eigen values that are purely imaginary at the bifurcation point $\mu = \mu^*$ which is named in part (a). Then in μ the real part of the eigen value is zero, but its rate of change, the slope, is positive a little to the right, of μ^*. The equilibrium is hyperbolic and so by linearized stability analysis there are stable and unstable foci predicted in (b) and (c). The Hopf bifurcation theorem demonstrates the existence of a stable limit cycle. The orbits of the attractors can be represented as a fixed point of the discrete maps in a lower dimensional space. This method of representation is the contribution of Poincare, which is often called Poincare maps. Poincare map connects the world of continuous flow in some dimension to the world of discrete maps in a space one-dimension lower. The lower dimensional entity gives the information regarding the higher dimensional one. Some more important theorems are discussed below

Bendixsons' Negative test

Let f and g define a vector field $\Omega = (f, g)$ in a simply connected region $D \subset R^2$. If divΩ has fixed sign in a region D, then Ω have no cycles in D.

Bendixson- Dulac Theorem

Given the system

$$\dot{x} = f(x, y)$$
$$\dot{y} = g(x, y)$$

(2.22)

where f and g are smooth in a simply connected region D, let B(x, y) be a smooth function in D such that

$$\frac{\partial(Bf)}{\partial x} + \frac{\partial(Bg)}{\partial y}$$

(2.23)

has fixed sign in D. Then the Eq. (2.19) has no closed trajectories in D.

These are some of the general theorems that help to reduce the possibilities in one's search of trajectory characteristics. However all these theorems are useful if the equation of motion is known. If on the other hand one starts the search from the real world data set generated by an experiment, the above theorems are to be viewed as restrictions to be taken into account in writing the equations of motion as inferred from the data set generated by an experiment.

2.4 Stochastic Resonance

Stochastic resonance is a phenomenon in nonlinear noisy systems whereby weak signals get amplified using noise. The amplification of feeble information requires three basic requirements, a threshold, a periodic signal and a source of noise that is inherent in the system. The response of the system undergoes resonance like behaviour as a function of noise level and hence this phenomenon is called stochastic resonance. Stochastic resonance is quantified by measuring changes in the intensity of a peak in the power spectrum. These quantities are readily measurable and are very useful in the study of signal amplification due to stochastic resonance. In a system with inherent noise the amplitude of the periodic signal used for the extraction of weak signals can be manipulated by changing the noise levels. In stochastic resonance effect the amplitude of the periodic signal first increases with the increasing noise levels, reaches a maximum value and then decreases. Thus frequency of the driving period has a very important role in the extraction of information. At resonance condition in the power spectrum one can observe peaks at frequencies other than the driving periodic frequency. This spectral amplification is an indication of the presence of information in the system.

Another parameter that is used for characterization is the signal to noise ratio (SNR). Instead of looking for peaks in the power spectrum, the amount of signal present in the background noise is estimated. Thus in this case stochastic resonance *becomes a problem of extracting* the signal from the background noise. However in real systems it is difficult to observe stochastic phenomenon using power spectrum

or SNR methods. The more reliable method that has been used for natural processes is Resident time distribution. In this the output of the process is considered as a stochastic point process by setting two crossing levels. The time interval elapsed to switch from one crossing level to another is noted. This time represents the residence times between two subsequent switching events. The statistical properties of this distribution are found out using the probability theory. In the absence of periodic forcing function, the residence time distribution has an exponential form. In the presence of periodic forcing one can observe a series of peaks. However the existence of peaks in the residence time distribution need not necessarily indicate the presence of a fundamental frequency and its subharmonics. Before the phenomenon the occurrences are randomly spaced that do not correspond to any definite spectral component.

Deterministic chaos resembles the feature of noise on a coarse-grained time scale. Hence with a periodic forcing function it is possible to extract weak signals embedded in a chaotic signal in which the noisy perturbation are due to chaotic signal. Stochastic resonance is an information- transmitting phenomenon that exploits the noise in a self-optimizing manner. In human brain dynamics as the system has inherent noise this phenomenon may have wider implications in understanding the dynamics of brain.

METHODS IN NONLINEAR TIME SERIES ANALYSIS

The main aim of nonlinear time series analysis is to understand the dynamics of a system where all that is available is a single variable time series. Unlike in linear time series analysis, the data is represented in a state space rather than in time or frequency domain. The representation of data in state space is the hallmark of nonlinear time series analysis. The ultimate purpose of such analysis is to identify all dynamical variables and possibly derive the equation that is governing the system with predictive capability. In nonlinear method a time series is embedded in a state space by a trajectory and as time evolves this trajectory may be attracted to a subspace called an "attractor". The characterization of this attractor by different measures is the landmark of nonlinear dynamical analysis of a time series. The different methods of nonlinear time series analysis is discussed in this chapter. A brief overview of linear time series analysis and the limitations of linear methods are also presented.

3.1 Linear Time Series Analysis

The basic assumption in linear time series analysis is that the source emits spectrally sharp monochromatic signals, which might be contaminated by broad band interference. To identify the signal of interest from the unwanted background and study the characteristics of the data using statistical or spectral tools is the aim of linear time series analysis. The commonly employed methods are linear statistical inference, autocorrelations, Fourier analysis and power spectrum representation.

A linear system is one that permits superposiability and hence can be represented by a differential equation. These equations with constant coefficients can have only exponential or periodic solution. Any irregular output is considered as due to linear system driven by irregular input. In linear stochastic process, a measurement of the state at a specified instant can be regarded as derived from an underlying probability distribution for observing different values or sequences of values. For an unknown probability distribution, mean, variance and other related quantities form estimates of the signal characteristics. However, these estimates cannot give any information regarding the time evolution of a system. The time evolution of a system dynamics can be obtained from the autocorrelations of a signal s (t). The autocorrelations of a signal with lag T is given by

$$C_T = \frac{1}{\sigma^2} \left(\langle s(n)s(n-1) \rangle - \langle s \rangle^2 \right) \tag{3.1}$$

where σ^2 is the variance, s observed signal and the bracket $\langle\ \rangle$ denotes the average. If the signal is observed over continuous time, one can define autocorrelation function C (τ) where τ =T δ t, δt being sampling time and T the lag.

If the measurements are drawn from a Gaussian distribution or joint distribution of multiple measurements are also Gaussian, then this forms a random process and would be fully described statistically by mean, variance and autocorrelation function. If a signal is periodic in time, then its autocorrelation function is also periodic. A stochastic process has decaying autocorrelation and the

rate of decay depends on the nature of the process. Another method of representing the signal is in Fourier space. The Fourier transform establishes a correspondence between the time and frequency domain. The Fourier transform of a signal s (t) is defined as

$$\tilde{S}(f) = \frac{1}{\sqrt{2\pi}} \int_{-\infty}^{\infty} s(t) e^{i2\pi ft} dt \qquad (3.2)$$

The inverse Fourier transform is

$$S(t) = \int_{-\infty}^{\infty} \tilde{S}(f) e^{-2\pi ft} df \qquad (3.3)$$

Both the transforms are invertible. These linear transformations give information regarding all regular structures in a data set.

The power spectrum of a process is defined as the squared modulus of the continuous Fourier transforms. It is the square of the amplitude of the frequency contributes to the signal. According to Wiener-Khinchin theorem, the Fourier transform of the autocorrelation function is equal to the power spectrum. Power spectrum is useful in studying the oscillations in a system. Spectrum consists of sharper or broader peaks at the dominant frequencies and their integer multiples. Noise in a system adds a continuous floor in the spectrum. Thus, noise and signals are clearly distinguishable and that they are additive. To track the temporal changes, spectral analysis is performed on consecutive segments of a long time series.

In developing models in linear time series analysis, the observations at a particular instant of time say s (n) is related to observations at the earlier instant and the driving forces at the earlier instant. This becomes

$$s(n) = \sum_k a_k s(n - k) + b_k g(n - k) \qquad (3.4)$$

The coefficients a_k and b_k are determined by least square fit and g (n) is some deterministic or stochastic forcing function. From the dynamical point of view the above mentioned model consists of simple linear dynamics. The first part of the model is called Autoregressive and the second part Moving Average (Papoulis, 1984). The choice of coefficients should be consistent with any knowledge one has of spectral peaks in the system. Once the coefficients are established then the model is used for prediction.

3.2 Limitations of linear time series analysis

The irregular output from a system is considered as due to irregular forcing function in linear domain. However, it is now clear that there are nonlinear dynamical systems, with a certain underlying dynamical equations that can produce irregular output even with well-defined regular input. Such systems, which are sensitive to initial conditions, are called chaotic systems. The power spectrum in such cases is broad band and Autocorrelation function shows an exponential decaying behaviour with a lag like stochastic process. Thus from autocorrelation function it is not possible to distinguish chaotic system from a stochastic system.

The frequency / power spectrum represents the number of oscillations and its harmonics present in a system. In the spectrum, sharper or broader peaks are observed at the dominant frequencies and their harmonics. The noise adds a continuous floor. For a chaotic system, however there will be a broad continuous part in the spectrum even in the absence of noise. Thus, it is very difficult to distinguish noise from chaotic system.

In linear modeling, the dynamics is represented as a sum of simple linear dynamics. Hence linear models fail to represent the chaotic behaviour observed in nonlinear systems, as nonlinearity is an essential condition for chaos (Abarbanel et al., 1993). However to choose models from data alone is still a difficult task in linear as well as in nonlinear domain. In nonlinear modeling the main departure from linear model is to realize that the dynamics evolve in a multivariate space whose size and structure is dictated by the data itself.

3.3 Nonlinear Time Series Analysis

Classical physics focuses on linear systems where small measurement errors of the current state of the system result in small errors in the future state. In other words the error does not grow with time. Although several nonlinear equations are dealt in classical domain they however have closed form of solutions or are represented as linear approximations. In linear domain, given the dynamical equations and the initial conditions the future as well as past can be predicted. Those systems that are not predictable are being treated as stochastic. The stochastic

systems has a large number of variables governing the dynamics and such systems are studied using molar description in terms of average behaviors and / or probabilities as provided by statistical mechanics.

Apart from linear theory and stochastic theory, deterministic chaos theory offers a third alternative. According to chaos theory, nonlinear systems with a few variables can result in random like time series. If the parameters of such nonlinear systems are slightly changed, small difference in initial condition can produce an "exponential" divergence in the behaviour of the system. The chaotic systems are generally referred as systems sensitive to initial conditions. The exponential divergence results in loss of information of the initial state and loses the predictive capability. However, if the system is dissipative then its asymptotic behaviour will be attracted towards a finite region of the phase space. Study of attractors, form the basis of nonlinear dynamical theory of dissipative systems.

The nonlinear time series analysis is based on the theory of dynamical systems. In dynamical system theory, a time evolution of a state of a system is represented as a trajectory in state space. The dynamics of a system is then understood by studying the dynamics of the corresponding points in state space. Mathematically, a dynamical system is represented by either first order ordinary differential equations with order depending on degrees of freedom or of discrete time variable. The state equation is then written as

$$\frac{d}{dt} X(t) = f[t, X(t)] \qquad\qquad t \in \Re \qquad\qquad (3.5)$$

31

in the case of continuos evolution and

$$X(n + 1) = F[X(n)] \qquad n \in L \qquad (3.6)$$

in the discrete case. A sequence of points X (n) or x (t) solving the above equations is called a trajectory of the dynamical system. Depending upon the initial conditions and the functions that represent the system, the trajectory will diverge and move away to infinity or stay in a bounded domain as time proceeds. This " object" or collection of points so formed in the phase space is called an attractor. For chaotic system, the corresponding attractors are complicated geometrical objects. They are called strange attractors. The characterization of attractor using the parameters like dimension, entropy, Lyapunov exponents, spectrum of singularities, unstable periodic orbit etc leads to the knowledge of dynamics of the system. In nonlinear time series analysis, one tries to understand the geometry and dynamics of the system by studying one of the variables as time series. The time series is a scalar measurement of some physical quantity that depends on the current state of a system. The overall approach requires one to adopt a different frame of reference that moves away from previous methods of data analysis.

3.4 Methods in Nonlinear Time series Analysis

Different methods of nonlinear time series analysis is discussed in this section. A delay reconstruction method is usually employed in nonlinear analysis for

the investigation of the dynamics of a complex system from time series. In this method, the time series s (t) is reconstructed as

$$y(n) = [s(n), s(n+T), s(n+2T), \ldots\ldots\ldots\ldots, s(n+(m-1)T)] \qquad (3.7)$$

where T is the time lag and m the embedding dimension with y(n) as elements of the correlation matrix. This reconstruction does not represent the original state space; rather it is an equivalent representation since for data analysis, the original phase space is not required. From the correlation matrix, the number of variables requires to specify the dynamics as well as the time evolution of the dynamics is obtained. This mode of embedding a system dynamics as an attractor in phase space is the analytic feature of nonlinear time series. The important tasks however is to know the appropriate embedding dimension, to unfold the attractor completely. As per Whitney's embedding theorem an attractor with D dimension can be embedded in R^{2D+1} and according to Taken's delay embedding theorem the delay reconstruction represents the entire dynamics of the system. Thus $X_{n+1} = F(X_n)$ is equivalent to $(s(X_n), s(F(X_n)), s(F*F(X_n)), \ldots\ldots\ldots\ldots)$ which is equivalent to a set of co ordinates. The function F that couples different degrees of freedom is reflected in the single variable time series. The components of delay vectors are mutually independent. Thus, it requires only one variable to understand the dynamics of entire system as this one variable contain all information regarding other variables due to coupling.

3.4.1 Grassberger- Procaccia Method

The most popular method to characterize an attractor based on geometry and dynamics proposed by Grassberger and Procaccia (1983a; 1983b), known as GPA. The two commonly evaluated parameters using this algorithm are Correlation dimension, D2 and Kolmogorov entropy, K2. The Correlation Dimension is a geometric parameter of the attractor that corresponds to number of independent variable require to specify the state of the system at any given instant, whereas Kolmogorov entropy is a dynamic parameter which characterizes the dynamical evolution of a system. The Grassberger – Procaccia method considers one of the variables of a system equation as a single variable time series, reconstructs its state space attractor using Time delay embedding theorem (Abarbanel et al., 1993) and evaluate the dimension and entropy of the attractor. This is done without the governing dynamical equations necessarily being known. The ability of Time delay embedding to reconstruct the system attractor in state space lies in the coupling among the variables controlling the system and as a result one variable will carry *all* information regarding other variables. This embedding method produces a smooth mapping of system's evolution in state space.

Consider a single variable time series obtained from a nonlinear system that consists of N data points sampled evenly with a sampling time Ts. Each data point represents the projection of full state vector that consists of current values of all variables required for characterizing a system. The obtained time series is embedded in a large enough m dimensional state space as

$$X_i = [v(i), v(i+T), v(i+2T), \ldots\ldots, v(i+\{m-1\}T)] \qquad (3.8)$$

where X represents the state vector, v represents the single variable time series, m being the embedding dimension and T, the time lag which need not be equal to sampling time Ts. The Correlation Dimension is then evaluated by considering correlations between points of a long time series on the attractor in state space and defining correlation integral as

$$C_m(r) = \lim_{N \to \infty} \left[\frac{1}{N^2} \sum_{i,j=1}^{N} H\left(r - \left| X_i - X_j \right|\right) \right] \qquad (3.9)$$

$$= \int_0^r d^m r'\, c(r') \qquad (3.10)$$

where H (x) is the Heavyside function, c (r') is the standard correlation function, m the embedding dimension and $|X_i - X_j|$ is the Euclidean distance between the vectors X_i and X_j. In short $C_m(r)$ estimates the total number of neighbors within a sphere of radius r in an m dimensional phase space. The main assumption of this algorithm is that the $C_m(r)$ behaves as a power of r for small values of r.

Thus

$$C_m(r) \sim r^{d,} \qquad (3.11)$$

where d is closely related to D2.

35

The Correlation dimension D2 is defined as

$$D2 = \lim_{r \to 0} \frac{\ln C_m(r)}{\ln r} \qquad \text{as } m \to \infty \qquad (3.12)$$

In practice, however D2 is evaluated by finding the slope of logarithms of $C_m(r)$ and r for successive higher values of r. This measure is a lower bound of Fractal Dimension.

Several other algorithms have been proposed to evaluate the dimension of an attractor (Pritchard & Duke, 1992). In many of these methods the dimension is defined as an exponent that scales the " bulk " of an object with linear distance and this is determined by taking log " bulk " over the log distance. In GPA, this bulk is the Correlation integral. The GPA is widely used compared to other methods because computation of correlation integral is straightforward and is efficient. Further distance (r) can be started from a low value, smallest inter point distance, and can be varied until the C (r) reaches its maximum value, i.e. 1. However other criteria required for the successive implementation of this method is the identification of proper time lag T, appropriate embedding dimension m and the determination of linear scaling region in the plot of log $C_m(r)$ and log (r).

The embedding dimension must be larger than the Correlation dimension. If the embedding dimension is very large then the endpoints of the reconstructed vector will be decorrelated resulting in inflation of estimated dimension. On the other hand, if the embedding dimension is not large enough there will be under estimation of

36

dimension. In GPA, the value of m is varied from 1 to higher values until the estimated dimension saturates. This estimated dimension at saturation is taken as Correlation Dimension. No recipe is given in GPA for the selection of time lag required for reconstruction. In the case of unlimited noise free data, any arbitrary lag T can be chosen. Nevertheless, the real data set is noisy as well as limited. This requires a proper choice of time lag. If the lag is small then the endpoints will be approximately equal and the reconstructed attractor will be essentially diagonal in state space. This phenomenon is called *redundance* (Pritchard & Duke, 1992). If time lag is too large the structure of the reconstructed attractor will be lost and this is called *irrelevance*. The methods commonly employed for the determination of embedding dimension is False Nearest Neighbors or Singular Value Decomposition and for the selection of time lag, Autocorrelation function or Average Mutual information criteria. These methods are discussed in subsequent sections.

Computation of Correlation Dimension from time series has achieved widespread popularity and several papers have been published reporting dimension of several systems. (Kantz & Schreiber, 1999). However, it is difficult to know the reliability and accuracy of these measures. Further problems due to temporal correlations and intrinsic oscillations are present in many of these results. To avoid pitfalls Theiler (1988) modified GPA by rejecting those pairs of points that are close in space as well as in time. Thus Correlation integral is defined as

$$C_m(r) = \frac{2}{(N - n_{min})(N - n_{min} - 1)} \sum_{i=1}^{N} \sum_{j=i+n_{min}}^{N} H\left(r - \left|X_i - X_j\right|\right) \quad (3.13)$$

where $n_{min} = \dfrac{t_{min}}{T_s}$, T_s being the sampling time.

The t_{min} can be determined by the method suggested by Provenzale et.al. (1992). In fact the modification proposed by Theiler and others do not guarantee that the estimated dimension of EEG is the true dimension of the system attractor. Again GPA is suitable only for stationary data set while EEG is nonstationary in nature. However, the estimated Correlation dimension of EEG can be viewed in a relative sense for making comparisons between different states of human brain.

Another measure, which was proposed by GPA that characterizes an attractor, is Kolmogorov entropy. This measure which is specific to dynamical system gives the degree of "chaoticity" of the system or the long time average rate at which the information is generated by the system or equivalently the rate at which current information about the system is lost. K2 is computed from the time series as

$$C_m(r) \cong r^{D2} \exp\left(-mTK\tilde{2}\right) \tag{3.14}$$

then

$$C_{m+1}(r) \cong r^{D2} \exp\left(-(m + 1)TK\tilde{2}\right) \tag{3.15}$$

From the above

$$K\tilde{2}(r) = \frac{1}{T} \ln\left\{\frac{C_m(r)}{C_{m+1}(r)}\right\} \qquad (3.16)$$

then

$$K2 \cong \lim_{\substack{m \to \infty \\ r \to 0 \\ T \to 0}} K\tilde{2}(r) \qquad (3.17)$$

Many researchers concentrate more on accurate determination of D2, only a few have given importance to the dynamical aspects of the attractor. The determination of entropy is significant as they give information regarding the Time Scales involved in the dynamics of a system. Apart from the proper choice of embedding dimension and time lag the results obtained from GPA depends on data length, precision of Digitizer, effect of filter and many others (Rapp, 1993). If parameters are seen in a relative sense the effect of many of the above mentioned can be minimized by carefully applying the algorithms. However, the problem due to nonstationarity is still unresolved. Therefore, in the next section we discuss a Nonstationary process from the nonlinear dynamical point of view.

3.4.2 Nonstationary Process

" A stochastic process is called *strict sense stationary* if all its statistical properties are translationally invariant under time. A stochastic process is called *wide sense stationary* if its mean is constant and its autocorrelation depends only on the difference $\tau = t_1 - t_2$ " (Papoulis, 1984).

A process, which violates the above definition, is usually considered as a nonstationary process. A time series is said to be stationary if its statistical quantity up to second order to be constant or all transition probabilities from one state of the system to another is independent of time within the observation period. This requires the condition that the parameter of the system remains constant and the dynamics are contained in the time series sufficiently frequently. There are tests to determine the stationarity of a time series (Isliker & Kurths, 1993). However, for a nonlinear dynamical system, especially human brain, the approach requires a different frame of reference that may move from the previous view of nonstationary process. If a process involve several time scales a stationary data set can be obtained only if the length of the data set is sufficiently larger than the longest characteristic time scale involved in the dynamics of a system. Thus, identification of different time scales becomes crucial to understand the nonstationary nature of a data set. From the nonlinear dynamical point of view the understanding of nonstationary process essentially is to identify the different time scales in the process and it is not merely a statistical property.

Some of the algorithms have been developed which claim to be useful for analyzing nonstationary data set. These are Pointwise Scaling Dimension (Farmer et al., 1983), Point D2 (Skinner et al., 1991) and the method proposed by Havstad and Ehler (1988).

3.4.3 Pointwise Scaling Dimension (PWSD)

This method was proposed by Farmer et al (1983) in which the correlation integral is evaluated by considering a reference vector X_i and finding all pairs of points within a radius r by spanning and probing the vector X_j over the entire epoch. Since reference vector is chosen sequentially for each point in the time series, the dimension is estimated as a function of time as well as its position on the attractor.

This continuously estimating dimension assumes that the reference vector, which spans only a short interval, would remain stationary and would dominate the calculations, making the overall estimate less sensitive to nonstationarity. This is considered as a modification of GPA. In this algorithm, also the nonstationarity is not well defined. Further, this also assumes stationarity within a short interval of the epoch.

3.4.4 PD2 Algorithm

The PD2 or Point D2 estimate of Correlation dimension was originally developed by Skinner and his group (Skinner et. al., 1991). In this algorithm, also the correlation integral is evaluated fixing the X_i and spanning the X_j vector over the whole data series in an m dimensional state space. Unlike in Pointwise scaling dimension algorithm this method does not consider all the vectors but considers only those X_j vectors that must arise from subepoch that produces scaling characteristics similar to those surrounding the X_i vector. It rejects unsuitable estimates that do not result in linear scaling or clear convergence. This eliminates the effect of artifacts or

noise or insufficient sample of stationary subepoch. The PD2 does not take into account all possible pairs of distance as in GPA nor all vector difference with respect to a particular reference vector as in Pointwise Scaling Dimension. This considers its own subspecies of stationary data epoch.

It has been pointed out that both PWSD and PD2 are better than GPA in estimating dimension from a nonstationary data. However PD2 seems to be effective compared to PWSD even for a small epoch of 1 sec or less (Elbert et al., 1994). Skinner and his associates used a 500ms data record from olfactory bulb of the rabbit during behavioral quiescence and reported that this small epoch is necessary to achieve statistical stationarity (Mitra & Skinner, 1993). After the presentation of a novel order, again 500ms data appear to be stationary within this condition. However, they found that D2 estimate increased compared with the *control*. Another group, (Rapp et al., 1990) found that EEG data of 1sec remain stationary statistically, but the estimated Dimension D2 of a target stimulus is quite different from non-target stimulus. In both the above-mentioned experiments Skinner found that the Dimension estimate does not shift to a unitary value rather changes continuously. This change may be due to a variety of rapid nonstationary changes. This observation clearly indicates that there exists a large class of time scales involved in the dynamics of human brain.

Even though both the above mentioned algorithms indicate the significance of nonstationarity they do not take into account the significance or relevance of time scales.

3.4.5 Havstad – Ehler Method

Much of the uncertainty in estimating dimension due to nonstationarity requires the use of small data sets, covering only small intervals. In this method, the obtained time series is divided into different overlapping or nonoverlapping windows. The dimension is evaluated for each window with a slightly different procedure than GPA. This allows the dimension estimate as a function of time.

The scalar time series is reconstructed in state space using the method of time delay as $X_I = \{v_{iaT}, v_{iaT-ibT}, \ldots\ldots\ldots, v_{iaT+(m-1)bT}\}$ where v is the time series, aT, the time interval between the first elements of successive vectors and bT, the time lag between vector elements and m embedding dimension. The data set for dimension estimation consists of N vectors and M reference vectors (M<N). In this method instead of calculating the number of pairs of vectors within a radius r, the radius is predetermined and the distance from a reference vector to each of N vectors within r are noted. From this number of vectors j within a predetermined r, the Correlation Dimension is calculated as

$$D_c(m) = \frac{\ln(j)}{\langle \ln r \rangle} \tag{3.18}$$

where $\langle \ \rangle$ denote the average. Euclidean norm is used to calculate the distance between the vectors. To avoid prominent distortion of slope in ln (j) and $\langle \ln r \rangle$ a certain minimum number of vectors are skipped on either side of the reference vector. Thus a reliable estimation of dimension is obtained by careful choice of

43

intervals between vectors and between reference vectors and neighbor vectors so that the vectors are adequately independent, by proper choice of time lag and by averaging ln (r).

The algorithms discussed so far tries to minimize the errors in dimension estimation due to nonstationarity but does not incorporate the notion of nonstationary process as such. The proponents of PD2 claim that their algorithm is superior to others, however does not define nonstationary process. They reject some of the vectors in the correlation integral estimation, which does not give similar scaling as the surrounding vectors of reference vector. Whether this rejection is valid when the process involves a large class of overlapping time scales is not mentioned. The method proposed by Havstad and Ehler has been employed in this work as it considers the dynamics within a window and considers at least in some sense the time scales involved in the dynamics within that window. Further, it has been found that it gives more reliable estimation of D2 especially for high dimension signals like those of EEG.

3.4.6 Selection of Time Lag

According to embedding theorem, any time lag can be used to reconstruct the attractor in state space. However, for practical cases the time lag for reconstruction of attractor is to be selected appropriately to avoid the problem of redundance, due to small value of lag or irrelevance, due to a large value of lag. The two commonly employed methods for the determination of time lag are Autocorrelation function and Average Mutual Information.

In autocorrelation function, the time lag is selected accordingly for the two-measurement $v(n)$ and $v(n+T)$ for linear independence average over the observations. For this a linear autocorrelation function is calculated as

$$C_L(T) = \frac{1}{N} \frac{\sum_{k=1}^{N}(v(k+T) - \bar{v})(v(k) - \bar{v})}{\frac{1}{N}\sum_{k=1}^{N}(v(k) - \bar{v})^2}$$

(3.19)

where N is the number of data points and $\bar{v} = \frac{1}{N}\sum_{k=1}^{N}v(k)$

and selecting the time lag that passes through first zero. In certain cases when multiple peaks are present in the Power spectrum, the time lag is selected as the number of digitized values in a quarter cycle of one of the higher dominant frequencies. In this prescription only linear dependence are considered.

Average Mutual Information (AMI) is a probabilistic measure, which is a generalization of auto-correlation function to nonlinear domain. It is defined by the expression

$$I(T) = \sum_{k=1}^{N} p\big[v(k), v(k+T)\big] \log_2\left[\frac{p\big[v(k), v(k+T)\big]}{p\big[v(k)\big]p\big[v(k+T)\big]}\right]$$

(3.20)

where $p(v(k))$ is probability of measuring $v(k)$ and $p(v(k), v(k+T))$ is the joint probability of measuring $v(k)$ and $v(k+T)$. The time delay required for reconstruction

45

is selected to be the value at which the first minimum in the average mutual Information (AMI) plot of I(T) versus T appears. If there is no minimum in the plot, then the time delay T is that value at which I(T)=Imax / 5. Here a probability distribution associated with each system governing the possible outcomes of observations on them. This method considers all kinds of nonlinear correlations unlike ACF where it takes into account only the linear ones (Fraser & Swinney, 1986).

The proponents of AMI claims that this method is superior as it considers all types of nonlinear as well as linear correlations whereas opponents argue that this method is suitable only for 2 dimensional case not for fully reconstructed state space. Further, the choice of first minimum and not subsequent minima needs a justification. A consensus is that time lag be selected so that the state space plot show maximum scatter. Again, this type of selection of time lag from any one of the above criteria is suitable for dimension determination, for the estimation of dynamical parameter like entropy this choice could introduce discrepancy since a finite lag would imply an averaging process and any time scale within the time lag will not be taken into account. Till now there is no good prescription available for the accurate estimation of time lag.

3.4.7 Embedding Dimension

It is very tedious, especially for a high dimension system to compute the correlation dimension by changing the state space dimension from a small value to

higher values until the estimated correlation dimension saturates. If an acceptable minimum embedding dimension can be estimated, then the correlation dimension need to be evaluated by embedding the attractor higher than the minimum embedding dimension obtained, thus reducing excessive computation. The method of False Neighbors (Kennel et al., 1992) observes the behaviour of near neighbors of the attractor as it unfolds into higher dimension. A reliable estimation of minimum embedding dimension is obtained by identifying false neighbors.

Consider r^{th} nearest neighbor $y_r(i)$ of the vector $y(i)$ in an m dimensional space. The Euclidean distance between the points $y(i)$ and $y_r(i)$ is

$$R_m{}^2(i, r) = \sum_{k=0}^{m-1} \left[y(i + kT) - y_r(i + kT)\right]^2 \qquad (3.21)$$

As the attractor unfolds into the next dimension, i.e. m+1, the Euclidean distance at this dimension is

$$R_{m+1}{}^2(i, r) = R_m{}^2(i, r) + \left[y(i + mT) - y_r(i + mT)\right]^2 \qquad (3.22)$$

Any point in state space is designated as false neighbor if

$$\left[\frac{R_{m+1}{}^2(i, r) - R_m{}^2(i, r)}{R_m{}^2(i, r)}\right]^{1/2} = \frac{|y(i + mT) - y_r(i + mT)|}{R_m(i, r)} > R_{tol} \qquad (3.23)$$

where, R_{tol} is some threshold. It is sufficient to consider only the nearest neighbor ($r=1$) and scan the entire orbit points and find out the number of false nearest neighbors. For a limited data set, a second criterion is required that considers the extremity of the attractor. The second criterion as

$$\frac{R_{m+1}(i)}{R_A} > A_{tol} \qquad (3.24)$$

where

$$R_A^2 = \frac{1}{N} \sum_{i=1}^{N} [y(i) - \bar{y}]^2, \bar{y} = \frac{1}{N} \sum_{i=1}^{N} y(i) \qquad (3.25)$$

A nearest neighbor that fails either test is declared false neighbor.

Apart from determining the embedding dimension from geometric consideration of attractors another method which is commonly used in noise reduction can be used for finding the dimension of phase space. Singular value decomposition, which is related to Principal Component Analysis, is used to decompose the trajectory matrix into singular value matrix and unitary matrices. Only the significant singular values are retained. In this transformation, the reconstructed state vectors are transformed into the orthonormal basis vectors. The number of significant singular values gives the embedding dimension of the space.

3.4.8 Unfolding Dimension

The parameters correlation dimension and Kolmogorov entropy give information regarding the degree of freedom, dynamical state as well as rate of dissipation of a dynamical system. In spite of several limitations of obtaining these parameters from real data it has been found that these measures can be used in a relative sense to study various conditions of brain by analyzing EEG. This triggered the enthusiasm of researchers to apply it to clinical diagnostic purposes. Even though these measures specify different states of human brain, any of these measures do not indicate as yet any individual specificity and functional stability.

The information regarding the geometry and dynamics are considered only for the state space dimension larger than the minimum embedding dimension. Any information for lower than the minimum embedding dimension is discarded. Schmid & Dunkii (1998) proposed a concept called unfolding dimension that measures the rate at which an attractor unfolds as state space dimension increases. In this method a plot of D2 versus dimension (m) is obtained for value of m as low as 1 to higher values and to this plot a fit using a biparametrization is obtained as

$$D2(m) = b_0\left[1 - \exp\left(\frac{-m}{m*}\right)\right]$$ (3.26)

where b_0 indicates the attractor dimension and m* the unfolding dimension which gives the rate at which an attractor unfolds. By applying this method to EEG, these

researchers could note the intra individual stability and functional specificity in the case of schizophrenia and remission as well as for normal.

3.4.9 Testing for Nonlinearity

A discussion in this chapter will remain incomplete without a mention about the detection of nonlinearity in time series. The general notion in nonlinear dynamical analysis is that if a saturated value of noninteger dimension value is obtained in GPA then the system is considered as chaotic. However, it has been found that the so-called 1/f– like stochastic systems also result in saturation. This refers to those series whose power spectrum varies as $(1/f)^a$. When a>0, the saturation occurs at 2/(a-1). To detect nonlinearity present in the series Theiler et al. (1992) introduced a discriminative test. In this method some linear process is specified as null hypothesis, then surrogated data sets are generated which are consistent with this null hypothesis. Finally, a discriminative statistics is computed for the original and each surrogated data. If the computed value for the original data is significantly different from the ensemble of values for surrogated data, then the null hypothesis is rejected and *nonlinearity is detected*. The surrogate data sets are randomized sequences whose statistical and / or spectral properties are similar to the original time series. Three types of generating surrogated data set are Phase randomized, Fourier shuffled and Gaussian scaled surrogate sets.

Phase randomized surrogate data set is generated by obtaining the Fourier transform of the original data and the phases are then randomized. One then

evaluates the inverse Fourier transform. The process gives linearly correlated noise with the same mean, variance and power spectrum as the original data but the phase information is destroyed.

In Fourier shuffled surrogate, first phase random surrogate of the series is obtained for the original data. The amplitude of the original and phase randomized are rank ordered and each value of the surrogated set is replaced by its corresponding amplitude from the original data to get a new series. This series has the same amplitude as the original data but in a shuffled manner. This is used for measuring sensitiveness in amplitude change as well as autocorrelation.

The Gaussian scaled surrogates are designed to test the null hypothesis that, all though the dynamics of the observed signal is linear it may be subjected to nonlinear distortions. The original signal is transformed into another signal by a static nonlinear filter. The filter is static in the sense that the output of the filter depends only on the current value of the original signal. First a time series having independent identical Gaussian distribution is formed, and then this series is reordered so that its ranking agrees with the series obtained from the nonlinear filter. The reordered series has the same Gaussian distribution as the filter output series and it is then Fourier transformed, phase angle shuffled and inverse is taken to get the surrogate data set. The final surrogate is obtained by rendering the filter output series so that it follows Surrogate data set.

Serious criticism has been raised regarding the chaotic nature of EEG by conducting surrogated data analysis (Rapp et al., 1991). These researchers claimed that EEG might have a simpler stochastic description and chaotic dynamical nature of EEG may be spurious. However, it has been shown that surrogated data analysis may not be sufficient to prove the stochastic nature of EEG (Pradhan & Sadasivan, 1997) by performing analysis on numerical data of classical chaotic systems, mixed sine waves, white Gaussian, colored Gaussian noises and various traditional EEG activity bands. White Gaussian noise and classical chaotic systems are discerned by surrogate data set, colored Gaussian noise and mixed sine waves with less number of sinusoids show behaviour similar to low dimensional system. But EEG show saturation and limiting correlation dimension in all bands.

Rapp (1990) has pointed out that the misapplication of nonlinear dynamical methods can produce fallacious results especially when applied to biological data. Nevertheless Rapp presented a general procedure, which is found to be very useful for the analysis of complex signals. The analysis of data requires a thorough understanding of the phenomenon. A brief account of the procedure with the same rule as presented by Rapp is presented below

- *Never skimp on House keeping*

  The crucial aspect in these experiments is data acquisition. Usually the data is acquired using Data acquisition card coupled to a computer. In this case data is to be checked before and after transfer to the computer. Further packaging protocol, amplifier gain and digitizer resolution should be checked. The entire experimental set

up especially data acquisition unit should be checked with simulated signals. A random signal can then be used to test the accuracy of the set up and dynamical analysis algorithms. In short a good documentation of data is very essential for this kind of analysis.

- *Test for Digitizer Saturation*

The digitizer should not be in saturation region. The maximum and minimum value of the analog signal should be within the working range of the digitizer. A 12-bit resolution is desirable.

- *Visually inspect the data*

A visual inspection and comparison with the analog version of the data is useful for identifying artefactual spikes and silent intervals introduced by the digitizer.

- *Determine the natural time scale of the signal*

A proper selection of the sampling time is very important. If the sampling rate is high then the memory requirement is large. On the other hand less sampling time reduces the information content. Evaluating the autocorrelation function of the signal and finding the first minimum time lag can make a proper choice of natural time scale of the system. However for a noisy data set this first minimum may be a local minimum and a global minimum may provide a better estimate. Many investigators take 1/e of its original value, as a measure of the signal's time scale. The autocorrelation function is robust to noise and can give a good measure of time scale.

53

- *Find the spectral properties of the signal*

Even though there are several limitations for applying the spectral analysis for nonlinear systems, this method is suitable for qualitative analysis of EEG signals. Hence prior to the application of nonlinear dynamical method, looking for known rhythms can make a check of the algorithms.

- *Testing for stationarity in time domain*

Most of the algorithms developed in nonlinear dynamics require the condition of stationarity. However the condition of stationarity may have different notion in nonlinear domain. It is not clear whether the spectral stationarity and classical statistical measures provide accurate information regarding the nonstationarity nature of EEG data. Even then it still seems helpful in estimating the stationarity using these measures.

- *Testing for stationarity in the Embedding space*

Instead of looking for stationarity in time domain Eckmann, Kamphorfst and Ruelle (1987) introduced a novel method for checking the stationarity in phase space. In this method nearest neighbors are discovered and plotted for each point and the pattern obtained is observed.

- *Construct phase portraits with different time lags*

Two dimensional phase portrait is plotted with different time lag to obtain the visual indication of two-dimensional geometry of the time series. This method however does not provide definite indication of the dynamics of the system.

- *Finding an appropriate embedding of the phase space.*

Several methods are proposed to find the appropriate embedding dimension. These are viz. 1) The autocorrelation function 2) Mutual information 3) Higher order autocorrelation functions 4) False nearest neighbors and its variants 5) Legendre polynomials 6) Continuity Statistics 7) Diagonal expansion 8) Singular value spectra are some of the proposals.

- *Apply geometrical filter*

The application of filter in time domain has several drawbacks. Hence geometrical filters seems to be better in noise reduction as they operate in phase space and not in time domain. These filters can also give misleading results if not applied properly.

Besides above-mentioned procedures it has been suggested that all dynamical measures should be validated with Surrogate data. Since the aim of the present investigation is not to establish chaos or otherwise, the study of surrogated data has been neglected and considered only the obtained parameters for a comparative study, which may lead to clinical applications.

3.5 Analysis of Signals

In linear as well as in nonlinear methods the primary tasks are to find the signal, the space in which the system can be represented, classification of signal and developing a model based on the characteristic parameters. While the objectives are

the same, the methods of analysis are entirely different. In linear domain, one assumes a dynamics that satisfies superposition theorem. In nonlinear dynamics this assumption is not tenable.

The main task is the signal separation and one must establish the differences between the information bearing signal and interference. The problem of identification of signal from noise is common for linear and nonlinear observer. The observer assumes that in a linear system the source emits sharp spectral signals and it is very easy to distinguish these spectral lines contaminated by broad band interference. Since the difference between the signal and unwanted background is clear, Fourier techniques can be used for separation. Further Fourier decomposition can also be used if the signal and contamination are located in quite different bands. As it has been already mentioned in a nonlinear system, it is difficult to assess the information content in broad band environment using Fourier representation. In a nonlinear system, the pure signal and the noise do not remain separate for all times as in the case of linear dynamics, but they may combine in a nonlinear fashion to generate stochastic resonance modes. Hence in the nonlinear domain, reconstruction of the signal in phase space by applying the various nonlinear noise reduction methods (Kostelich & Schreiber, 1993) separates the signal from noise. The geometric structure in phase space is characteristic of each chaotic system as the behaviour is fundamentally multivariate. In the current studies of nonlinear signal processing, there is three distinct direction of signal separation. First, the evolution equation of the system is known and one has to extract the signal from the knowledge of the dynamics. Second, with a signal measured at an earlier time as a

reference signal one can establish the statistics of the evolution of the attractor and use this statistics to separate from the subsequent transmission the chaotic signal from the contamination. The third case is the most difficult one in which a one time measured signal is only available and one make models based on this signal. There is no knowledge of either the reference signal or the evolutionary equation

After the identification of signal, the next step is to represent the signal in correct space. In the case of linear system, the natural choice is to represent the signal in Fourier / Canonical vector space. If the source is invariant under translations in time, the sines and cosines form the natural basis functions in which the original signal is expanded with coefficients. Thus, the classifying parameters are the coefficients of harmonic functions, represented by sharp spectral peaks in the Fourier spectrum. If the source has transients or significantly high frequency content with many localized events in time domain, the linear transform such as wavelets are suitable for such localized events. In the case of chaotic signals, the Fourier representation again fails, as the process is multivariate. With a suitable phase space the parameters derived are the invariants of the orbit like Lyapunov exponents, various fractal measures, linking numbers of unstable periodic orbits etc. For developing models the parameters of the model are derived, to be consistent with the spectral peaks in linear case whereas in the case of nonlinear model the parameters are found consistent with the invariant classifiers like Lyapunov exponents, dimensions etc. Some of these invariants are quantities that are unchanged under various operations on the dynamics or the orbit as well as small variations in initial conditions. This indicates that they are insensitive to initial conditions. Some of the

invariants are further unchanged under the smooth change of coordinates and some, topological invariants, are purely geometrical properties of the vector field describing the dynamics. Some of these are used to establish the predictability of the nonlinear system. Many of the chaotic systems are unpredictable due to instabilities in phase space and the sensitivity to initial conditions. System identification in nonlinear chaotic systems means establishing a set of invariants for each system of interest and then comparing observations to that of library of invariants. Another area that has wide applications in engineering is the signal synthesis. The main task is to study the synchronisation of chaotic sources and thereby use these sources for communication. Research in this direction has already been initiated which will be discussed in the subsequent chapters.

There are both promises and problems with the approaches of nonlinear analysis of signals. The promise is that the nonlinear data analysis in combination with powerful nonlinear dynamical theory will give information regarding the dynamical variables of the system. The problem is that whether the algorithms developed in nonlinear domain actually detects chaos or another mathematical transformation adding little new information in the understanding of the system.

ELECTROENCEPHALOGRAM AS A TIME VARYING SIGNAL

A brief account of characteristic of Electroencephalogram as a time varying signal is discussed in this chapter. An account of clinical implication of the characteristics as well as chaotic phenomenon observed in neural system is also presented.

4.1 Electroencephalogram

The electroencephalogram (EEG) is the recording of electric potentials generated in the cerebral cortex due to involved mechanism of large number of neurons. Generation mechanism of action potential in axon of a single neuron is essentially due to the sodium-potassium pump while the generation mechanism in synapses are essentially a physico-chemical process. in the case of axon, it has potassium ion fluid inside and sodium ion enriched fluid outside. Hence there is a negative electrochemical potential field across the axon membrane of the order of 80 mV. In the case of myelinated axon, there are unmyelinated regions situated at regular intervals and these are called nodes of Ranvier. The potential firing takes place at these nodes. However in certain cases the whole nerve is unmyelinated and action potential can occur at any point along the length of the nerve. At the arrival of a signal, at the nodes of Ranvier, a sodium gate open and there is avalanche of sodium ions entering the nerve, thereby raising the potential to 40mV. This is a sharp increase and is called the first phase of potential firing. However, there is a threshold

59

and if the signal does not excite the process this firing does not take place. The second phase is a slow recovery to the equilibrium negative state of - 80mV during which the nerve discharges the sodium ions and get it enriched by the potassium ion inside the nerve. Often the second phase offshoots the equilibrium level coming to a level of about 100mV and then come back to the equilibrium level of 80mV. The time duration between the initial phase and the final phase is called the Refractory time. A peculiarity in this process is that the amplitude of these firings is independent of the stimulus strength, while the firing frequency has a linear dependence with the stimulus strength. This shows that the process is indeed nonlinear and the fact that there exists a threshold in the process introduces certain randomness. Hence the whole process of nerve response to a stimulus is a random nonlinear process.

In the case of a synapse, the process is entirely different. The presynapse has vesicles that deposit its content of neurotransmitters into the synaptic cleft. This in turn reduces the electric resistance in the postsynaptic membrane and it activates either calcium ions if it is an excitatory process or chloride ions if it is an inhibitory process resulting in an action potential firing or its inhibition. This is a physico chemical process, but the physical characteristics of the action potential firing are independent of whether it is a sodium-potassium pump action or a synaptic transduction. The fact that there is no attenuation of the amplitude is very significant and this indicates that the whole signal transduction is not akin to a flow of current in a conductor. The amplitude of the action potential remains constant along the axon. This is because it derives energy for its propagation from the nerve itself. The generated potential travels from the axon hillock to the terminals where the

60

depolarisation releases neurotransmitter causes an excitatory or inhibitory potential in other neurons. The action potential itself causes only a very brief current, which does not penetrate far into the extracellular space.

The potentials generated by large number of neurons are *integrated* at various stages of its propagation from input to the central nervous system and back to the action muscle stage. Integration of electric potential in the cortex occurs mainly at the vertically oriented pyramidal cells of the cortex. These pyramidal cells can achieve these functions because of the following reasons. (1) The dendrites of the pyramidal cells extend to nearly all layers of the cortex, guiding the flow of potentials generated by postsynaptic potentials at either the cell body in deep layers of the cortex or at dendrites in the more superficial layers through the entire thickness of the cortex. (2) These neurons are closely packed and oriented parallel to each other, facilitating spatial summation of the currents generated by each neuron. (3) Groups of these neurons receive similar input and respond to it with potential changes of similar direction and timing. The currents generated by these neurons summate in the extracellular space and are limited to the cortex. However, a small fraction penetrates through the meningeal coverings, spinal fluid and skull to the scalp where it causes different parts of the scalp to be at different potential levels. This constitutes EEG. Though EEG is produced by involved mechanism of large number of neurons it is difficult to provide a valid explanation in terms of the underlying single neuronal processes.

4.1.1 Nature of EEG patterns and their characterization

A variety of patterns appear in "*normal*" EEG and it is difficult to characterize a normal EEG. However, it is believed that there are a few abnormal patterns in EEG. Hence, usually EEG is defined based on the presence of abnormal patterns. Although abnormal brain functions are reflected in EEG, it is not essential that normal EEG reflect only normal brain functions. However, most abnormal EEG pattern indicates abnormal brain function. Also, there may be abnormal patterns in EEG of persons without any brain disease. Therefore, a visual inspection fails to provide accurate diagnosis of brain function. Some of the abnormal patterns identified in clinical diagnosis are spikes and sharp waves, certain slow waves and amplitude changes, which are known to be abnormal in different age group. Further EEG characteristics depend on age group also. The normal EEG undergoes enormous changes from premature period upto the age of 19 years, whereas normal EEG in general show very little changes in the age group of 20 to 60 years. Above 60 years of age, some of the abnormal patterns are considered as normal.

For visual inspection of EEG, the understanding of different waveforms is important. The different waveforms identified are as follows. These waves with uniform appearance due to symmetrical rising and falling are called regular waves. Some of them similar to sine waves are called sinusoidal. Other regular waves are arch-shaped or saw-toothed. A transient is an activity that can be clearly distinguishable from its background activity. It may be a single wave or a sequence of two or more waves. Spike has duration of 20 to 70 msec whereas sharp wave has

duration of 70 to 200 msec. A spike may be followed by a slow wave and form a spike - and - wave complex which may have a frequency of less than 3 Hz. In some cases there may be two or more spikes called multiple spike complexes. Spikes and sharp waves are generally considered as abnormal patterns. Single spikes and sharp waves and complexes which contain spikes and sharp waves and last for less than a few seconds are called interictal epileptic form activity. The longer lasting activity of spike and sharp waves and of some other types are called ictal pattern.

Based on frequency EEG waves are classified:

- Delta waves – under 4Hz

- Theta waves – from 4 Hz to under 8 Hz

- Alpha waves – from 8 Hz to under 13 Hz

- Beta waves – over 13 Hz.

There are waves in EEG that extends across the boundaries of the above mentioned frequency bands. Waves under 8 Hz are generally called slow waves whereas waves above 13 Hz are called fast waves.

The amplitudes of EEG are in microvolts and they are classified as low (under 20 microvolts), medium (20-50microvolts) and high (over 50 microvolts). The differences in amplitudes observed from the corresponding two sides of the brain has great clinical significance, provided it has to ensure that it is not due to external factors like unequal spacing and impedance of the recording electrodes, difference in amplifier gain and several such other factors. The distribution of the

63

activity is also important from clinical point of view. This can be observed by placing electrodes at different locations on the scalp. Eight channel recordings are the ones normally used. However, sixteen or more channels can provide a better spatial resolution. Generalized distribution refers to that activity which occurs at the same time over most or the entire headspace. Lateralized distribution refers to activity that appears only or mostly on one side of the head. This type of activity suggests abnormality. Some normal patterns may also appear on one side of the head at one time and later occurs on the other side after a few seconds or minutes without being abnormal. Focal activities are also observed and are restricted to one or a few adjacent regions.

Another measure that is often used is the phase relation. In this context phase refers to polarity and timing of components of waves in one or more channels. If the trough and crest of waves in one of the channels coincide with any of the waves in other channels, then these waves are said to be in phase. If peaks are pointing in opposite direction then they are said to be out of phase or phase reversal. Similarly, if two activities occur at the same time they are said to be synchronous. Waves that occur at the same time on both sides are called bisynchronous. This term corresponds to the activities between two sides of the brain. The waves that occur in different channels without any relation in time to each other are called asynchronous. If waves occur in one region at one time and in another region at a different time are said to be independent.

4.1.2 Normal and Abnormal EEG patterns

The normal EEG of an adult shows various types of activity. Alpha rhythm is the most common one with regular waveform and often sinusoidal in nature. The frequency ranges from 8Hz to 13 Hz in different subjects and is almost constant in any one subject. The frequency of alpha rhythm in the two hemispheres is same. A slight decrease in frequency is the indication of abnormality in that hemisphere. The phase relation over different parts of the brain may vary. Individual alpha waves are not synchronous in different areas in normal EEGs. The amplitude of this rhythm is greatest and persistent in occipital and parietal regions. Alpha rhythm may appear in recordings from a frontal electrode referred to an electrode on the ear. The physiological significance of alpha rhythm is still unknown. Beta rhythms are less common compared to alpha waves. They appear either in a wide distribution or limited to the frontal or posterior head regions. Beta rhythms over 30 Hz usually have very low amplitude. These rhythms disappear during drowsiness and sleep. The amplitude of the beta waves is usually lower than the alpha waves and amplitude and distribution is symmetrical. The ratio of beta to alpha activity increases with age but this ratio does not have any known clinical significance. The presence of beta activity in an older person reflects better cerebral function than its absence. Like alpha, the physiological significance of beta rhythms is also not clear. Another rhythm seen in less than 10% of EEGs are Mu rhythm that consists of arch shaped waves at 7-11 Hz. This type of wave seen in central or centro-parietal regions appears in trains' upto a few seconds. Mu waves intermix or alternate with beta activity and has a frequency similar to alpha waves. Nevertheless this rhythm is seen

when alpha rhythms are blocked. Mu rhythm is normally intermittent and asynchronous.

An EEG is *considered* abnormal, if it contains any of the abnormal patterns like epileptic form activity, slow waves, amplitude abnormalities or any of the pattern resembling normal activity but difference in frequency, reactivity or other features. The epileptic form activity can be of three types, Localized, generalized or special patterns. Similarly for slow waves, the patterns are localized, generalized or bilaterally synchronous and for amplitude abnormalities, localized and general amplitude changes. Each pattern is identified either with general cerebral pathology or specific neurological diseases. Local epileptic form activity is due to a focal irritative lesion of the cerebral cortex whereas generalized epileptic form activity is associated with a variety of conditions that increase the excitability of subcortical centres, or wide parts of cortex or both. Special epileptic form activity has a great variety of pathological correlates. Local slow wave is due to damage of white matter of the hemisphere whereas generalized asynchronous slow waves are due to involvement of subcortical white matter than of the cerebral cortex. Bisynchronous slow waves are due to involvement of subcortical and cortical grey matter. Amplitude changes are often due to superficial lesions or decrease of production of electrocortical potentials.

Different types of neurological diseases can cause cerebral lesions. Many diseases causes more than one types of cerebral lesions however not all types of neurological diseases can cause EEG abnormality. In some cases, EEG may show

abnormality without any evidence of diseases. This is because visually the pattern appears to be normal the hidden information is not completely revealed. This has been demonstrated in a previous work in which they showed that even after the epileptic seizure the EEG appears to be normal. However many of the dynamical features are quite different from those prior to seizure (Lalaja et.al.,1987). As such, there is no method to quantify the information content present in EEG. Fourier analysis may appear to be the natural choice. However being a linear method is totally inadequate, since it fails to characterize much of the nonlinear information present in the signal.

4.1.3 Dynamical aspects of EEG

The usual brain mapping scheme such as X ray computer aided tomography (X-ray, CT scan), Positron Emission Tomography (PET) or Magnetic resonance imaging (MRI) maps the blood flow in the brain and not directly the neuronal activity. However; they give information regarding the large time scales. EEG is the only signal that has information regarding large class of time scales. Hence, the EEG study could give greater information regarding the activity in the complex system. Eventhough the present clinical diagnostic value of EEG is low, recent developments in nonlinear dynamics enable one to determine various measures from EEG and can hope to obtain a deeper understanding of hidden information from EEG. In nonlinear dynamics, EEG is considered as a time series. This however represents the entire dynamics of brain. However, a proper functional marker has yet to be developed from EEG. Otherwise the characteristic parameters obtained from nonlinear

dynamical method or any other method would not give a deeper understanding of the brain functioning as compared to that obtained from EEG reading by visual inspection. The problem of fixing a base line (normal) in nonlinear domain is still not solved. This is because the parameters are found to be highly sensitive to psychological state of the subject (Lalaja, 1990) and thus many results obtained are psychologically integrated rather than psychologically invariant.

In linear systems as the frequency content are important spectral measure by Fourier analysis are widely used to study the different rhythms in EEG. In this however, it is also assumed that EEG signals have a random component due to random firing of large number of neurons. An EEG series is usually considered as a linear stochastic process. Based on this assumption standard digital signal processing tools like FFT, autoregressive, and autoregressive moving models are utilized for the analysis of these signals. The brain activity in waking state is desynchronised whereas there occurs partial synchronisation during eyes closed condition. However, during sleep there appear various transitional states. Low amplitude and highly periodic slow wave activity is seen in deep anaesthesia. Spikes and waves are usually associated with epileptic seizure while high alpha activity and increased coherence appear during meditation. The psychotic or mental disorder has not yielded any specific spectral characteristics. The cognitive activities or intensive mental tasks have not produced any discerning patterns in EEG different from background activity with the application of spectral measures (Pradhan, 1999). The broad band nature of EEG found in various states of brain activity does not provide any additional information thus makes it difficult to understand the dynamics of brain in linear

analysis (Jansen & Brandt, 1993). Nevertheless nonlinear dynamical analysis provide information during these activities. A brief review of efforts from the nonlinear point of view in the analysis of brain dynamics is presented in the next section.

4.2 Chaos – Neurons to Brain

Although, a great deal of study has been conducted by observing the spectral properties of the EEG, the dynamical aspects are still not known clearly. The nonlinear dynamical analysis is currently tried in finding these characteristics. A brief review of work on nonlinear dynamical analysis of EEG and brain function is presented here. To understand the brain from EEG from nonlinear dynamical point of view, the methods developed in nonlinear dynamics and deterministic chaos is employed. Several "invariant" parameters have been developed to understand complex system. The parameters like metric dimension, entropy and Lyapunov exponents are commonly suggested parameters of which dimension, especially correlation dimension is widely used. The algorithms for evaluating these parameters are developed for complex systems in general. However, due to limitation in applying these algorithms many of them have been modified. The algorithms and their modifications are presented in the next chapter. Here a brief review on applications of chaos theory from Neurons to Brain is presented.

With the development of nonlinear dynamical methods and theory of deterministic chaos, a great deal of interest has been shown by several investigators to observe chaos from neurons to brain. In neuron dynamics the behaviour of normal

silent neurons can be viewed as a fixed point of a dynamical system (West, 1990). Similarly, the train of periodic pulses can be represented as a limit cycle and irregular behaviour as a chaotic attractor. The first evidence of chaotic behaviour in isolated neuron was observed by Hayashi et al. (1982). This group showed aperiodic behaviour when excited by sinusoidal stimulation. Initially the neuron-produced entrainment with an applied stimulus gradually became aperiodic. Chaotic behaviour is also observed in two types of giant neurons: in the isolated oesophageal ganglion of Onchidium verruculatum and marine pulmonate mollusk (Hayashi et al., 1983, 1987). Chaotic activity is also observed in the interspike interval as well as in the membrane potential under various types of sinusoidal stimulation. The attractor was reconstructed using Poincare map. Many nonlinear features were observed in the giant axon of squid Doryteuthis bleekeri (Aihara et al., 1985).

Many of the above-mentioned experiments require a highly concentrated ionic medium and high forcing sinusoidal stimulus to produce self sustained activity. Further, the neurons are isolated from the body, which is far from the real situation. Matusumoto and co workers (1987) showed for the first time chaotic activity under regular trains of current pulses instead of sinusoidal current. Pulse train also produces chaotic behaviour in the giant axon of squid, immersed in normal seawater (Aihara et. al., 1984). On evaluating the correlation dimension at two different points of axon it has been found the values are 3.2 and 3.4 indicating a stable propagation of this behaviour along the axon. Chaos thus is seen in any information processing. Based on chemical induction (cocaine) L. Stagnalis Holden et. al. (1981) showed the existence of chaotic oscillations in pond snail. They used a high concentration of

aminopyridine on mollusk and found that on prolonged exposition neuron passes through a range of periodic and irregular behaviour in which each state persisted for several minutes. Due to strong nonlinearity, the single cells can exhibit chaotic behaviour. The significance of chaotic behaviour in the functioning of a given cell and its interaction with other cells remains an unsolved problem. Pratap (2000) has made an effort in this direction.

Moving towards practical situation, study of cell assemblies in animals provides an insight into the behaviour of neuron in association with other cells. Rapp and colleagues conducted a correlation dimension analysis (Rapp et al., 1985) of interspike interval of 10 single neurons of which three showed a relatively low fractal dimension (2.2 – 3.5), two gave value between 5 and 7 and the rest behaved randomly. The limitations pointed out are absence of information regarding fast firing neurons and sufficient data length to detect high dimensional chaos. To understand the chaotic activity of brain due to motor activity, Mpitsos and co workers (1988) deafferented the cerebral ganglion in the mollusk Pleurobranchaea californica, a sea slug and observed patterns corresponding to rhythmic motor related activity. They found decrease in autocorrelation function, correlation dimension between 1.75 and 2.5 and positive Lyapunov exponents (0.15 – 0.55 bits /sec). They also did a study to understand the chaotic nature of motor pattern generation considered as an artificial neural network model with one input unit, one output unit and four hidden units. They found this network is capable to distinguish various chaotic signals. Thus, they concluded that the information exchange between various parts of the brain is coded in as various degrees of chaos. Freeman and associates

investigated the perceptive events in the olfactory system of rabbit (Freeman, 1979, 1987) and developed a model of the bulb with nonlinear-coupled ordinary differential equations. The rabbits were trained to respond to two different odors in different ways. After conducting study based on Freeman's model it was concluded that during this process the bulb operates as a global dynamical system. This interpretation is due to the observation of evoked pattern in the whole bulbular surface (Yao & Freeman, 1990).

Another type of activity seen in biological data is the reaction of the system to a learnt odor. In this case, the surface EEG has an almost coherent state that vanishes during expiration (Skarda & Freeman, 1987). The next type of modelled biological activity is that of an epileptic seizure. Based on the model of Freeman it was concluded that during seizure the transmission between the bulb and other parts of the system collapses. The correlation dimension is found to be around 2.76. The recovery from seizure is not yet understood. Roschke and Basar showed in cats that during sleep the auditory cortex, the hippocampus and the reticular formation can be characterized as in a state of hypersynchrony over the whole cortex. Signals in auditory cortex showed the highest correlation dimension followed by those in reticular formation and then in hippocampus. They also suggested the detection of chaotic activity in high frequency window.

Several papers have been presented regarding the dimensional analysis of EEG (Jansen & Brandt, 1993). Many of these investigators used the dimension estimate algorithm of Grassberger and Proccaccia (1983). Babloyantz and their group

72

(1985) presented the first report of estimation of dimension. Later several investigators reported the dimension of EEG, the values ranging from 1 to 8. Though the reliability of these estimates are still on trial, a great promise is seen to apply these concepts for various conditions of brain (Rapp, 2000). The general finding in spite of discrepancy in values are the eyes closed EEG found to be of lower dimension compared to eyes open. During mental task, the dimension value increases. A brief summary of the dependence of dimension of human EEG on various conditions of brain is given Table 4.1. The list is incomplete. However, this gives a clear indication of importance of nonlinear dynamical methods of analysis to various emotional, cognitive, perception, personality, aging and different states of consciousness as also under different pathological states of the subject.

Table 4.1: Dimension value under various conditions of brain

State of the brain	Dimension.
Coma (appalic syndrome)	Decreased compared to wakefulness.
Anaesthesia (with sedatives)	Reduced compared to wakefulness and dreaming.
Sleep	Markedly reduced during deep sleep compared to wakefulness and dreaming.
Menstrual cycle	No difference during different phases of the cycle.
Ageing – 7 years' upto 50 years.	Monotonous increase with age intelligence, increased in intelligent persons when no stimulus presented.
Musically sophisticated versus untalented subjects.	Markedly reduced during regular rhythmical music in subjects preferring simple music.
Focused attention.	Reduced compared to imagery and rest attentiveness.
Creativity	Slightly increased compared to convergent thinking
Positive feelings	Increased compared to negative feelings during rest condition.
Love	Pronouncedly reduced in persons in love compared to persons not in love.
Pain	Reduced during thermic pain compared to control condition.
Smoking	Reduced in smokers after smoking
Clonazepam (antiepileptic)	Increased compared to plecebo
Carbamazepin (antiepileptic)	No change compared to placebo
Parkinson disease	Increased during performance and imagination of complex tasks.
Schizophrenia	Markedly increased in frontal lobe, reduced parietal lobe.
Chronic pain	Increased during imagined pain in pain patients and pain sensitive persons compared to rest condition and healthy persons.

74

Brain is the most complex system in the universe and there is no theory as such that explains the functions of brain. The present scientific theories are based on the few fundamental principles and the phenomenon observed in a few experiments. Some neural models have been proposed to understand the functioning of brain. Physiologists and psychologists apply these models for clinical purposes. Physical scientists on the other hand use these models for solving complex problems with the help of computational network that mimics some of the functions of brain. Work in this direction has led to the development of an interesting computational method called "Artificial Neural Network". This chapter presents a general overview of different neural models that have been applied in Neural network theory.

Nerve cells are the cellular constituents of the brain specialized for rapid intercommunication. On the application of strong stimulus, these nerve cells generate potential pulses with amplitude constant and firing frequency depending upon the stimulus strength. There is immense complexity in neural interconnectivity and the overall system is very complex. There are about 50 neurotransmitters and depending upon the type of receptor proteins embedded in the neural membrane, neurotransmitters and currents either depolarize the membrane so that the neuron is excited or else they hyperpolarise it so that the neuron is inhibited. The common neurotransmitters are acetylcholine and γ- amino-butyric acid. There is a high degree of randomness in neural firing.

75

Hodgkin & Huxley (1952) formulated a mathematical equation based on the observation of generation and propagation of action potential in squid axon. These equations eventhough are very complicated, provide fairly accurate representation of generation and propagation of action potential. The first neural network model was proposed by McCulloch and Pitts (1943). They proposed a network that can perform problems like simple arithmetic, classifying, storing and retrieving finite data set, recursive application of logic rules etc. The neural model consists of a set of binary elements, which are neurons that are either on or off and the output of each neuron depends upon the input in which weights are fixed. Influenced by this model von Neumann developed the first digital computer using the model and logical notation developed by McCulloch & Pitts. Although binary logic was adequate to prove the model proposed by McCulloch & Pitts it was not satisfactory as a brain model. One of the most striking aspects of the nervous system is its ability to perform in the presence of noise with unreliable elements. The nervous system also has the ability to respond to related but differing stimuli and show a degree of tolerance to perturbations of its inputs. All these features are difficult to realize with the binary model. Despite these limitations, McCulloch-Pitts model is important in the sense that it can embody whatever operations and processes those that can be described in logical terms. Winograd & Cowan (1963) constructed a redundant neural network in which they utilized a distributed representation of information. This provides an insight into the functioning of neural networks in the brain even if some of the units are damaged. Eventhough the different brain regions are specialized for different functions, the scale of such a localization of function need not extend down to a single neuron. In short, there is the collective dynamics of neurons that give rise to a

76

specific task. Hebb proposed that the connectivity of the brain is continually changing as an organism learns differing functional tasks, and the cell assemblies are created by such changes. Hebb postulated that repeated activation of one neuron by another, across a particular synapse, increased its conductance to that group of weakly connected cells, if synchronously activated. This would tend to organize into more strongly connected assemblies. The representation of information is distributed. The study of various changes in neuronal activity is called Neurodynamics. Rashevsky and coworkers started the field of Neurodynamics in which they used calculus rather than logic to study neural nets. They represented the activation and propagation in terms of differential equations and tried to make contact with the related applications in the physical problems (Cowan & Sharp; 1988).

Hebb's model triggered the development of adaptive neural networks that can learn to perform specified tasks. Thus, pattern classification and pattern recognition became the central theme for building neural networks. The major approach in pattern recognition problem was the result of Perceptron model. Perceptron model is a modification of McCulloch-Pitts model with modifiable interconnections that can be used to classify certain sets of patterns that are distinct. It consists of a set of 'sensory' units connected to a set of 'motor' units. Initially the weights are set arbitrarily so that stimulation will result in arbitrary output. However, depending upon the process and the error in the output the weights are adjusted to get the desired response. Adaline is a closely related variant of perceptron model. The difference between Adaline and Perceptron lies in the training procedure.

There are several limitations of Perceptron and Adaline models. These models fail to recognize several of the simple patterns like T and C and this is due to the nature of McCulloch-Pitt's neurons. Further, implementing the function ' x or ELSE y' and its negation requires several units. The limitation is overcome with the introduction of modified architecture with 'hidden units'. Though Perceptron or Adaline model with only single layer units is not computationally universal, the problem of assigning credits to the hidden units in multilayer perceptron models is unsolvable. The limitation of single Perceptrons and Adaline models can be overcome with a more complex architecture incorporating hidden units with modifiable connections. The notable feature of the Perceptron is that its memory is distributed and therefore less likely to be disrupted by damage. However, the Perceptron model does not address the associative feature of human brain. Taylor(1964) introduced the neural net with associative memory that is similar to Perceptron model with no hidden units, except that the units are not McCulloch-Pitts units. The net learns to associate different sensory patterns through repeated presentation of pairs of patterns. In Taylor's net associated memory is stored in a distributed fashion. Later Taylor introduced a more elaborate net that is capable of forming associations with paired stimuli in a more reliable and controllable way. A similar net was introduced by Steinbuch that consists of a planar net of switches interposed between arrays of 'sensory' receptors and 'motor' effectors. This scheme is called Learning Matrix. Learning matrices have a simple mathematical structure and their performances can be readily analyzed. Several network models with associative property have been proposed following the work of Steinbuch. Marr (1969) proposed a theory that explains the function of cerebellum in animals to make

78

delicate and precise voluntary movements and the mechanism of temporary storage of memory in hippocampus. Marr's theory is interesting as it assigns specific function to each neuron in a part of the brain.

Most noteworthy among all these models are that proposed by Anderson and Cooper (1978). Eventhough the functions of individual neurons in many parts of the brain have been well understood the manner in which large interconnecting network of neurons produce mental activity by collective process that is not well understood. This is true especially when one tries to understand the activity of single cells its role in higher cortical function or to localize any region of the nervous system in which the memory is stored. A basic problem in understanding the organization of memory in biological system is to understand the vast information storage and retrieval mechanism of a system composed of vulnerable and relatively unreliable elements. The problem of distribution of memory over a large number of cells has been addressed in Anderson & Cooper's model.

Anderson and Cooper introduced a class of neural models for the acquisition and storage of distributed memories that display features such as recognition, association, generalization and some of the features of mental behaviour associated with animal memory. It has been suggested that much of the learning and resulting organization of the central nervous system occurs through some kind of modification of the efficacy or strength of at least some of the synapses, thus altering the relation between presynaptic and post synaptic potentials. A small but coherent modification of large number of synaptic junctions can result in distributed memories. The

79

neurons of the primary sensory areas display various forms of stimulus selectivity, i.e.: they may respond preferentially to a tone of a given frequency, a light spot of a given color, a light bar of certain orientations etc. Thus, stimulus selectivity is considered as the general property of sensory neurons and conjecture that development of such selectivity obeys some general rule.

In a distributed memory the simultaneous or near simultaneous activities of many different neurons are considered. A large spatially distributed pattern of neuron discharges, each of which might not be very far from spontaneous activity, could remain important even if this is hard to detect.

In developing the model Anderson and Cooper considered N neurons 1,2,.....,N each of which has some spontaneous firing rate r_j^0. Then a vector has been defined whose component are the difference between the actual firing rate r_j of the jth neuron and the spontaneous firing rate r_j^0. Thus

$$f_j = r_j - r_j^0 \qquad (5.1)$$

Two such banks of neurons are connected to one another by replacing the multiplicity of synapses between axons and dendrites by a single ideal junction. This summarizes logically the effect of all the synaptic contacts between the incoming axon branches from neuron j in the F bank and the dendrites of the outgoing neuron i in the G bank neurons. F is concerned with incoming signals and G with responses.

Although the firing rate of a neuron depends in a complex and nonlinear fashion on the presynaptic potentials, there is usually a reasonably well defined linear region. The firing rate g_i of neuron i in G is mapped from the firing rates of all the neurons f_j in F by

$$g_i = \sum_{j=1}^{N} A_{ij} f_j \qquad (5.2)$$

The neural activity f in the F space is mapped into the neural activity g in the G space and this can be written in a compact form as

$$g = Af \qquad (5.3)$$

where A is a matrix with elements A_{ij}.

Thus it is in modifiable mapping of the type A that the experience and memory of the system are stored. In contrast to machine memory, which is local, the animal memory is likely to be distributed and addressable by content or by association. It is convenient to write the mapping A as

$$A = \sum_{\mu\nu} C_{\mu\nu} g^{\mu} \times f^{\nu} \qquad (5.4)$$

Parikh and Pratap (1984) developed an evolutionary model in the framework of nonequilibrium statistical mechanics as developed by Brussel School. In

81

developing the model, they followed the Anderson and Cooper's method to simulate the memory effects. Consider a network of N neurons that are all linked to each other. In the absence of input, the neurons have a certain amount of spontaneous activity, which is described by the firing frequencies r_j^0. The firing frequency is random in time and r_j^0 is considered as random variable having a distribution around the time-averaged mean. The difference between the actual firing rate r_j and the spontaneous firing rates r_j^0 is represented as

$$h_j^0 = r_j - r_j^0 \qquad (5.5)$$

The same stimulus can lead to firing patterns that vary from trial to trial, but the average of the firing rates is roughly constant. Therefore, the frequencies h_j^0 are also random variables distributed about appropriate mean values. In order to simulate the memory effects consider the time interval $-\infty$ to 0 (at instants $\beta_1, \beta_2, \ldots\ldots, \beta_K$) there have been K experiences and associated correlations, defined by certain input and output firing rates. Denoting input and output firing rates as f_j^ν and g_i^μ respectively, where ν and μ take values from 1 to K and i, j=1,....,N neurons for all the past K events. Here f_j^ν are the afferent frequencies of the νth species at the instant j and g_i^μ is the efferent one. By defining the state of the neural network at t=0 by a distribution function $\rho\left(\left\{g_i^\mu\right\}, \left\{f_j^\nu\right\}, \left\{h_j^0\right\}, t = 0\right)$. The problem is to obtain the distribution function $\rho\left(\left\{g_i\right\}, t\right)$. If $G\left(\left\{g_\alpha\right\}\middle|\left\{g_i^\mu\right\}, \left\{f_j^\nu\right\}, \left\{h_j^0\right\}, t - \tau\right)$ is defined as a transition

probability, which takes the state at t-τ to t, then one can obtain $\rho\left(\{g_i\}, t\right)$ by writing an evolution equation as

$$\rho\left(\{g_\alpha\}, t\right) = \int_0^t \int d\{g_i^\mu\} \int d\{f_j^\nu\} \int d\{h_j^0\} G\left(\{g_\alpha\}\big|\{g_i^\mu\}, \{f_j^\nu\}, \{h_j^0\}, t - \tau\right)$$
$$\times \rho\left(\{g_i^\mu\}, \{f_j^\nu\}, \{h_j^0\}, \tau\right) d\tau \tag{5.6}$$

It may be noted that the time appears in the transition probability as t-τ and Eq. (5.6) is non Markovian in nature.

In this equation, G is the kernel in the integral equation. This kernel G maps the input stimulus at t=0 into an output at t>0. Different hypothesis about the synaptic changes would lead to different forms for G.

The evolutionary model proposed by Parikh and Pratap became the starting point of developing a nonlinear nonequilibrium model of Neurodynamics. As the equation is non Marckovian in nature, it takes into account all the past experiences in predicting the future. This would also mean that all the time scales play a very significant role in the dynamics. The time scales that could exist in a neural system are discussed in chapter 7. Again a new parameter called "concept" has been introduced. Thus the "concept" is "learnt" if the set of output firing rates approaches a characteristic set of numbers on repeated input of the same type. This model is a general evolutionary model of a distributed memory with the "Kernel" in the equation simulates the changes in the synaptic behaviour produced by external stimuli.

83

SYNCHRONIZATION PHENOMENON IN INTREACTING SYSTEMS

The characterization of systems from time series using the nonlinear dynamical methods employs a notion of phase space and different parameters derived from this space. Eventhough this method is powerful in understanding the temporal evolution of a system, an effort has also been made to understand the spatio-temporal dynamics. In this however, the time series is reconstructed using not only the temporal variables but also spatial co-ordinates. This is found not suitable for understanding the dynamics of complex systems. To understand such systems it is essential to know the dynamics of subsystems or *interactions* among subsystems. Recently developed methods of understanding the interactions between subsystems include phase synchronization method proposed by Kurth's group (Rosenblum et al., 1996), methods of False neighbors and other related methods to study the synchronization of chaotic oscillators. It has been found these parameters and methods have applications in various branches of science and engineering. The notion of synchronization and phase is quite different from classical definitions. Mathematical modeling and simulation as an appropriate tool to uncover the mechanisms of coordination in physiological systems is difficult, since one cannot have control on the various parameters. However, a qualitative knowledge of collective dynamics of the system can be made from the study of time series that is being generated. Hence, it would be worthwhile to discuss this newly developed concept in detail.

6.1 Phase Synchronization Using Hilbert Transform

Synchronization, which is a basic phenomenon in physics, has been defined in classical sense, as adjustment of frequencies or phases of periodic oscillators due to weak interactions. This notion of phase synchronization has been applied to chaotic systems also. Nevertheless, one needs a clear definition of phase in such systems. Due to interaction of two or large number of chaotic sub systems, states of systems can coincide while the dynamics in time can remain chaotic. In phase synchronization method, the importance is given to phase locking without giving much importance to amplitude. An ideal case would have been to study the coherence i.e., phase as well as amplitude synchronization. Since this method is developed for chaotic systems where the amplitude is chaotic, phase synchronization is defined as appearance of certain relation *between the phases of interacting sub systems*.

It has already been mentioned that in this domain the phase has to be defined clearly. In the case of periodic oscillators, the dynamics of stable periodic oscillations are represented by a stable limit cycle in phase space. Thus the phase can be defined as

$$\frac{d\phi}{dt} = \omega_0 \tag{6.1}$$

where $\omega_0 = 2\pi/T_0$, T_0 being the period of oscillations. When a small periodic force with frequency Ω is acting on periodic oscillations the phase is obtained as

$$\frac{d\phi}{dt} = \omega_0 + G(\phi, \psi) \qquad (6.2)$$

where

$$\frac{d\psi}{dt} = \Omega \qquad (6.3)$$

$G(.)$ is 2π periodic in both arguments.

Here the phase corresponds to zero Lyapunov exponents while amplitude corresponds to negative exponents. When two periodic oscillators interact the synchronization can be defined as

$$\left| n\phi(t) - m\psi(t) \right| < Constant \qquad (6.4)$$

or weaker condition of frequency is

$$\omega = \left\langle \frac{d\phi}{dt} \right\rangle = \frac{m}{n}\Omega \qquad (6.5)$$

where n and m are integers and $\langle \ \rangle$ denote the average. In the presence of small noise there occurs phase slips whereas in the presence of large noise the above mentioned properties are destroyed.

In the case of chaotic system, it is not possible to give a general definition of phase. Pikovosky et al. (1997) considered three definition of phase.

(a) The phase is defined by considering a projection of attractors in the (x,y) plane and finding the smeared limit cycle around the origin or some point which can be considered as the origin and attributing to each rotation. It is defined as

$$\phi_n = 2\pi \frac{t - t_n}{t_{n+1} - t_n} + 2\pi n \qquad t_n \le t < t_{n+1} \qquad (6.6)$$

where t_n is the time of the nth crossing of the secant surface. This definition coincides with the definition of phase in the case of periodic oscillators. From nonlinear dynamical point of view, this definition of phase corresponds to the direction in phase space with zero Lyapunov exponents. The problem of this method is to find a proper Poincare surface and hence this method is difficult for experimental signals.

(b) The second definition however uses the same concept as previous one but the phase is defined as the angle between the projection of phase point on the plane and a given direction on the plane. Thus phase

$$\phi_p = \arctan\left(\frac{y}{x}\right) \qquad (6.7)$$

where x and y are the coordinates corresponding to x-axis and y-axis respectively. This also has same drawback as the previous one. Further, the above ϕ_n and ϕ_p do not coincide on a time scale less than the average period of oscillations.

(c) The above mentioned definitions require a reconstruction of attractors in phase space and finding an appropriate projection. This in fact is difficult for experimental signals with a small amount of noise. The third definition of phase uses a different concept such as analytical signal processing. In this approach the instantaneous value of phase and amplitude for an arbitrary signal s(t) is calculated by defining a complex analytic signal Ψ(t) as

$$\psi(t) = s(t) + i\tilde{s}(t) \tag{6.8}$$

where $\tilde{s}(t)$ is the Hilbert transform of s(t).

$$\tilde{s}(t) = P.V \frac{1}{\pi} \int_{-\infty}^{\infty} \frac{s(\tau)}{t - \tau} d\tau \tag{6.9}$$

where P.V stands for principal value in the Cauchy sense.

Thus, amplitude and phase of an arbitrary signal is uniquely defined. The Hilbert transform $\tilde{s}(t)$ of s(t) can be considered as a Fourier convolution of s(t) and $1/\pi t$. Hence Fourier transform $\tilde{S}(\omega)$ of $\tilde{s}(t)$ is the product of Fourier transform of s(t) and $1/\pi t$. The instantaneous frequency ω (t) may have negative values as it is the rate of change of ϕ (t) and these values are neglected to have only positive frequencies that are meaningful. Hence for a physically relevant frequency

$$\tilde{S}(i\omega) = -iS(i\omega) \tag{6.10}$$

This can be obtained by passing the signal s(t) through a filter whose amplitude response is unity and phase response is constant with $\pi/2$ lag at all frequencies. Although the method using Hilbert transform defines phase of a signal, its validity on the definition of phase of a dynamical system is questionable. However, an important advantage of analytical signal concept is that the phase can be easily obtained from the measured scalar time series.

The above three definitions of phase have been applied to some of the standard chaotic oscillators. As there is no unique definition of phase, the phase is defined here is in a reasonable and consistent way.

The experimental evidence for phase synchronization is given by Parlitz et. al. (1996). They showed the experimental evidence of phase synchronization in two unidirectionally coupled Rossler systems implemented on an analog computer. For irregular, nonstationary and noisy bivariate data a new method in the framework of phase synchronization has been developed by Tass et.al.(1998). This method is used to detect alternating epochs of phase locking from nonstationary data thereby extracting information regarding the interdependence of weakly interacting systems. This method is used to understand the part of the nervous system involved in the tremor muscle activity of Parkinson's disease. The synchronization between the activity of remote brain areas in humans and the muscle activity is understood by means of noninvasive measurement. Based on the work of Stratonovich (1963), the synchronization of noisy system is viewed as appearance of peaks in the distribution of the cyclic relative phase. Strong noise can cause phase slips; hence phase

synchronization is considered only in a statistical sense. Phase synchronization is not equivalent to correlation. However it reveals the different characteristics of the system interdependence.

The information regarding the phase synchronization is extracted from bivariate data by computing phase of each data set $\phi_1(t)$ and $\phi_2(t)$ by Hilbert transform. Because of phase fluctuations and slips due to noise, the histogram of relative phase distribution, $\psi_{n,m}$, is plotted. The $\psi_{n,m}$ is obtained as

$$\psi_{n,m}(t) = n\,\phi_1(t) - m\,\phi_2(t) \tag{6.11}$$

The deviation of this relative phase $\psi_{n,m}$ from a uniform one is quantified by defining two measures called n: m synchronization indices. In the first measure, the synchronization index is found based on the Shannon entropy.

$$S = -\sum_{k=1}^{N_b} p_k \ln p_k \tag{6.12}$$

where N_b is the number of bins and p_k is the probability of finding points in the kth bin.

Synchronization index is then defined as

$$\rho_{nm} = \frac{S_{max} - S}{S_{max}} \tag{6.13}$$

where n:m is the phase locking ratio and $S_{max}= \ln N_b$. $\rho_{nm}=0$ corresponds to uniform distribution which represents zero synchronization and $\rho_{nm}=1$ correspond to Dirac like distribution representing perfect synchronization.

In the second measure, an index based on conditional probability has been defined. In this each interval is divided into N_b bins, Then for each bin k,

$$1 \leq k \leq N_b$$

$$r_k(t_j) = M_k^{-1} \sum e^{i\phi_2(t_j)}$$
(6.14)

for all j, such that $\phi_1(t_j)$ belongs to k^{th} bin is evaluated. If there is complete dependence between the two phases, then $\left| r_k(t_j) \right| = 1$ while it is 0, when there is no dependence.

These two measures quantify the degree of co ordination of different signals. This has been applied effectively to study the heart beat and respiratory dynamics (Rosenblum et.al.,1998) as well as to study co ordination of brain regions with muscle activity (Tass et.al., 1998).

6.2 Method of False Nearest Neighbors

Earlier to the method proposed by Rosenblum, Abarbanel and his group proposed another method of chaotic synchronization (Rulkov et al, 1995) in which they considered a unidirectionally coupled system. The system consists of an

autonomous driving system and a response system in which the driving system does not depends on the parameters of the response system. In this interacting system, there exists a relation between the variables of the driving system d(t) and the variables of the response system r(t). During synchronization the transformation can be represented as

$$r(t) = \psi(d(t)) \qquad\qquad (6.15)$$

In simple cases, the transformation will be a straight line in x-y plane. If the transformation is complex, the projection will be a complicated geometrical object. In this case the method that gives the information regarding this transformation is the projection of attractors of driving and response system that identifies mutual false nearest neighbors. This type of synchronization is called Generalized Synchronization (GS). If a synchronization relation mentioned above exists the chaotic attractor of the response r(t) has a relation to chaotic attractor of the driving system attractor d(t). This relation can be found out by looking for a geometric connection between the driving and response system that preserves the identity of neighborhoods in the state space.

Consider a set of points X(i) and Y(i) in state space of the driving and response system respectively. Select an arbitrary point in the driving system X_n in the phase space of the driving system. Let there exist generalized synchronization condition (6.14). Suppose the nearest phase space of this point has a time index n_{NND}, then the point Y_n in the space of the response system will have point Yn_{NND} a close

neighbor as long as there exists relation between the driving and response systems. Next step is to find a parameter that relates the driving and response system that preserves the identity of neighborhoods in the space. This is a kind of correlation between observed dynamic variables, one from the driving system and one from the response system. If the distance between two nearest neighbors are small then

$$Yn - Yn_{NND} = \phi(Xn) - \phi(X_{NND}) \approx D\phi(Xn)(Xn - Xn_{NND}) \qquad (6.16)$$

where $D\phi(Xn)$ is the Jacobian matrix of transformation evaluated at location Xn. Similarly find the time index corresponding to response vector Yn and locate its nearest neighbor Yn_{NNR} which comes at time index n_{NNR}. Since there exists a relation as given in Eq.(6.15)

$$Yn - Yn_{NNR} = \phi(Xn) - \phi(X_{NNR}) \approx D\phi(Xn)(Xn - Xn_{NNR}) \qquad (6.17)$$

Thus the parameter, Mutual False Nearest Neighbors (MFNN) is evaluated as

$$MFNN = \frac{|Yn - Yn_{NND}|}{|Xn - Xn_{NND}|} \frac{|Xn - Xn_{NNR}|}{|Yn - Yn_{NNR}|} \qquad (6.18)$$

In experiments, this parameter is evaluated from time series by reconstructing the attractor using time delay embedding with time lag from average mutual information. When the driving and response systems are synchronized, MFNN should be unity at all points. Usually modified MFNN parameter is found as it is very much suitable for

93

experimental signals. In this, the response time series is embedded in the space R_E of

dimension d_r, which is then fixed. This dimension d_r must not be less than the

minimum dimension necessary to unfold the attractor corresponding to the response

time series. All distance will be computed in this space. d_d is a variable greater than

the embedding dimension of the driver attractor. For each d_d select an index n and

find its nearest neighbor of point d(n), which comes at time index n_{NND}. Find the

nearest neighbor $r(n_{NNR})$ of point r(n) in the response embedding space. Then a ratio

is formed as

$$\frac{\left| r(n) - r(n_{NND}) \right|^2}{\left| r(n) - r(n_{NNR}) \right|^2} \tag{6.19}$$

To compensate for the increase of MFNN parameter in high dimensions due to the

sparseness of the phase space population, the above expression is divided by the

same parameter computed for the driving system. Thus, the modified MFNN is

obtained as

$$P(n, d_r, d_d) = \frac{\left| d'(n) - d'(n_{NNR'}) \right|}{\left| d'(n) - d'(n_{NND}) \right|} \frac{\left| r(n) - r(n_{NND}) \right|}{\left| r(n) - r(n_{NNR}) \right|} \tag{6.20}$$

where d' are vectors of the driving time series embedded in the space dimension d_r

and d' ($n_{NND'}$) is the nearest neighbor of point d'(n) in this d_r dimensional space. This

parameter should on the average be of order unity for synchronized trajectories and

this parameter is greater than unity for unsynchronized trajectory. During onset of

synchronization, the ideal method is to examine the statistical distribution of MFNN. By constructing a histogram of a set of MFNN parameters one can obtain the reliable information about the system. However, to reduce the computation an average of MFNN parameter can also be employed for studying the synchronization phenomenon in systems.

6.3 Phase Definition using Poincare map

The definition of phase from Hilbert Transform takes into account only the observation that the phase changes linearly with the time. However for a system with high degree of nonlinearity and stochasticity there can be intrinsic oscillations of phase and this is not taken into account.

Hence, a new method has been introduced in which the information regarding the phase is obtained from Poincare map. In this the signal is reconstructed in a two-dimensional map with x(n) on the X-axis and x(n+T) on the Y-axis. A vector is defined connecting the coordinates $[x(n),x(n+T_d)]$ and $[x(m), x(m+T_d)]$. The time lag T_d required for reconstruction is obtained from Average mutual information criteria. The amplitude and phase is defined as

$$A = [x_m\text{-}x_n]^2 + [x_{m+T} - x_{n+T}]^2 \qquad (6.21)$$

$$\phi = arctan \frac{x_{m+T} - x_{n+T}}{x_m - x_n} \qquad (6.22)$$

Here the amplitude refers to the length of the vector in the Poincare map. In this method m determines the *length scale* at which the phenomenon is to be observed. The choice of m depends upon the degree of noise as well as the time scales involved in the process. For a noise free system m can be selected as $n+T_j$ with $T_j=1$ whereas for a noisy system m should be selected as $n+T_d$. Further as the signal is reconstructed in Poincare space, all nonlinearity and intrinsic dynamics are included. The results of phase from Poinacare map and its relevance on real data set is presented in results and discussion of chapter 10.

6.4 Coherence Index

Coherence is another phenomenon that can characterize the dynamics of a system. In this, the distribution of amplitude and phase from a single variable time series is considered and the coherence index is defined from the histogram of amplitude and phase. The motivation behind this methodology is based on the work of Lanczos and Gellai (1975). In this, these authors studied the amplitude – phase plot (similar to polar plot) of a set of data obtained from the Fourier transform of the random numbers. They erected a set of random numbers as ordinates in a Cartesian coordinate system, at equidistant points on the abscissa in the interval $(-\pi, +\pi)$. The numbers $y_0, y_1, y_2, \ldots\ldots\ldots, y_{2n-1}$ can then be written as a finite Fourier series as

$$ y_j = \frac{a_0}{2} + \sum_{k=1}^{n} \left[a_k \cos\left(\frac{\pi j k}{n}\right) + b_k \sin\left(\frac{\pi j k}{n}\right) \right] $$

$$= \frac{a_0}{2} + \sum_{k=1}^{n} C_k \cos\left(\frac{\pi jk}{n} - \Theta_k\right)$$

$j=0,1,\ldots\ldots,2n\text{-}1$ and $k=1,2,\ldots\ldots\ldots n$ (6.23)

where a_k, b_k as well as C_k, Θ_k are all random variables. a_k, b_k as well as C_k, Θ_k are all determined in the usual manner and the relations of C_k, Θ_k with a_k, b_k are the usual ones viz.,

$$C_k = \left[a_k^2 + b_k^2\right]^{\frac{1}{2}} \quad \text{and} \quad \Theta_k = \arctan\left(\frac{b_k}{a_k}\right) \qquad (6.24)$$

It has been observed that a plot of these vectors show bunching in the unit circle. If the original data set were strictly random then the vector distribution in the unit circle would have been uniform. On the other hand bunching of vectors would indicate the presence of an attractor. This implies that one can write a given series as a sum of two or more distinctly different Fourier series. This can also be interpreted as that the given series can be decomposed into two or more series having different fundamental frequencies or different time scales. Hence, for a system with multiple time scales information regarding this can be obtained from plotting the circular plot as suggested by Lancos and Gellai. The presence of chaos is an adequate evidence for incompatible frequencies. Based on the above theoretical formulation one can define an index incorporating both amplitude and phase coherence. For this phase and amplitude is evaluated from Poincare map from the Eq. (6.21) and Eq. (6.22). In evaluating the phases one has to take into account the sign of the numerator and the

denominator to determine the quadrant in which the vector is situated. From the phase and amplitude values histograms are drawn for amplitude and phase distribution respectively. Based on the Shannon entropy (Tass et.al.,1998) the distribution is quantified as

$$S = -\sum_{k=1}^{N_b} p_k \ln p_k \qquad (6.25)$$

where p_k is the distribution in the kth bin and N_b is the total number of bins. For normalizing this term S_{max} is defined as

$$S_{max} = \ln N_b \qquad (6.26)$$

Then the amplitude coherence is defined as

$$\rho_a = \frac{S_{max,amp} - S_{amp}}{S_{max,amp}} \qquad (6.27)$$

and in a similar manner phase coherence is defined as

$$\rho_p = \frac{S_{max,ph} - S_{ph}}{S_{max,ph}} \qquad (6.28)$$

These definitions are however different from those of Tass et.al.(1998). In that the histogram is plotted for a relative phase distribution of a bivariate data where as in

98

this method a single time series is considered. The Coherence index is defined as the

harmonic mean of phase and amplitude coherence as

$$C_i = \frac{2\rho_a \rho_p}{\rho_a + \rho_p} \hspace{4cm} (6.29)$$

Since this is defined for a single time series characterizing the attractor this can be

used for the characterization of the attractor along with other measures like attractor

basin, embedding dimension, generalized attractor dimension, generalized

dimension, entropy, Lyapunov exponents etc. Instead of considering the distribution

of phase from a single time series a similar measure can be derived from the

histogram of relative phase / amplitude distribution from bivariate data and they are

called Phase synchronization index, Amplitude synchronization index and

Synchronization Coherence index respectively. The Phase synchronization index has

been derived by Tass et al. (1998), however two more new parameters are introduced

considering the relative amplitude of the vectors in the Poincare map.

TIME SCALES IN NEURAL SYSTEM

In understanding the collective dynamics of a nonlinear, nonequilibrium system it is essential to know the various time scales involved in the process. Many investigators in the study of complex systems have ignored the role of time scales. Prigogine (1962) has introduced the concept of time scales in the dynamics of a system in developing a theory of nonequilibrium statistical mechanics. Later Balescu (1975) has stressed its significance in the dynamics of a nonequilibrium system. Eventhough several physical and chemical systems have been studied in this framework, it was Pratap who formulated for the first time the time scales in neural system. In this chapter the significance of time scales in nonlinear time series analysis of EEG has been studied in the theoretical framework of collective dynamics. The derivation of different time scales and its role in neural dynamics have also been discussed in this chapter.

The understanding of dynamics of brain from the EEG recorded from the scalp is an active area of research in nonlinear time series analysis. EEG is recordings of electric potentials generated in the cerebral cortex by a large number of neurons and are generally classified, based on frequencies as alpha (8 to 13Hz), beta (more than 13 Hz), theta (4 to 8Hz) and delta (less than 4Hz). The action potentials generated by neurons are *integrated* at various stages of its propagation from the input point to the central nervous system and back to the action muscle. These

generate collective modes, which in the cortex are recorded as EEG on the scalp. It has been pointed out that the amplitude of the action potential generated by the individual neuron is constant while the firing frequency is a *linear* function, as far as measurements go, of the applied stimulus strength. A simple addition of these amplitudes however cannot reproduce the observed characteristics of EEG. Hence the integration process should be an involved mechanism. Further it has been found that the electrical characteristics of the action potential are quite different from those of EEG. The characteristic time scales of different waves of EEG is of the order of 0.1 second where as that of the action potential is ~ 1 milliseconds. A factor of hundred between two time scales implies that the human brain has a wide range of time scales resulting in being highly nonlinear and that it is thermodynamically open with feedback and feed forward processes. Hence the construction of general time scale starts with identifying different characteristic parameters in neuron dynamics.

The human brain consists of about 10^{10} neurons of which about 1 to 2% is active and they are connected in a certain pattern. These connections change with the input signals. Hence to study the collective effects in the cortex one has to take into account the dynamics of the individual neuron, which contribute towards the collective effects. The most significant feature in the neuron dynamics is the firing potential, ϕ which is the basic unit of information transmitted along the nerve fiber. In the neural firings a potential change is generated due to changes in Sodium and Potassium ion conductance across the membrane of an axon. This is highly nonlinear, which is however a single neuron process. It is known that there exists a resting potential −80 mV and a threshold potential −50 mV. If the potential

differences across a membrane are less than 50 mV there is no firing. But if it is greater than the threshold value, a firing takes place, and the peak potential of this is about 40 mV. Thus each firing has amplitude of about 100 mV and one of the most significant features of this is that the amplitude of this firing is independent of the strength of the stimulus. Furthermore the firing as it proceeds along the length of the axon does not get attenuated. The fact that the signal intensity is not attenuated as it travels from one point to another both spatial and temporal indicate that the generation process is essentially nonlinear and nonequilibrium in nature. Further the system is thermodynamically open; hence feedback and feedforward mechanisms are operative. Thus the process is distinctly different from the usual electrical conduction in a cable. Here the firing takes place at the various nodes of Ranvier in a sequential manner. The velocity of propagation forms another important parameter in the neuron dynamics. The electrical signals propagated along the length of the axon has a finite measurable speed and is about 100 m/sec. Besides the velocity of propagation which is the rate of travel of the nerve impulses is also constant. It is worth mentioning that this is much less than the speed of light, which is taken as the interaction speed in electrodynamics. Next is the firing frequency, which is the inverse of the *refractory time*. It is usually about 1000 Hz and is inversely dependent on the stimulus strength. If two successive stimuli separated by a certain time interval are applied to the nerve fiber, the behaviour of the fiber will depend on the refractory time. Immediately after a nerve impulse has been initiated, the given part of the fiber is in the absolute refractory state, i.e. it cannot be excited again. This is followed by a relative refractory state in which the threshold potential is somewhat increased. Hence at a given instant, one can classify neurons on the basis of the

refractory time. The same neuron can have different refractory times at different instants, but they all have a greatest lower bound. Hence the number of neurons firing with a specified refractory time is time dependent. The duration of the entire refractory time varies from one to a few milliseconds. Since the firing potential is electrical in nature, they are generated by the various ions such as sodium, potassium, calcium etc., and these are characterized by the electrical charge (e) and ion mass (m). The movement of charge that flows between two consecutive nodes of ranvier is represented as axon current. This consists of two parts, a displacement current component through the membrane capacity and an ion current through the membrane. A signal received by one nerve or a group of nerves will be communicated to a large number of nerves by a cascading process, through axonal tree, the branches of which end in synapses connecting them with other cell bodies and dendrites. This cascade process however will not connect all neurons in the system but will end up with the distribution of regular tubes and stripes. Hence one can define a number density (n) that represents the number of neurons per unit volume. This can also be defined as the fraction of affected neurons to total neurons in a unit volume. The chemical processes also play a significant role in the signal transmission by changing the conductivity of the medium. This is included by a nondimensional parameter, ε_o representing the conductivity. These parameters along with the numerical values are given in Table 7.1.

Table 7.1: Different parameters used in the construction of general time scale

Name	Symbol	Dimension	Order of magnitude
Action potential	ϕ	$(MLT^{-2})^{1/2}$	10^{-1} volts
Propagation speed	V	LT^{-1}	100 m/seconds
Firing frequency	ν	T^{-1}	1000 Hz
Ionic charge	q	$(ML^3 T^{-2})^{1/2}$	1.6×10^{-19} Coulomb
Ionic mass	m	M	10^{-27} Kg
Ionic density	n	L^{-3}	2mM
Medium effect	ε_o	-	-
Ion plasma frequency square	$\omega_p{}^2$	T^{-2}	$10^3 z \mu^{-1/2} n^{1/2}$ rad /sec

Using these parameters, a dimensional analysis following Balescu (1975) has been performed to obtain the general time scale as.

$$T = \phi^i V^j e^k \nu^p m^q n^r$$

$$= (MLT^{-2})^{i/2} (LT^{-1})^j (ML^3 T^{-2})^{k/2} (T^{-p}) (M^q) (L^{-3r}). \qquad (7.1)$$

Equating powers of M, L and T on both sides we have

$$i/2 + k/2 + q = 0 \qquad \text{(power of M)} \qquad (7.2)$$

$$i/2 + j + (3/2)k - 3r = 0 \qquad \text{(Power of L)} \qquad (7.3)$$

$$-i - j - k - p = 1 \qquad \text{(power of T)} \qquad (7.4)$$

There are only three equations with six unknowns, so expressing p, q and r in terms of i, j and k as

$$p = -i - j - k - 1 \tag{7.5}$$

$$q = -i/2 - k/2 \tag{7.6}$$

$$r = (-3/2)i + (1/3)j + (1/2)k \tag{7.7}$$

Substituting (7.5), (7.6) and (7.7) in (7.1) a general time scale is obtained as

$$T = \Gamma v^{-1} \tag{7.8}$$

where Γ is a dimensionless quantity defined as

$$\Gamma = (\phi^2 n^{1/3} / mv^2)^{i/2} (V n^{1/3} / v)^j (\varepsilon_0 e^2 n / mv^2)^{k/2} \tag{7.9}$$

Expressing $i/2 = x$, $j = y$ and $k/2 = z$ as these parameters are real numbers the dimensionless constant Γ becomes

$$\Gamma = (\phi^2 n^{1/3} / mv^2)^x (V n^{1/3} / v)^y (\varepsilon_0 e^2 n / mv^2)^z \tag{7.10}$$

Thus a general time scale T is obtained as

$$T = \Gamma v^{-1} = a^x b^y c^z \quad (\text{ say }) \tag{7.11}$$

The dimensionless quantity consists of three parts, the first one depends on the electrodynamic variable ϕ besides the dynamic variable firing frequency. This is the resistance per unit length per unit time. The second term consists of only mechanical

105

variables and is the ratio of the distance traveled by the signal during a refractory period to a characteristic length defined by $n^{1/3}$. In the third term however one can write ($\varepsilon_o\, e^2\, n\, /mv^2$) as ($\varepsilon_o\, \omega_p^2\, /v^2$) with ω_p as the ion plasma frequency. The third term is the ratio of the square of the plasma frequency to the firing frequency and this characterizes the collective behaviour.

In summary (7.11) consists:

 a: ratio of electric frequency to firing frequency.

 b: ratio of mechanical frequency to firing frequency.

 c: ratio of plasma frequency to firing frequency.

The x, y and z are natural numbers. It could be real or complex, rational or irrational or integers. If they are complex, the process could have an amplitude and phase. If they are rational, the frequencies are compatible while if the frequencies are irrational, they are incommensurate. From (7.11) it is very clear that there exists three fold infinite time scales in the system. This point is very important in the analysis of EEG signals. Further, this clearly shows that the electrical, mechanical and plasma frequencies can be independent. However they can also get coupled by the choice of x, y and z. By proper choice of variables x, y and z some of the known relevant time scales can be obtained and they are derived below.

1). Sodium Potassium pump: The sodium potassium pump depends on the threshold potential and hence on ϕ. Since it is a chemical process depending on the number of sodium ions going in and potassium ions coming out during depolarization phases, the time scale should depend on mass and number density, but not on the firing frequency. To get relevant time scale corresponding to this process, one must choose

y = z = 0 and x = -1/2. Thus relevant time scale for this process is with $\phi \sim$ millivolts and n ~ 100

$$Tp = (m / \phi^2 n^{1/3}) \sim 10^{-7} \tag{7.12}$$

2.) *Synaptic transduction*: In the synaptic transduction, the process depend on the dielectric characteristics of the synaptic cleft as also on the speed at which the signal arrive at the pre synapse as well as the threshold potential. However, there is no explicit dependence on the number density, since there is randomness in the injection of neurotransmitters in the cleft due to the discharge of vesicles. A time scale is constructed by a proper choice of x, y, z viz. x= -y = z = -1/2. Thus the time scale is obtained as

$$Ts = (mV \, v / \varepsilon_0 \, \phi^2 \, \omega_p^2)^{1/2} \tag{7.13}$$

3.) *Collective modes*: At various stages in a neural system, there are integration processes operative. The threshold potential is a consequence of the integration process. In a single neuron or in the case of synaptic transduction the process is always collective in nature. Also in the case of EEG signals, the process is indeed a collective one which do not exhibit all the apparent regularities seen in a single neuron firing sequences or the signal transmission from a pre synapse to a post synapse. If we consider this as a self-consistent process, which is in general responsible for the collective modes, then the relevant time scale is the interaction time scale,

$$Ti = (\varepsilon_0 \, \omega_p^2)^{-1/2} \tag{7.14}$$

.and, this is obtained by setting x = y = 0 and z = -1/2.

Thus different time scales suitable for different mechanism could be derived from the general time scale. There may be other relevant parameters, however in this formulation only some of the known ones is considered. In the absence of an understanding of neuronal activities one cannot stipulate the domain of x, y and z. Hence, by substituting values of x, y and z arbitrarily a few more time scales are derived and are presented in Table 7.2. It is evident from the table that there exists a large class of time scales with a wide range of magnitude. The different values of ionic density would give different values of x, y and z. However, in this construction the ionic density is taken as 10^6 m^3.

Table 7.2: Time scales

Name	X	y	Z	Time scale	Order of magnitude
Mechanical	0	−1	0	$(V n^{1/3})^{1/3}$	10^{-4}
Refractory	0	0	0	v^{-1}	10^{-3}
Electromechanical	1/4	−1/2	−1/4	$(\phi/Vevn^{2/3})^{1/2}$	10^{7}
Electromagnetic	1/2	0	-1/2	$\phi/e\,Vn^{1/3}$	10^{19}

Various algorithms developed till now in the evaluation of ergodic parameters are suitable only for stationary data set (Grassberger & Procaccia, 1983a). However for nonstationary data set, these parameters are slowly varying functions of time (Pradhan & Dutt, 1993). Hence in choosing the data length, the number of data

points must be sufficiently large in comparison with natural time scale in the system. This requires the identification of different time scales involved in the dynamical process.

Many authors in studying the dynamics of human brain have ignored the role of time scales. Parikh and Pratap (1983) developed an evolutionary equation in the framework of nonequilibrium statistical mechanics developed by Prigogine and his Brussels School in which the significance of time scales has been stressed. Further Pratap(2000) formulated a theory of sensory transduction considering the interaction time scale. Considering the time scales one can develop nonequilibrium statistical mechanics of brain.

ATTRACTOR POTENTIAL FROM TIME SERIES

Recent studies of brain using the methods of nonlinear dynamics have revealed that the human brain dynamics involve a variety of highly nonlinear nonequilibrium dynamics. In these studies, the dynamics is understood by evaluating invariant parameters from the Electroencephalogram recorded on the scalp and treating it as a time series. The invariant parameters have been developed in the framework of deterministic chaos theory and are used for characterizing the brain under various pathological conditions (Elbert et al, 1994). This suggests that this kind of analysis could be useful for the development of a non-invasive diagnostic tool. The effort has already been started in this direction. However, a consistent theory has yet to be developed that incorporates all kinds of nonlinearity and stochasticity. Pratap (2000) has formulated a nonequilibrium statistical mechanics of brain function by considering the cortical activity as due to a gas of attractors. The evolution of this attractor gas is represented in a phase space spanned by the attractor invariants. The local properties are evaluated by defining a single attractor time – dependent mapping function. This theoretical framework forms the foundation of attractor potential that has been discussed in detail in this section.

There are about 10^{10} neurons in the cortex domain of which only a few percent are active at any given time. Even this small percentage which is a large number of neurons in the brain give rise to complex dynamics. In a single neuron

dynamics, the input to a neuron generates an action potential, which acts as a stimulus for the adjacent cell, giving rise to excitation. At each cell, there is an integration process of large number of stimuli and the process is an involved mechanism. At the Central Nervous System, various signals arriving from the different paths are again integrated in a highly nonlinear manner generating new signals and these signals are propagated to various muscles. The dynamics of the afferent and efferent propagating signals in the presence of random background firing was worked out by Anderson and Cooper (1978) to explain the higher functions of the brain such as association, recollection and generalization. Parikh and Pratap (1984) proposed a general formalism in the framework of nonequilibrium statistical mechanics and the results of Anderson and Cooper are obtained as a special case. Besides, these authors defined a new parameter called the *concept* to explain the learning process. The neural system is highly complex with feedback and feedforward mechanisms making the system thermodynamically open and in nonequilibrium state. Hence, the dynamics should necessarily be dominated by positive and negative feedback mechanisms rendering this to be statistical and nonlinear in character. Some of these features were incorporated by Cowan (1991) in formulating the stochastic neurodynamics based on a Master equation approach. In this approach, the basic formulation was based on linear dynamics and nonlinearity was introduced in a nonlinear stochastic equation. In another approach quantum mechanics (Pribram, 1991) and Greens function (Bressloff, 1995) has been used. However, in both these approaches nonlinearity was not taken fully into account. Apart from these analytic approaches a different view point was adopted by McCulloch and Pitts (1943) in which each stimulus excite a certain group of neurons

which in turn excite a larger population establishing thereby a pattern of excitation for each stimulus. This realistic approach became the starting point of Neural Network Theory. In Neural Network theory, the two functions evaluated are the Cost function and transfer function. Cost function is obtained by minimizing a function of the difference between the input training signal and the output signal. The transfer function on the other hand plays the role of interaction between the neurons. However in the method proposed by Pratap, a Γ space spanned by the invariant parameters are defined and an ensemble is constructed in this space. Then a Liouville density satisfying the Liouville equation is postulated. A formal solution is then projected onto a subspace using a diagrammatic technique as in classical field theory. The formulation is given in detail in the next section, but it has yet to make in roads into the realm of practical application.

In formulating the nonequilibrium statistical mechanics of brain function the invariant parameters selected for the construction of Γ space are Embedding dimension E_i, its Basin measure B_i, Generalised dimension D_{iq}, generalised information entropy K_{iq}, the new parameter Coherence index C_i and the corresponding Lyapunov exponents λ_{iq}. The trajectories of a dynamical system reconstructed in phase space will cluster in a subspace if there is a deterministic component. This subspace is called the Embedding space and E_i denotes its dimension. The dimension of this subspace is an integer. The *'object'* that formed in the subspace by the clustering of trajectories is called an Attractor. The set of initial conditions that produce the trajectories that end up on the attractor are called the attractor basin and this is denoted by B_i. To determine the attractor dimension, an

attractor is divided into a large number of cubes of volume ε. If V is the total volume

of the attractor, then the number of cubes is V/ε. If $N(\varepsilon)$ is the minimum number of

cubes required to cover the entire attractor, then one can define a dimension called

Capacity dimension D_F as

$$D_F = \underset{\varepsilon \to 0}{Lt} \frac{\ln(N(\varepsilon))}{\ln\left(\frac{1}{\varepsilon}\right)} \qquad (8.1)$$

If P_i is defined as the probability of finding a point on the attractor taken at random

in the ith cell, then

$$P_i = \frac{N_i(\varepsilon)}{N} \qquad (8.2)$$

where N is the total number of cubes which cover the entire attractor and N_i is the

number of cubes covering the trajectory in the neighborhood of the ith cell. From this

probability a generalized dimension D_q that is related to qth power of Pi is defined as

$$D_q = \underset{\varepsilon \to 0}{Lt} \frac{1}{q-1} \frac{\ln\left(\sum_{i=0}^{N(\varepsilon)}(P_i)^q\right)}{\ln(\varepsilon)} \qquad (8.3)$$

where q is a real number and can have values from zero to infinity. D_qs are arranged

in a descending sequence such that $D_j > D_{j+1}$. For q=0, $D_0 = \dfrac{-\ln(N(\varepsilon))}{\ln(\varepsilon)}$ is known as

Hausdorff dimension and D_q for q=1 is called the information dimension. The value of D_1 is evaluated from Eq (8.3) by taking the limit of q $\rightarrow$ 1 carefully. Again for q=2, the dimension obtained, called the Correlation dimension is most widely used for characterizing experimental signals. The generalised dimension is defined by considering the probability of having a point of the trajectory at random in a specified cell.

In defining the generalised entropy a sequence of cells i_0 i_1 i_2 .... i_n are considered and a joint probability $Pi_{0....i_n}$ is defined. Using this joint probability, the generalised entropy is defined as

$$K_q = - \underset{\substack{\varepsilon \to 0 \\ n \to \infty}}{Lt} \frac{1}{q-1} \frac{1}{n} \ln\left(\sum_{i_0........i_n} \left[P_{i_0.........i_n(\varepsilon)} \right]^q \right) \qquad (8.4)$$

The Dimension and the entropy are respectively the geometric and dynamic parameters of the attractor.

The Lyapunov exponents indicate the sensitivity of the initial conditions and thereby the stability of the system. If a system is represented by a discrete functional relationship

$$x_{n+1} = F(x_n) \qquad (8.5)$$

theory is given below and the salient points are brought out by considering an electron gas, which has thoroughly been worked out.

8.2 Phase Space Representation

Consider a classical electron gas having N number of particles with a passive ion background to provide overall charge neutrality. Each particle has a canonical momentum $\bar{p}$ and a conjugate position variable $\bar{q}$. One now constructs a phase space of 6N dimensions spanned by 3N momenta and 3N coordinates and this space is called Γ space. In this space a single point represents the state of the entire system and the evolution of the system is represented by a trajectory. Here time is considered as a parameter as in classical dynamics. However the system is completely specified only if we know all the 6N variables at any instant of time (initial state), which is indeed impossible. Gibbs overcame this impasse by constructing identical systems (energy or Hamiltonian being the same) with all plausible initial states and constructed identical trajectories in the Γ space. These trajectories do not intersect at any given instant of time and hence can be compared to an incompressible flow in this space. Gibbs then asked the question: What is the probability that the system is at or in the close neighbourhood of a specified state point at time t. This probability in the Γ space is defined as

$$\rho = \rho\left(q_1, q_2, \ldots, q_N, p_1, \ldots p_N, t\right) \qquad (8.7)$$

116

This is called Liouville density and since there are no sources or sinks in the Γ space, this function satisfies a continuity equation

$$\frac{d\rho}{dt} = 0 \qquad\qquad (8.8)$$

The expanded version of the above equation would read as

$$\frac{\partial\rho}{\partial t} + \sum_{i=1}^{N}\left[\frac{\partial\rho}{\partial q_i}\cdot\dot{q}_i + \frac{\partial\rho}{\partial p_i}\cdot\dot{p}_i\right] = 0 \qquad\qquad (8.9)$$

The collection of the trajectories is called the Gibbsian ensemble. If the system is conserved, one can define a Hamiltonian that defines a parametric surface in the Γ space. However in general one can define a Hamiltonian that is a motion generating function and the time derivatives in Eq. (8.9) can be replaced with space derivative using Hamilton's equations.

8.3 Hamiltonian

A Lagrangian or Hamiltonian describes the dynamics of a system completely. If the system is conservative then the Hamiltonian is the energy of the system and one can define a Hamiltonian density, which can be used to write the equations of motion as

$$\dot{q} = \frac{\partial H}{\partial \bar{p}} \text{ and } \dot{p} = -\frac{\partial H}{\partial \bar{q}} \tag{8.10}$$

and on substituting these total time derivatives in Eq. (8.10) it results in

$$\frac{\partial \rho}{\partial t} + \sum_{i=1}^{N} \left[\frac{\partial \rho}{\partial q_i} \cdot \frac{\partial H}{\partial p_i} - \frac{\partial \rho}{\partial p_i} \cdot \frac{\partial H}{\partial q_i} \right] = \frac{\partial \rho}{\partial t} + \left[\rho, H \right] = 0 \tag{8.11}$$

where the square bracket is called the Poisson's bracket. This representation is restricted to conservative systems. However for most conservative systems where dissipative forces exist; one can go over to a time dependent Hamiltonian characteristic function formalism.

One can in general write the Hamiltonian as consisting of two parts, the kinetic and potential parts and write it as

$$H = H_o + \lambda H_1 \tag{8.12}$$

In this separation, a constant λ has been introduced which is used as a book keeping parameter. H_o is independent of $\bar{q}$ and H_1 of $\bar{p}$. Hence Eq. (8.11) takes the form

$$\frac{\partial \rho}{\partial t} + L_o \rho = \lambda (\delta L) \rho \tag{8.13}$$

where, L_o and δL are operators given by

$$L_o = \sum \frac{\partial H_o}{\partial p_i} \cdot \frac{\partial}{\partial q_i} \quad \text{and} \quad (\delta L) = -\lambda \sum \frac{\partial H_1}{\partial q_i} \cdot \frac{\partial}{\partial p_i} \qquad (8.14)$$

Eq. (8.13) can be formally integrated giving rise to a solution in the form of an integral equation of the Volterra type of the second kind viz.

$$\rho(t) = e^{-L_o t}\rho(o) + \lambda \int_0^t dt_1 e^{-L(t-t_1)}\rho(t_1) \qquad (8.15)$$

where $\rho(o)$ is the initial state (state at t=0).

Eq (8.15) can be iterated to all orders giving thereby

$$\rho(t) = \sum_{n=0}^{\infty} \lambda^n \int_0^t dt_1 \int_0^{t_1} dt_2 \ldots \int_0^{t_{n-1}} dt_n e^{-L(t-t_1)}(\delta L)e^{-L(t_1-t_2)}$$

$$\times(\delta L)\ldots e^{-L(t_{n-1}-t_n)}(\delta L)e^{-Lt_n}\rho(0) \qquad (8.16)$$

Eq (8.16) can also be written in the language of Green's function as

$$\rho(t) = e^{-L_o t}\rho(o) + \lambda \int_0^t d\tau G(t-\tau)\rho(\tau) \qquad (8.17)$$

where the definition of G is obvious from Eq.(8.16). Here an exact solution of the Liouville equation has been obtained which is of little consequence, since this does

not help one to evaluate local properties in the system. Since all observations are made at different points in the system, one has to obtain a weight function, which is a local function. This amount to obtaining a one-particle distribution function defined in a six dimensional μ space (molecular space) i.e. it is equivalent to mapping the dynamics in the Γ space to a subspace of dimension six. This is achieved by defining a relevant time scale.

8.4 Choice of time scale

There are essentially two methods in vogue viz. the one started by Yvon that is currently known as BBGKY (Bogoliubov, Born, Green, Kirkwood and Yvon) and the other developed by Prigogine and his co-workers known as the Brussels school. In the former case one integrates the Liouville equation Eq.(8.11) over all variable except one, and since the interaction potential connects this particle with another (in the case of two body interaction, the ensuing equation will have a source which is a functional involving f_2 or two particle distribution function. If one integrates all variable excepting two to obtain f_2 the resulting equation has again a source term which is a functional of f_3, again due to interactions. Thus the equation reduces to an open ended hierarchy and this is known as BBGKY hierarchy. One has to apply a closure by assuming the higher order distribution function is a function of lower order distribution function. Various people have effected different closures. This seems to be quite arbitrary.

Prigogine's method (Balescu, 1975) on the other hand chooses a specific time scale and from the infinite series, one picks up a subset of infinite terms corresponding to a specified time scale. This however is meaningful only if the various time scales existing in the system are widely separated as one has in plasmas. There it can be shown that relaxation time scale is about two orders of magnitude higher than the interaction time scale. Hence the distribution functions in the two different time scale have different characteristics. Therefore the one particle distribution function (OPDF) that one gets pertaining to a chosen time scale gives rise to averages which give correct estimates of local property. A detailed discussion of the electron gas problem together with a diagrammatic treatment is given in Prigogine. (1962).

This method however has to be modified when the time scales are close by or even overlap. This is precisely the case for the brain dynamics. Furthermore one does not know the exact interaction between neurons to write a realistic Hamiltonian. Hence a method has to be devised to get an idea of interaction in the brain system.

8.5 Model of Neurodynamics

Dynamics of a system is defined by interaction in the system. In the present case, the inferred data indicates the end result of all interactions in the system at the space time point from which the data is collected. Hence the effort must be to infer the plausible interactions in the system, which result in the final state indicated by the data set. This is a particular case of doing an inverse analysis of the data set to get an

insight into the interactions in the system. Hence one necessarily has to assume a model in which an interaction is postulated and examine whether the assumed model reproduces the output data. In the present analyses the model of human brain proposed by Parikh and Pratap (1991) is followed which has successfully predicted the EEG output from a normal person in the eyes closed state. In this the starting point is the integral equation proposed by Prigogine as given in Eq.(8.17).

Interaction in the human brain generates a large number of attractors specified by various characteristic parameter such as embedding dimension ε_i, attractor basin B_i, generalized metric dimension D_{iq}, generalized entropy K_{iq} and Lyapunov constant λ_{iq}/Lyapunov function. In this i is the attractor index and q are integers $0 \leq q \leq \infty$ for any specified i. The value q=0 for the ith attractor is known as Hausdorff dimension. q=1 is called the information dimension and q=2 is the two body correlation dimension. D_{iq} for q>2 are the higher order correlation dimensions and all these are geometric parameters specifying the shape of the attractor in a suitably chosen phase space. Similarly K_{iq} are the Shannon entropy and K_{i2} is known as Kolmogorov entropy of the ith attractor which is the measure of the information capacity of the system. Similarly $\lambda_{iq}= 0$ for any q implies that Lyapunov exponents do not indicate the stability/ instability of the system. In such a case one has to resort to Lyapunov functions.

The dynamics of brain can be simulated to the dynamic state of an attractor gas specified by the above parameters. At a given point 'A' in the skull space, if an

attractor of a specified set of parameters disappears at a certain instant and an identical (in all respects) one appears at a certain other point 'B' in the skull space at a later instant of time. One can treat this as an instance of scattering of the attractor from A to B. In the parlance of field theory, the attractor is annihilated at A and created at B.. One can define a velocity of transport of this attractor by evaluating the ratio $\dfrac{\overrightarrow{AB}}{\Delta t}$ One can also define a potential responsible for this scattering process in the space spanned by $\vec{X}$, $\vec{v}$, ε_i, B_i, D_{iq}, K_{iq}, λ_{iq} wherein $\vec{v}$ is the speed with which the attractor disappears and appears from A to B. It should be emphasized here that the above parameters are only a *certain* set of known "invariant" parameters and that this set is not closed by any means.

The dynamics in the attractor gas can be specified in terms of its parameters such as Embedding dimension E_i, its Basin measure B_i, Generalised dimension D_{iq}, generalised information entropy K_{iq}, Coherence index C_i and the corresponding Lyapunov exponents λ_{iq}. A Γ space is then constructed with coordinates X_i, V_i, E_i, B_i, D_{iq}, K_{iq}, C_i and λ_{iq} and in this space, the state of a given system which is completely specified by the above variables is represented by a point. The evolution of a system is represented by a trajectory in this Γ space. Following the usual methods of statistical mechanics, since initial condition is not known, one can construct replicas of the given system of all possible initial state and these give a Gibbsian ensemble. In this space then a probability distribution function ρ is defined as

$$\rho = \rho(\Omega, t) \qquad (8.18)$$

where

$$\Omega = \left\{\Omega_i\right\} = \left\{\overline{x}_i, \overline{v}_i, E_i, B_i, D_{iq}, K_{iq}, \lambda_{iq}, C_i\right\} \qquad (8.19)$$

ρ gives the probability of a system to be located at a point Ω in this Γ space at the instant t.

In the above i is the attractor label and q is a set of natural numbers from 1 to infinity. The probability function is normalized as

$$\int \rho d\Omega = 1 \qquad (8.20)$$

where $d\Omega$ is an infinitesimal volume in the Γ space as

$$d\Omega = \prod_i (dx_i)(dv_i)(dE_i)(dB_i)(dD_{iq})(dK_{iq})(d\lambda_{iq})(dC_i) \qquad (8.21)$$

Each pattern generated by a collection of neurons due to an external stimulus would generate a pattern of attractors in phase space. Hence, to study the dynamics of brain an approach is adopted in which the probability of generating a particular attractor distribution in the skull space is studied. To obtain this a reduced distribution function is defined as

124

$$f_{1....k} = \int \rho d\Omega_{k+1....N} \tag{8.22}$$

where i....k are the attractor labels. This equation would reduce to a single attractor distribution function as

$$f(\Omega_i, t) = \int \rho d\Omega' \tag{8.23}$$

where the prime indicates the variables of the ith attractor are not integrated. One can then write ρ as

$$\rho_N = \prod_{i=1}^{N} f_i + \phi_{1....N} \tag{8.24}$$

where the first term gives the uncorrelated distribution and the second term the dynamical correlations. Thus

$$f(\Omega_i, \Omega_j, t) = f(\Omega_i, t) x f(\Omega_j, t) + U(\Omega_i, \Omega_j, t) \tag{8.25}$$

where the integration is carried out over all the variable indices except i and j.

The Liouville density satisfies the continuity equation

$$\frac{d\rho}{dt} = 0 \tag{8.26}$$

and the Liouville equation is rewritten in full as

$$\frac{\partial \rho}{\partial t} + L_0(\rho) = \lambda(\delta L)\rho \qquad (8.27)$$

where L_0 is the Liouville operator without interactions and δL is the part of the operator which include interactions. λ is the interaction strength. By formally integrating the above equation the solution is obtained as a Volterra equation of the second kind as

$$\rho(t) = e^{-L_0 t}\rho(0) + \lambda \int_0^t d\tau e^{-L_0(t-\tau)}(\delta L)\rho(\tau) \qquad (8.28)$$

where $\rho(0)$ is an initial state. On iterating, to all orders one obtains an infinite series giving the complete correlation dynamics. From the infinite series so obtained after integration a subset of infinite terms, corresponding to a chosen time scale is selected and this subset is summed exactly. The Eq. (8.28) has the following physical significance. The exponential term in the operator transports the state from an earlier time to a later one. Here it is called a propagator. The first term on the right hand side transports the initial state to the instant t without any interaction and this is the known as the free flow term. The second term represents the response of the entire system at τ to the final state at t. The above equation can be written as

$$\rho(t) = \int_0^t d\tau G(t - \tau)\rho(\tau) \qquad (8.29)$$

where G is the transition probability which takes the system from an initial state to final state. This equation is called the evolutionary equation of Parikh and Pratap. This is the staring point of the dynamical study of neural system from nonequilibrium statistical mechanical point of view. On integrating Eq. (8.29) over all the variables except one pertaining to a specified state, one can write the single particle distribution function in terms of G as

$$f(\Omega_i, t) = \int_0^t d\tau \int d\Omega_j G(\Omega_i | \Omega_{ij}, t - \tau) \rho(\Omega_j, \tau)$$
(8.30)

where Ω_{ij} is

$$\Omega_{ij} = \begin{cases} \bar{x}_i - \bar{x}_j, \bar{v}_i - \bar{v}_j, E_i - E_j, B_i - B_j, D_{iq} - D_{jq}, \\ K_{iq} - K_{jq}, \lambda_{iq} - \lambda_{jq} \end{cases}$$
(8.31)

The appearance of (t-τ) as well as Ω_{ij} indicates that the equation depends on the entire previous history and hence the solution is *non Marcoffian* which reflects memory. There are different methods of solving the Liouville equation. (a) From an interacting system obtain an interaction potential and then the one particle distribution function. (b) Integrate the Liouville equation for a system of one particle interacting through a two-particle interaction potential to obtain a differential equation for f_1 for a source function depending on two-particle distribution function f_2. On integrating all variables except two, the source function would depend on f_3 and so on. This hierarchy is called BBGKY and imposing some constraints, this

127

hierarchy is broken. Bogoliubov 's ansatz is that in all the many particle distribution, the time is taken from f_1, particular the four particle distribution function $f_4 = f_2 \otimes f_2$ where $f_2 = f_2 (x_1, x_2, f_1(t))$. Prigogine's method is more meaningful as it incorporates the dynamics in different time scales. In the absence of any knowledge of G a functional form is generally assumed and the system is modeled to obtain a solution with the predictive capability.

Here a different approach is considered. As a first step to model the dynamics of brain from nonlinear dynamical point of view an effort has been made to find out the interaction potential, which appears in the Hamiltonian written as

$$H = H_0 + V_I.$$

where H_o is the kinetic energy part and V_I is the interaction "potential". To get information about the interaction potential from a time series, the method adopted is as follows: The data obtained as a time series consisting of N points taken at equally spaced time intervals is arranged in a delayed matrix as

$$C = \begin{bmatrix} f_1 & f_2 & \cdots\cdots & f_m \\ f_2 & f_3 & \cdots\cdots & f_{m+1} \\ . & \cdots\cdots & & . \\ f_n & f_{n+1} & \cdots\cdots & f_N \end{bmatrix} \qquad (8.32)$$

where $n = N-(m-1)$. Here m is the embedding dimension and C is a rectangular matrix. This is then subjected to a singular value decomposition (Broomhead &

King, 1986). Then C^TC where C^T is the transpose of the C is constructed. Here C is a nxm rectangular matrix and therefore C^TC would be a mxm symmetric square matrix, N being the total number of data points and m the embedding dimension. The eigen values and eigen functions of C^TC are determined. For an embedding dimension of m=15, there will be 15 the eigen functions Φ_1, Φ_2,...., Φ_{15} each a 15x 1 matrix with eigen values λ_1,..., λ_{15}.

In this since the attractors are dynamic in nature Φ as well as λ both functions of time including all the nonlinearities. The potential is evaluated from the Schrodinger like equation as

$$\left[H_0 + V_I(\Phi)\right]\Phi = \lambda\Phi \tag{8.33}$$

where Eq.(8.33) becomes

$$\left[-\Phi'' + V_I\right]\Phi = \lambda\Phi \tag{8.34}$$

where V_1 is a scalar function of the wave function thereby making (8.34) nonlinear. An inverse scattering calculation would give the effective potential at the specified point and with a specific velocity. The advantage in the above is that the set of Φs are all orthogonal. In dimensionless variables one can write (8.34) in matrix form as

$$V_1 = \Phi^T\Phi'' + \lambda \tag{8.35}$$

129

where the prime denotes differentiation with respect to its arguments. In (8.35) Φ is a column vector and hence Φ^T is a row vector and $\Phi^T\Phi=1$, since Φs are orthogonal. V_1 is a scalar function of Φ. Eventhough the attractor potential has been derived in view of modelling the dynamics of human brain there is no restriction to use these methods for other complex systems as well.

Thus in this chapter human brain dynamics has been presented as a collection of large class of attractors distributed in the skull space whose interactions produces a pattern of attractors. These attractor distributions is characterised by invariant parameters along with newly defined index, Coherence index. The various attractors consisting of both regular and strange, are treated as multispecies attractor gas and its state as a function of time is mapped on space spanned by these parameters. The known relations between these parameters and the invariant measures are exploited to develop a nonequilibrium statistical mechanics of the system. In this phase space, the state point describes the trajectories and for different initial states, from a set of non-intersecting trajectories a Gibbsian ensemble is constructed for the attractor distribution. Writing a Liouville equation, an evolutionary equation of the probability density is obtained. The attractor potential is derived to obtain the functional form of G and this functional form would then be a more realistic representation of the dynamics as it is derived from the real data. The results are presented in chapter 10.

EXPERIMENTAL DESIGN AND VERIFICATION OF METHODS

The methods of nonlinear time series analysis along with new methods developed in this work have been validated with several standard maps and equations. The basic idea is to understand the dynamics of the system from time series and infer the dynamics of the system. To understand the dynamical aspects from the nonlinear dynamical point of view the procedure generally adopted is to reconstruct the time series in an appropriate dimension with a proper choice of Time lag. The characterizing parameters are evaluated from this reconstructed signal. Thus for the evaluation of characterizing parameters, the time lag and appropriate embedding dimension have to be fixed. The methods used in this work for the evaluation of time lag, embedding dimension, correlation dimension and Kolmogorov entropy are given below

SET 1

1. *Average mutual information criteria* (Fraser & Swinney, 1986.) is used for the selection of time lag T_d required for the reconstruction of phase space.

2. *Global False nearest neighbors* is employed (Abarbanel *et.al.*, 1993) for the selection of appropriate embedding dimension

3. *Singular value decomposition* (Broomhead & King, 1986) is used for evaluation of the eigen values and eigen functions of attractor reconstructed from the signal. This is also a noise reduction method.

4. *Fixed Mass approach* (Havstad & Ehlers, 1989) is used for the evaluation of Correlation dimension and Kolmogorov entropy.

The above mentioned methods give the information from a single time series. However to understand the interactions thereby to study the synchronization of different regions of brain the methods adopted in this work are from Modern synchronization theory of dynamical systems. The methods are given below

SET 2

5   *Phase synchronization method using analytical signal concept* (Rosenblum *et. al.*, 1996) for understanding the coordination of subsystems.

6   *Generalized synchronization method using false nearest neighbors* (Rulkov et al., 1995) for understanding the global synchronisation.

New methods developed in this work to evaluate phase, coherence properties and the attractor potential are:

SET 3

7.   *Evaluation of phase from Poincare map.*

8.   *Determination of Phase synchronisation index, amplitude synchronisation index and Synchronisation Coherence index from Poincare map*

9.   *Phase coherence, amplitude coherence and coherence index.*

10.   *Evaluation of interaction potential- an inverse scattering method.*

Many of these methods are verified with standard maps and equations. *SET 3* is developed as a part of this work and the results are presented in the next chapter. The standard maps and equations used for verification are:

a) Logistic equation

b) Henon map

c) Rossler equation

d) Mixed sine waves

e) Random numbers

f) Coupled Rossler equation

9.1 Verification of Methods

a) Logistic Map

This is a one - dimensional map, which may be thought of as a simple idealized ecological model for the yearly variation in the population of an insect species. The population at n^{th} year uniquely determines the population at $(n+1)^{th}$ year and the equation is given as

$$X_{(n+1)} = rX_n \left(1 - X_n \right)$$ (9.1)

where r is the control parameter. At r=4.0 the data set obtained from this equation is chaotic for a set of initial conditions. The data obtained is plotted as time series and is given in Fig 9.1(a). The plot of ln C(r) Vs ln (r) is given in Fig 9.1(b). The correlation dimension D2 obtained is 0.9863 and the plot of singular values is given in Fig 9.1(c). The singular value plot shows that the embedding dimension is 2 for this system.
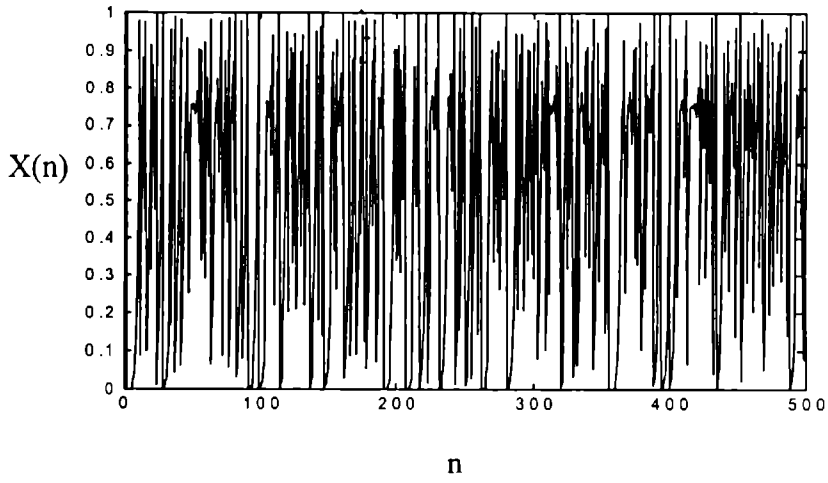
Fig 9.1(a): Time series of Logistic equation at r=4.0
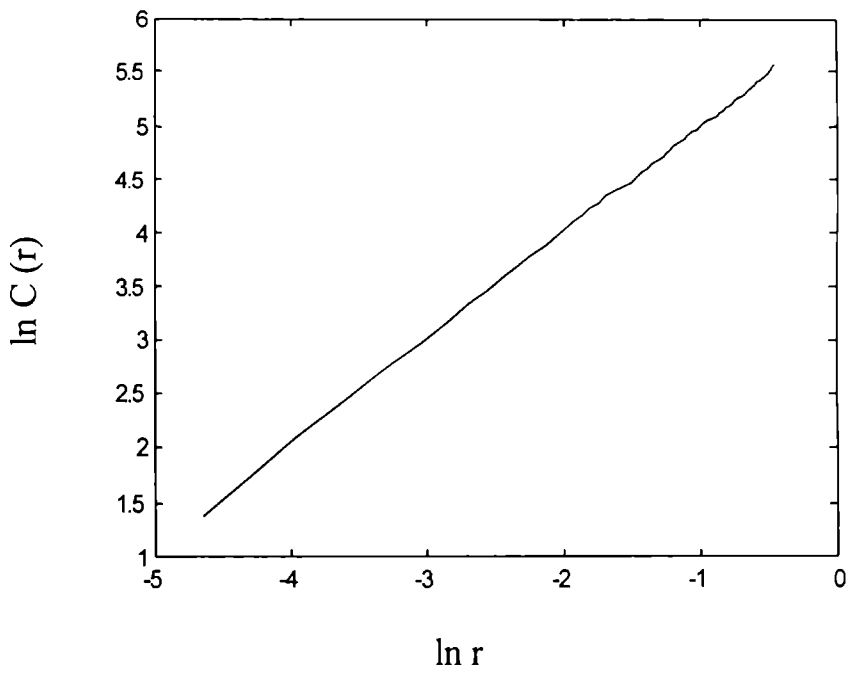
Fig.9.1(b): ln C(r) Vs ln r plot of Logistic equation
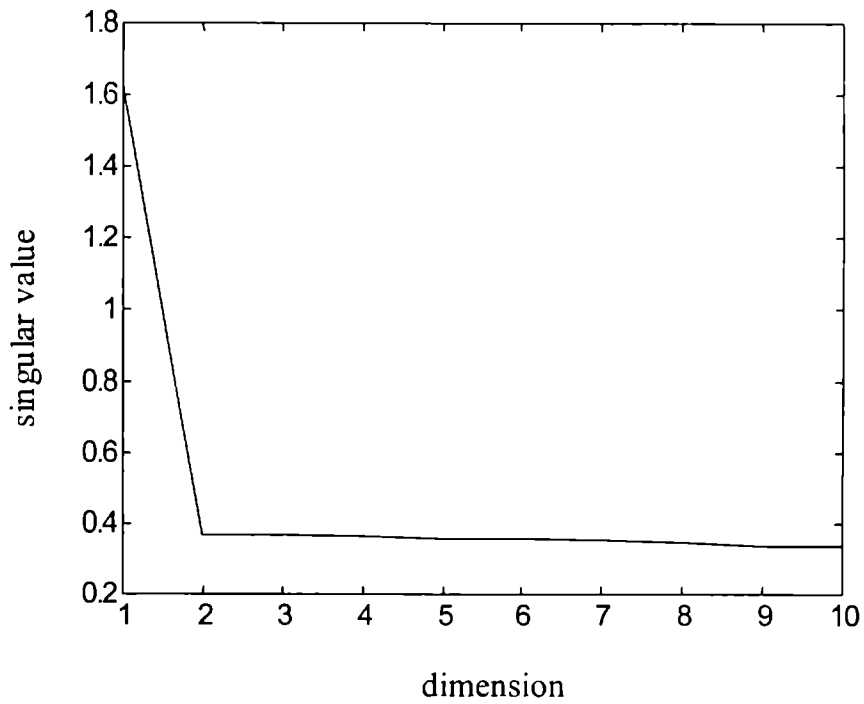
Fig 9.1(c): Plot of singular values of Logistic equation

b) Henon Map

This is a two dimensional map given by Henon

$$X(t + 1) = 1 - aX^2(t) + Y(t)$$
$$Y(t + 1) = bX(t)$$

(9.2)

which, yields irregular solutions for many choices of a and b. For a=1.4 and b=0.3 the sequence of output will be chaotic.

In evaluating the average mutual information it has been found that there is no minimum in the mutual information curve. In such cases the time lag is selected at value Imax/5 of AMI curve. In this case it is selected as n=5 as shown in Fig. 9.2(a).
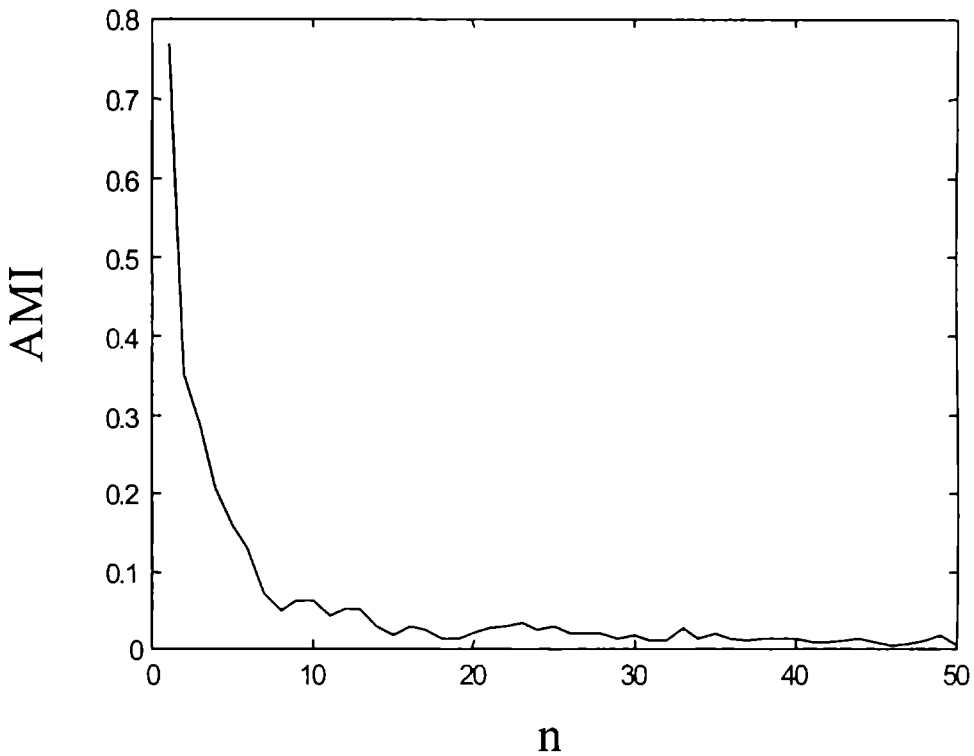
Fig 9.2(a): Average Mutual Information curve of Time series of Henon map. (n = 5)

However the percentage false nearest neighbor plot reaches a minimum value at a dimension of 2 and this is the embedding dimension of the system. Fig. 9.2(b) shows the plot of percentage false nearest neighbor against dimension. On evaluating D2 and K2 using Grassberger-Procaccia method, D2 is obtained as 1.23 and K2 as 0.46
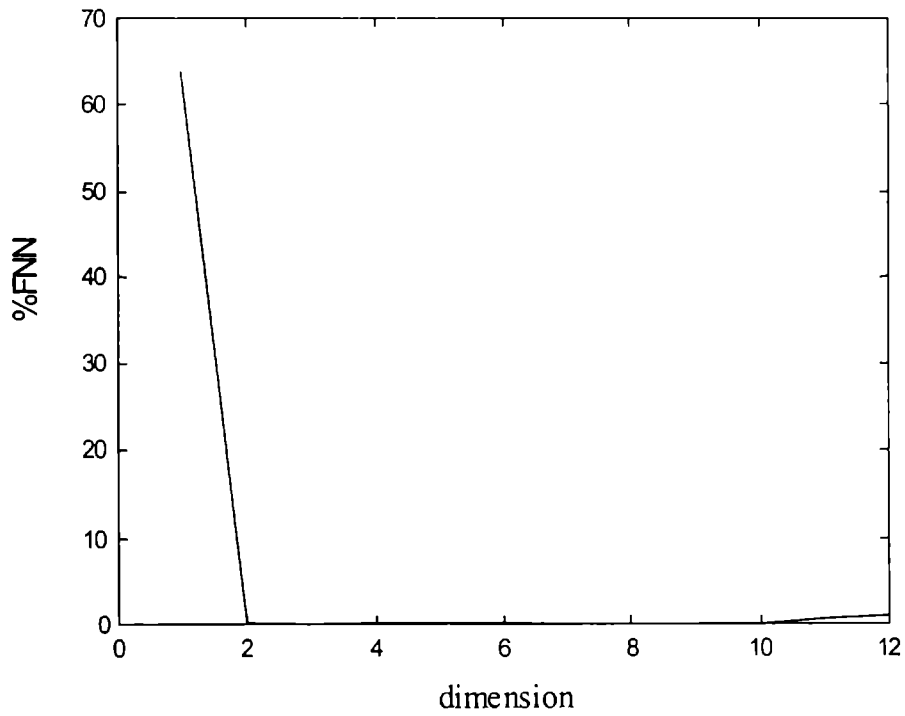
Fig. 9.2 (b): Percentage False Nearest Neighbor of time series of Henon map

c) Rossler Equation

The equation is

$$\frac{dx}{dt} = -\left(y + z\right)$$

$$\frac{dy}{dt} = x + ay \qquad\qquad (9.3)$$

$$\frac{dz}{dt} = b + z\left(x - \mu\right)$$

137

The parameters are a=0.2; b=0.2; μ=5.7. The equation has been numerically evaluated using a time step Ts = 0.0005 In all the three above mentioned equations 20,000 data points are generated and last 5,000 data points are selected to avoid the transients. The correlation dimension D2 is obtained as 1.76 and Kolmogorov entropy K2 is obtained as 0.101. The time lag Td from AMI is obtained as 35Ts.

c) Mixed Sine waves

The mixed sine wave is generated using the equation

$$y(t) = \sum_i A_i \sin(2\pi f_i t) \qquad (9.4)$$

with i=1 and f_1=7 Hz a time series with a single frequency is obtained. Then with i=2 and f_1=7 Hz and f_2=22 Hz a signal with incommensurate frequencies is generated. Further retaining f1=7 Hz and making f2=21Hz a signal with a fundamental and harmonics is generated. The amplitudes A_i are taken as unity. The sampling frequency used for numerically simulating the sine waves is selected as ten times the highest frequency component. The different waveforms are given in Fig. 9.3 and its representation in phase space is given in Fig. 9.4.

In the case of sine wave with a single frequency the phase space representation is a circle and in the case of commensurate frequencies it is represented as a distinct circles depending upon the frequencies present in the signal

as in Fig 9.4(c). In the case of incommensurate frequencies there are no distinct

circles as there is no rational relation between the frequencies as in Fig 9.4(b). This

mode of representation is useful when one is trying to evaluate the phase from

Poincare map.
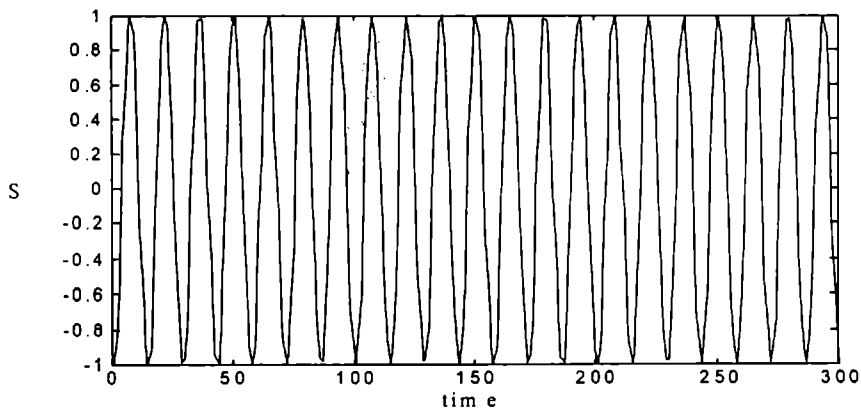
Fig. 9.3(a): Sine wave of frequency f=7Hz.
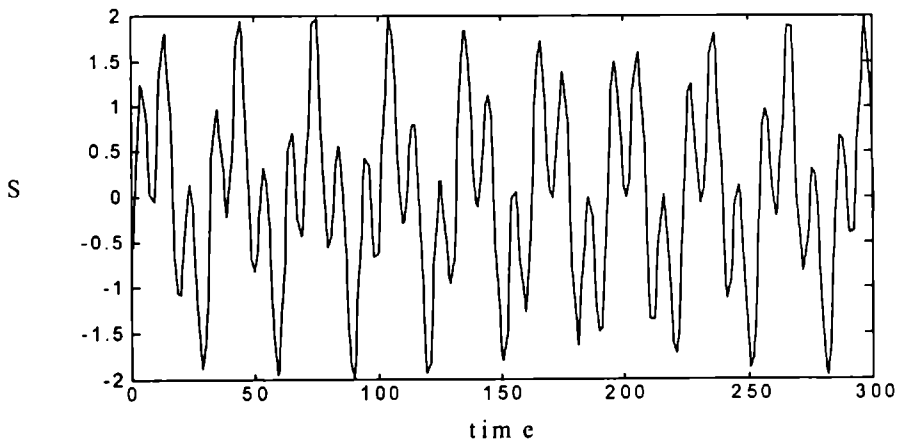
Fig. 9.3 (b): Mixed sine waves with frequencies f_1=7Hz and f_2=21Hz
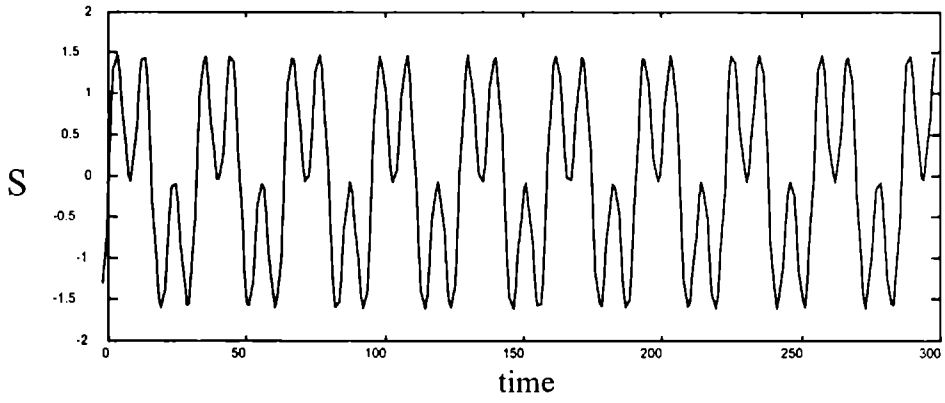
Fig. 9.3(c) = Mixed sine waves with frequencies f_1= 7Hz and f_2 = 22 Hz.
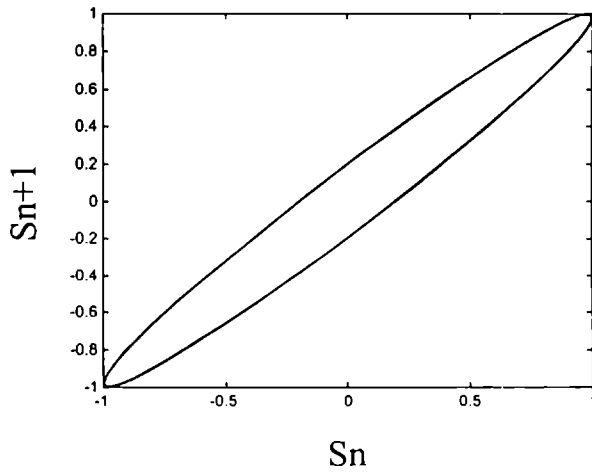
Fig. 9.4(a): Poincare map of Sine wave of frequency f=7Hz
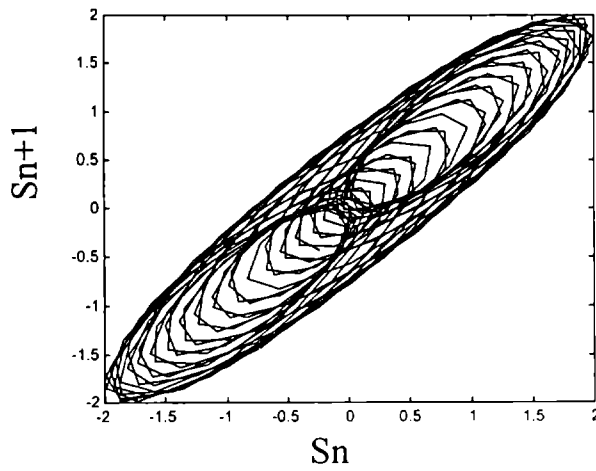
Fig. 9.4(b): Poincare map of Mixed sine waves of frequencies f_1=7Hz and f_2=22Hz

140
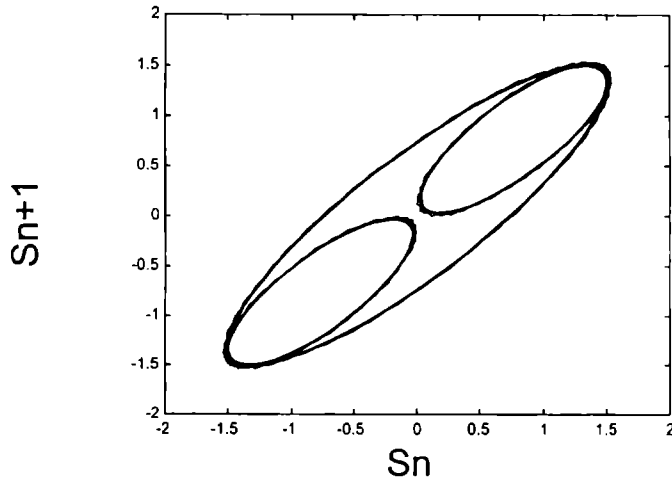
Fig. 9.4(c): Poincare map of Mixed sine waves of frequencies $f_1=7Hz$ and $f_2=21Hz$

D2 for sine wave of single frequency is $\cong 1.00$, for mixed sine wave with two frequencies that are incommensurate is $\cong 2.00$ and that of commensurate frequencies is obtained as $\cong 1.00$. K2 on the other hand for all the three cases is obtained as $\cong 0$. The plot of ln C(r) Vs ln r of mixed sine wave with incommensurate frequencies is given in Fig 9.5.
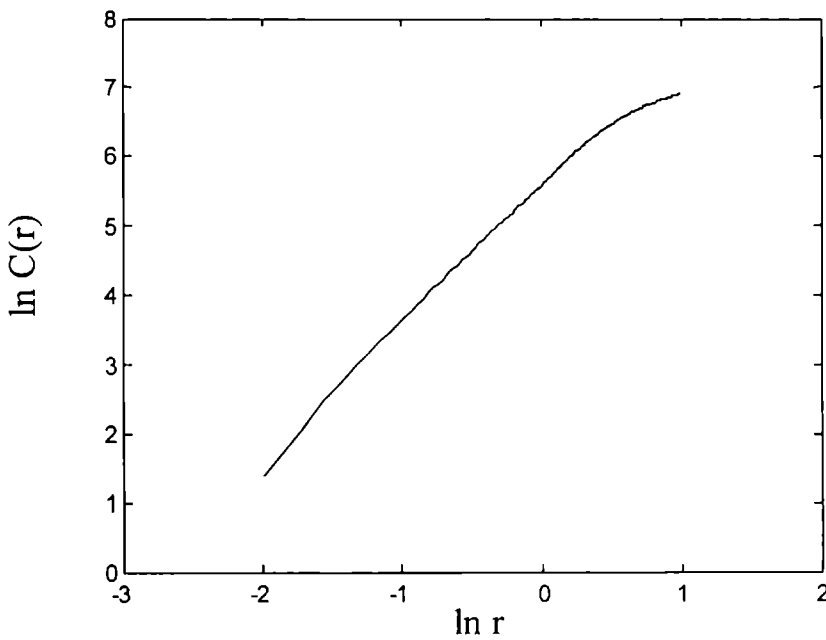
Fig.9.5: ln C(r) Vs ln r plot of Mixed Sine wave ($f_1=7Hz$ and $f_2=22Hz$). D2=2.003

141

The value obtained by finding the slope using linear fit of ln C(r) Vs ln(r) in the case of mixed sine wave with frequencies 7Hz and 22Hz is 2.003. Since there are two distinct independent frequencies the number of independent variables involved in generating the sine wave is 2 and this is reflected in the D2 value.

d) Random Numbers

Many of the computer generated random numbers are of low dimensional in nature. Hence a procedure is adopted by which data from different random number generators are randomly shuffled to get a data set of sufficiently high dimension. Poincare map is given in Fig 9.6
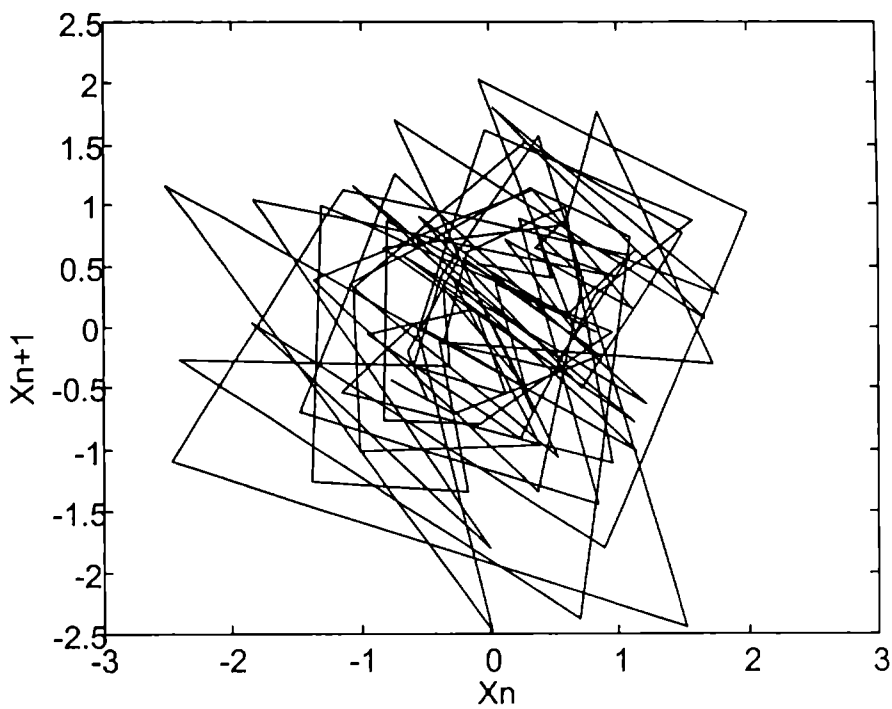
Fig. 9.6: Poincare map of random number.

In the case of Random numbers it is very clear from the Fig 9.7 that the percentage of False nearest neighbor never achieves zero or remains in a low value, indicating that the embedding dimension is very high.
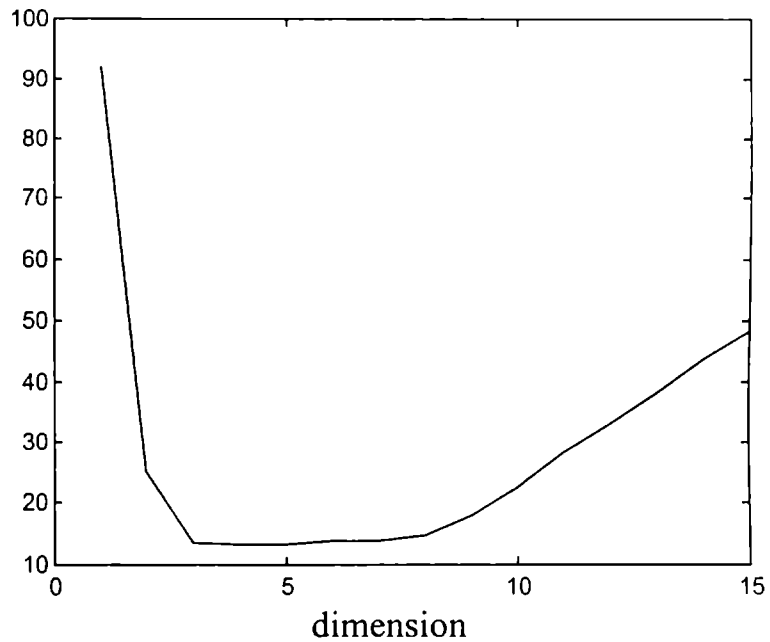
Fig. 9.7: Percentage False Nearest Neighbour of Random number

e) **Coupled Rossler equation**

The Rossler equations are coupled as given below. This set of equation is

$$\frac{dx_1}{dt} = -\left(y_1 + z_1\right)$$

$$\frac{dy_1}{dt} = x_1 + ay_1$$

$$\frac{dz_1}{dt} = b + z_1\left(x_1 - \mu\right)$$

143

$$\frac{dx_2}{dt} = -(y_2 + z_2) + c_1(x_1 - x_2)$$

$$\frac{dy_2}{dt} = x_2 + ay_2 \tag{9.5}$$

$$\frac{dz_2}{dt} = b + z_2(x_2 - \mu)$$

proposed by Rosenblum et al (1996) to study the phase synchronization of subsystems. The parameter values are a=0.15, b=0.2, μ=10 and c_1 is the coupling strength. In this x – variables form the drive system whereas the y- variables form the response system.

The set of equations proposed by Abarbanel (Rulkov et. al, 1995) and his group again is a coupled Rossler equation as in Eq. 9.5 with the parameter values, a=0.2, b=0.2, μ=5.7 and c_1 is the coupling strength. In this however as the coupling parameters are varied one could achieve the amplitude synchronisation. Using analytic signal phase of an arbitrary signal can be determined. However, to verify the method of phase synchronization the coupled Rossler equation with the parameters proposed by Rosenblum has been used. At a coupling value of c_1=1.5 the phase of the two systems are locked, while the amplitude remains chaotic. This locking is observed by calculating the phase difference of respective variables. Fig.9.8(a & b) gives the time series of y_1 and y_2 before phase synchronisation. The corresponding relative phase is given in Fig 9.9 (a). Fig. 9.8(c) gives the time series y_2 during phase synchronisation. There is no change in the time series of y_1 as the system is coupled unidirectionally. Fig 9.9(b) represents the relative phase of the drive and response during synchronisation.
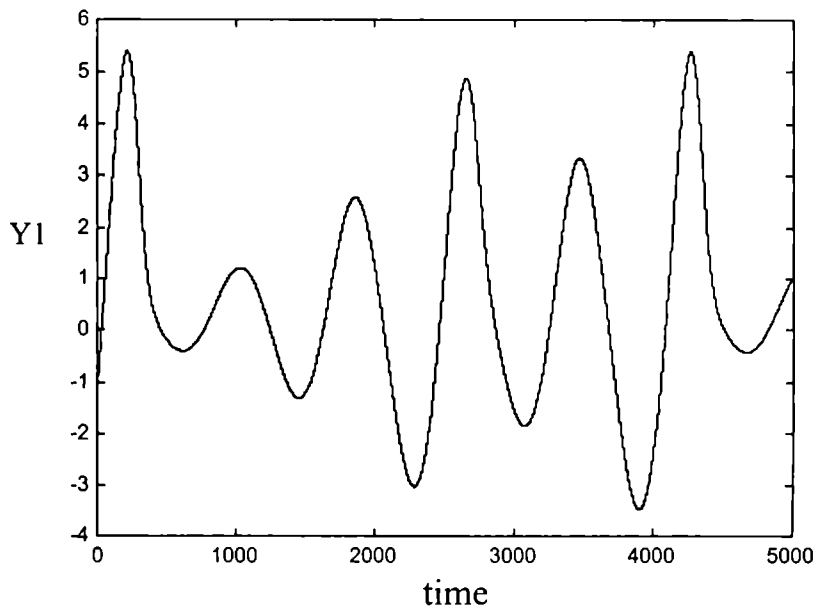
Fig 9.8(a): Time series of drive system of Coupled Rossler equation before phase synchronisation. ($c_1=0.3$)
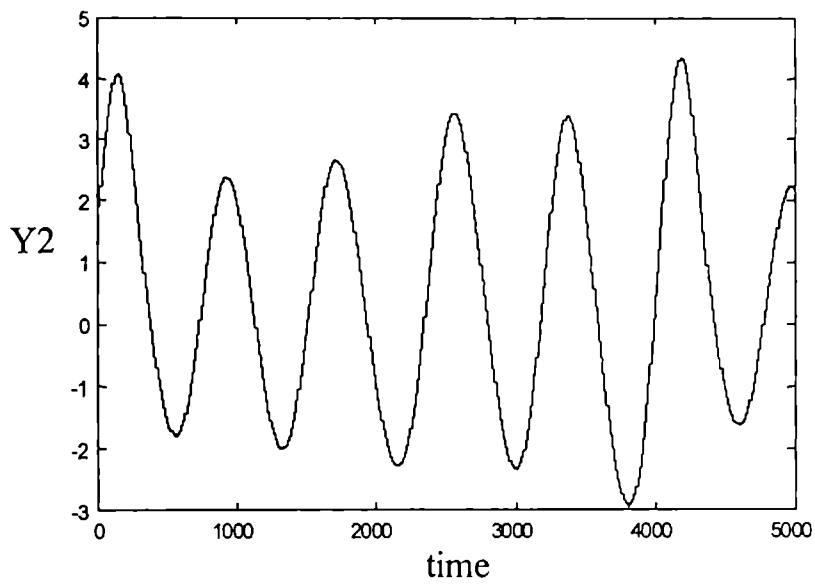
Fig 9.8(b): Time series of response system of Coupled Rossler equation before phase synchronisation. ($c_1=0.3$)
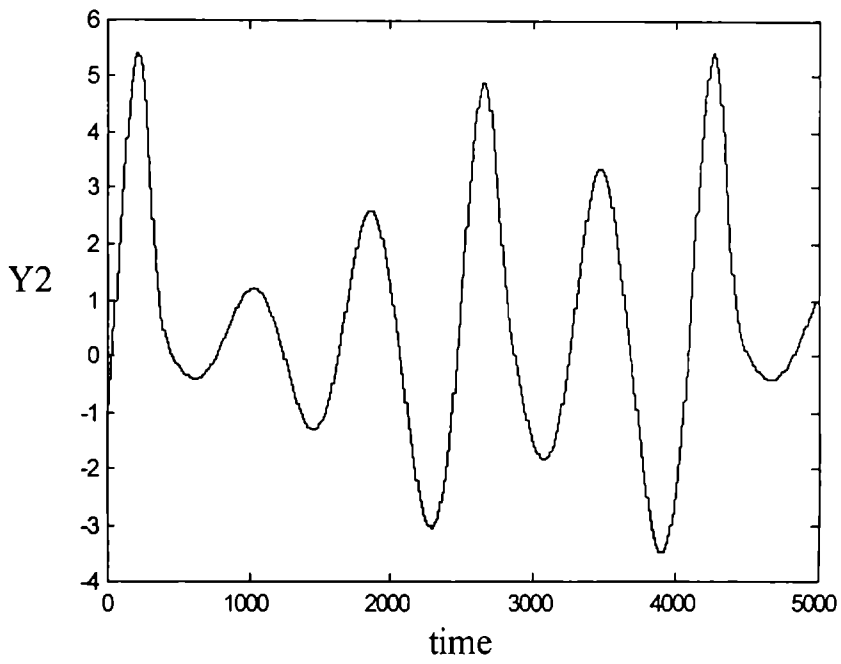
Fig 9.8(c): Time series of response system of Coupled Rossler equation during phase

synchronisation. ($c_1=1.5$)
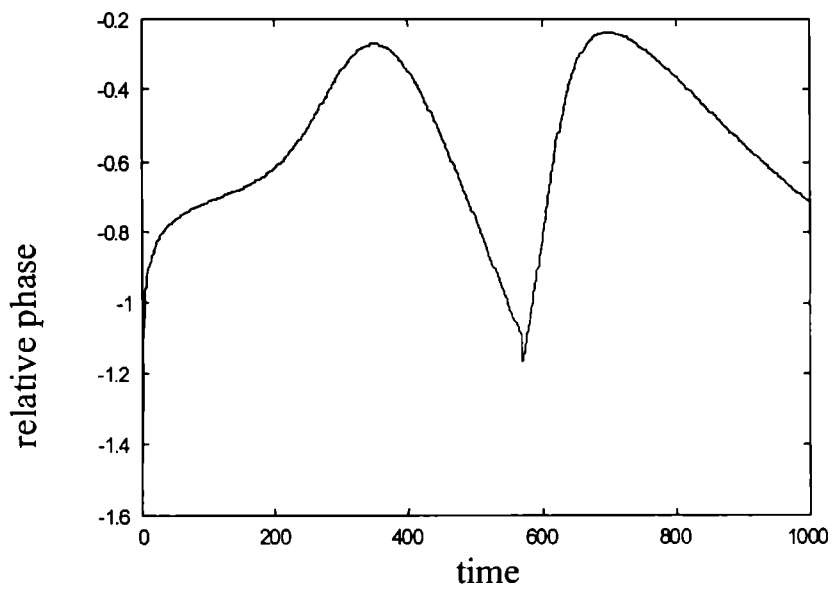
Fig.9.9(a): Relative phase variation of coupled Rossler equation before phase
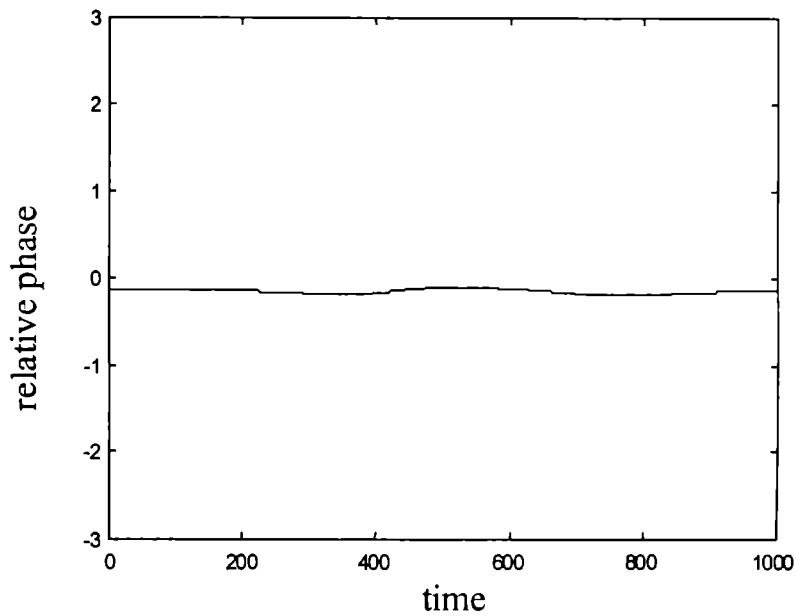
synchronisation

Fig.9.9(b): Relative phase variation of coupled Rossler equation during phase synchronisation

The Rossler equation with the parameter values proposed by Abarbanel is used for verification of Generalized synchronisation algorithm also called Global synchronisation. At a coupling value of $c_1=0.3$, the amplitudes are uncorrelated as shown in Fig 9.10(a) whereas for a coupling value of $c_1 =1.2$, the amplitudes are synchronised as shown in Fig 9.10(b). By finding, the MFNN index one can determine the generalized synchronisation. However the occurrence of phase synchronisation indicates the occurrence of generalized synchronisation not vice versa and hence the detection of phase synchronisation is important to understand the subtle aspects of the dynamics.
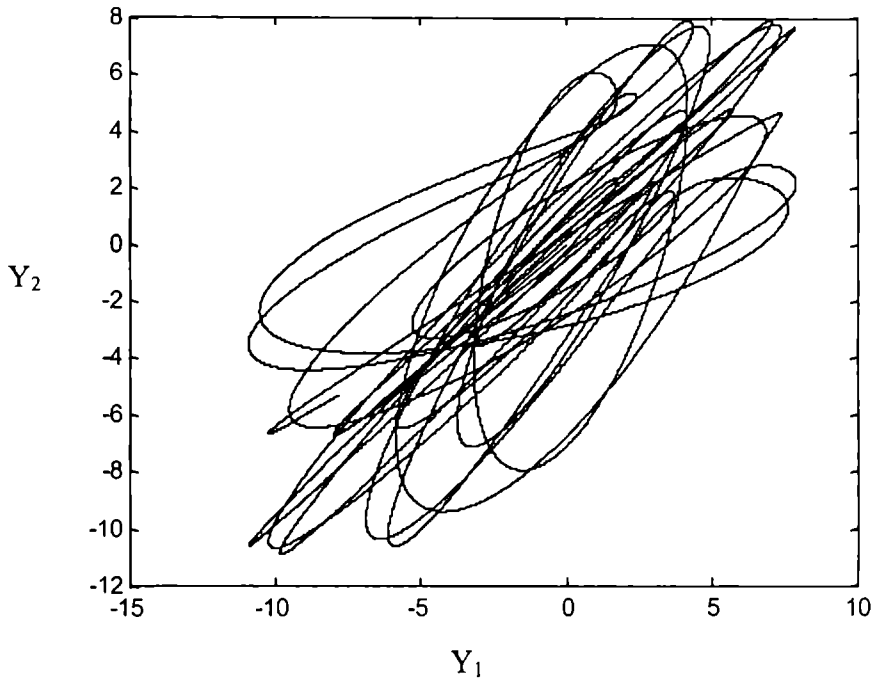
Fig 9.10(a) Y_1-Y_2 plot of coupled Rossler equation before amplitude synchronisation
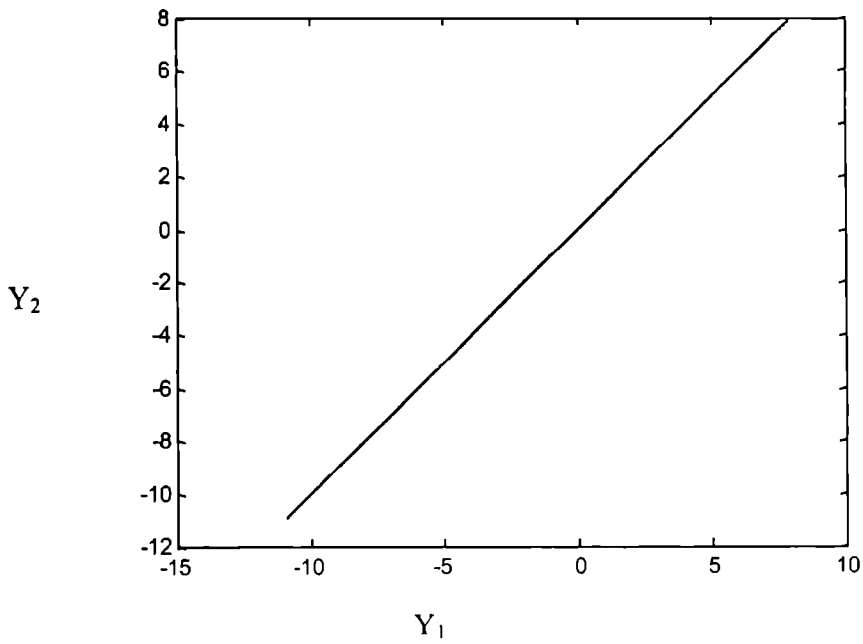
Fig 9.10(b) Y_1-Y_2 plot of coupled Rossler equation during amplitude synchronisation

The methods in SET 3 are developed as a part of this work. Hence, verification mainly depends upon the comparison with the existing methods. Thus, phase from Poincare map has been compared with the phase from analytical signal concept. To get a more reliable picture relative phase has been evaluated for the coupled system using Poincare map as well as Hilbert space. Phase synchronisation index, amplitude synchronisation index and Synchronisation Coherence index have been evaluated from a bivariate time series using relative phase / amplitude both from Poincare. The results are presented in the next chapter.

9.2 International 10-20 System

The International 10-20 system of electrode placement provides for uniform coverage of the entire scalp. It uses the distances between the bony landmarks of the head to generate a system of lines that run along and across the head and intersect at intervals of 10 or 20% of their total length. The electrodes are placed at intersections. The use of the 10-20 system assures symmetrical reproducible electrode placements and allows comparisons of EEG from the same persons and from different persons recorded in the same or different laboratories. The system is flexible: additional electrodes, which may be needed to accurately localize an abnormality can be incorporated by further subdividing the distances between the intersections.

The standard sets of electrode for adults are arranged as shown in Fig. 9.11. This arrangement consists of 21 recording electrodes and one ground electrodes. The recording electrodes are names with a letter and a subscript. The letter is an

abbreviation of the underlying region: Prefrontal or Frontopolar (Fp), Frontal (F), Central (C), Parietal (P), Occipital (O) and Auricular (A). The subscript is either the letter 'z' indicating zero or midline placement, or a number, indicating lateral placement. Odd numbers refer to the electrodes on the left, even numbers refer to electrodes on the right side of the head. The numbers increase with increasing distance from the midline except for the numbers of temporal and frontopolar electrodes that increase from front to back. The inferior frontal electrodes F7 and F8 are often called 'Anterior Temporal' electrodes because they fairly faithfully records activities from the anterior temporal area. In some pathological cases like scalp lesions it may be impossible to place electrodes in the positions of the 10-20 system. In these cases the electrodes should be placed as closely as possible to these positions and as symmetrically as possible on the two sides.
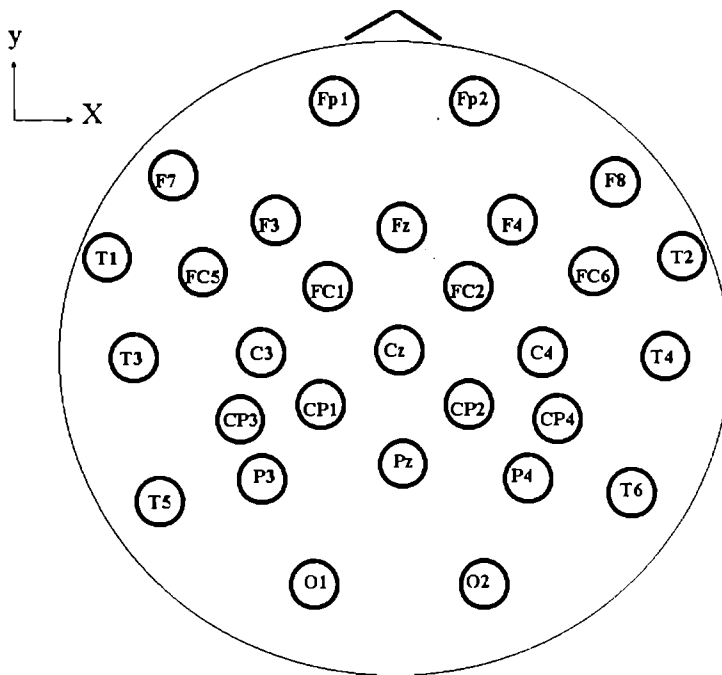
Fig. 9.11: Electrode placement in International 10-20 system

9.3 EEG Data

(data 1)

Five subjects who were known epileptics with uncontrolled seizures in the age group of 20 – 25 years were recruited for this study. Despite anticonvulsant medication the subjects showed seizure discharges in EEGs. The eight channels EEG data is collected using International 10-20 system with an EEG machine coupled to a PC using Analog to Digital Converter (DT- 2841) and an array processor (DT-7020). The eight scalp loci are Fp1, Fp2, F7, F8, T3, T4, O1 and O2. The sampling is done at the rate of 256 samples / sec / channel. The data is filtered using a bandpass (0.25 - 32Hz) fourth order butterworth filter twice cascaded. The data were visually screened to remove artifacts as well as to identify epochs containing epileptic discharges. Two experts who differed in their scoring by less than 5% performed the identification of epochs. The differences were resolved by discussion and a consensus rating was assigned to the discrepantly rated epochs.

The data from five normal volunteers without any history of neuropsychiatric illness or intake participated for acquiring data. Subjects were seated on a chair in a sound proof, electrically shielded room. Silver cup electrodes were attached as mentioned above at eight- scalp locii. They were instructed to be in a relaxed state. Online digital recording continued for 30-45 minutes for each subject and the procedure was repeated four times on the same subject. The signal were digitised at a sampling rate of 256 samples per channel per second.

(data 2)

The meditation EEG data set comprised of 16 channels of EEG data, which were acquired using an EEG machine (SynAmps, Neuro Scan, Inc. USA) coupled to a PC. The electrodes were placed as per the international 10-20 system of electrode placement. The corresponding electrode positions with that of the channel numbers are: Fp1 (1), Fp2 (2), F3 (3), F4 (4), F7 (5), F8 (6), C3 (7), C4 (8), T3 (9), T4 (10), P3 (11), P4 (12), T5 (13), T6 (14), O1 (15) and O1 (16). The data were acquired at a rate of 512 samples/channel/seconds and filtered using a bi-directional 150 order FIR digital filter with a bandwidth of 0.1–32 Hz. Three experts then visually screened the data and all suspected artifacts containing segments were deleted from analysis.

In order to understand the collective dynamics EEG from seven persons during meditation as well as before meditation is recorded. The meditation performed by the person is a form of meditation in Buddhist tradition called *Vipassana*. Vipassana is a Pali word – 'Vi' means in a special way and 'sana' means to see which translates into "look into yourself in a special way". This method of meditation is becoming popular in India and abroad[11]. Vipassana is a mindfulness of meditation whereas other forms of meditation fall under the category of concentration methods. " Seeing things as they are" is the feature of this method in which attention is turned into constant scrutinizing of each successive unit in thought continuum. Attention is focussed on one object but as thoughts, objects or feelings occur, they too are noticed and then attention is returned to the original focal object (Novak, 1996).

BRAIN DYNAMICS AS INFERRED FROM EEG

This chapter is the most important one in this thesis. All the results derived in the light of the discussion in the earlier chapters are presented in this chapter. The main aim of the present work is to study the collective dynamics from electroencephalogram and thereby investigate the possibility of applying the methods of nonlinear dynamics for clinical purposes. Further, this work also aims at developing a general framework to study the interactions in human brain. The starting point is the derivation of time scales in the framework of nonequilibrium statistical mechanics applied to biological system. Based on this framework the relevance of time scales on the dynamical parameters has been studied. This led to the study of collective dynamics of brain during cognitive process. However, the methods developed for study of collective dynamics using modern synchronization concepts have been modified to include non-linearity and stochasticity in dynamics. The new parameters developed such as phase coherence, amplitude coherence and coherence indices are applied to real data set. A method to find the effective potential from EEG time series has also been developed. This chapter is divided into three parts. In the first part the physical aspects of human brain dynamics has been discussed from nonlinear dynamical point of view. Second part deals with the cortical coordination and in the last part a general framework for evaluating the interaction in neocortex has been presented.

PART I: PHYSICAL ASPECTS OF HUMAN BRAIN DYNAMICS

In this section an investigation is conducted by viewing brain as a dynamical system. A study on nature of characterizing parameters during epilepsy and meditation is presented. Role of time scales in the nonlinear analysis of EEG during epilepsy is also discussed.

10.1 Significance of time scales in the analysis of EEG

The characterization of physical and biological systems in nonlinear domain is done using methods in nonlinear dynamics and deterministic chaos (Ott, 1993). The method of characterization depends mainly on the evaluation of ergodic measures such as dimensions, entropies, Lyapunov exponents' etc. These parameters are evaluated from a single time series. Eventhough, several physical systems have been characterized the evaluation of invariant parameter poses difficulty mainly due to presence of noise, nonstationarity, finite data length etc. (Rapp, 1993). The existence of chaos in human brain has been reported by many authors (Jansen et al, 1993) by evaluating some of the invariant parameters. The existence of chaos as well as the reliability of the methods has been questioned by introducing the method of Surrogated data analysis. However, the reliability of surrogated data analysis has been reexamined and it has been found that even this method is not quite infallible and is not suitable to distinguish colored noise from low dimensional chaotic signal. To resolve this pandemonium the present approach is to set aside the problem of existence or nonexistence of chaos and view the ergodic measures in a relative sense. Hence, an investigation has been conducted to understand the human brain from a

154

dynamical point of view. In this context the significance of time scales on nonstationarity and the information capacity has been discussed. The basic motivation is that if the time series were nonstationary then the different measures would also be time dependent unlike the case of stationary time series where these measures are independent of time.

Human brain dynamics involve three fold infinite time scales as has been discussed in the chapter 7. Many authors in studying the dynamics of human brain have ignored the role of time scales. Parikh and Pratap (1983) developed an evolutionary equation in the framework of nonequilibrium statistical mechanics developed by Prigogine and his Brussel School in which for the first time the significance of time scales in the collective dynamics of human brain has been stressed. Further, Pratap (2000) formulated a theory of sensory transduction considering the interaction of time scales. In this investigation the relevance of time scales in the nonlinear dynamical analysis of EEG has been performed.

EEG recordings of five subjects who were known epileptics with uncontrolled seizures in the age group of 20-25 years were used in this study (data1). The data from five normal volunteers without any history of neuropsychiatric illness or intake of any psychotropic drugs who were in the age group of 20-25 years were also collected. The data is reconstructed as a multivariate vector $X(i) = \{x(i), x(i+Td), \ldots\ldots\ldots, x(i+(m-1)Td\}$ with time lag $Td = n\ Ts$. Ts is the sampling time and n an integer, and Td is determined from average mutual information (AMI) criteria (Fig.10.1).
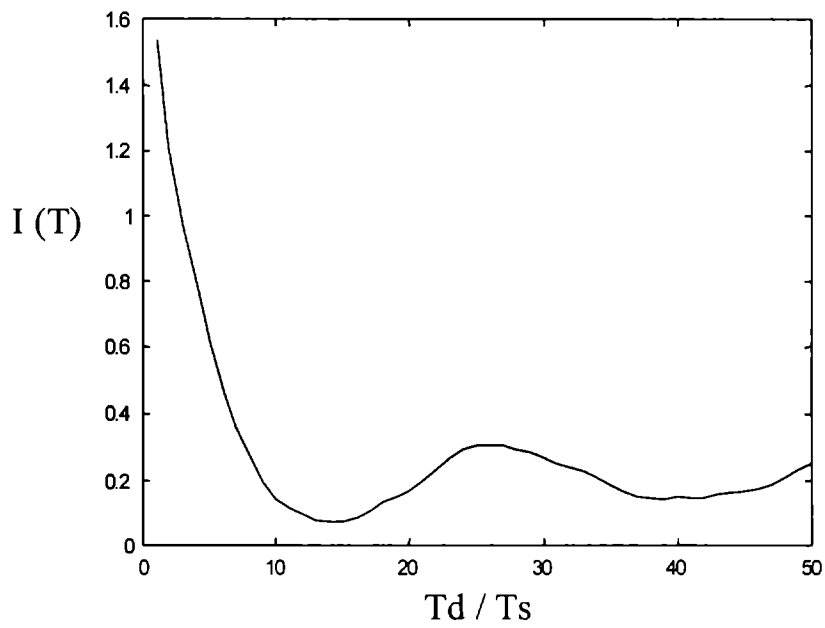
Fig. 10.1: AMI curve of Fp1 for a normal eyes closed data (n=14)
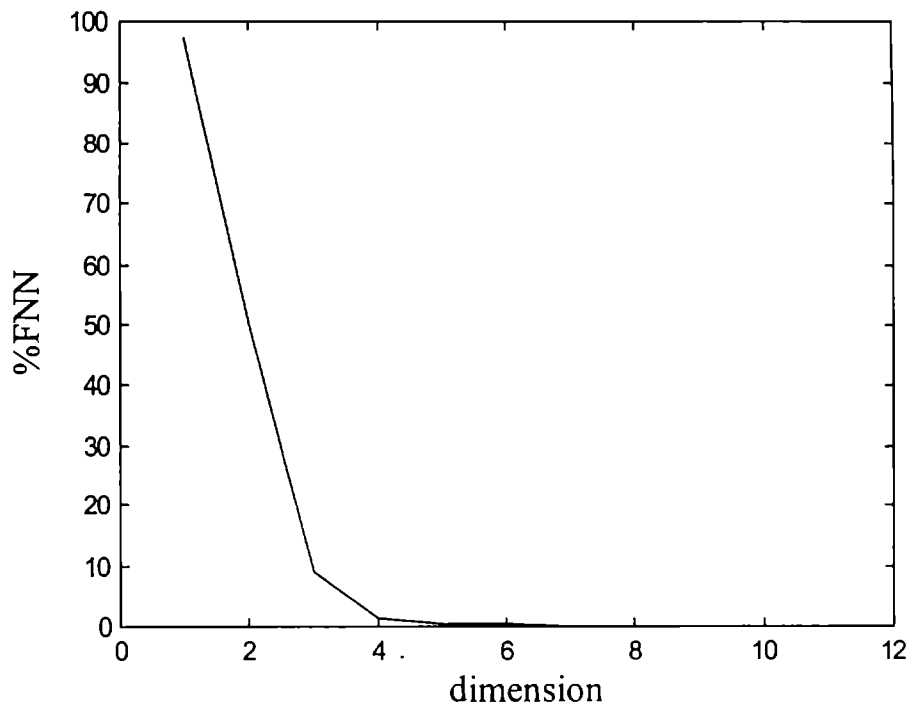
Fig. 10.2(a): Percentage of False Nearest Neighbor of normal eyes closed data at Fp1

The parameters Correlation dimension and Kolmogorov entropy evaluated with a few dimension values greater than the embedding dimension determined from the Global False Nearest neighbors with the threshold R_t fixed at 10 and A_t at 2. (Abarbanel et al, 1993). Percentage nearest neighbors against dimension for a particular window for the case of eyes closed and epileptic data are given in Fig 10.2(a) and Fig. 10.2(b) respectively. The data set selected from each channel simultaneously consists of 12000 data points and they are grouped into different nonoverlapping window of length 1000 points. The Kolmogorov entropy are calculated for each window.
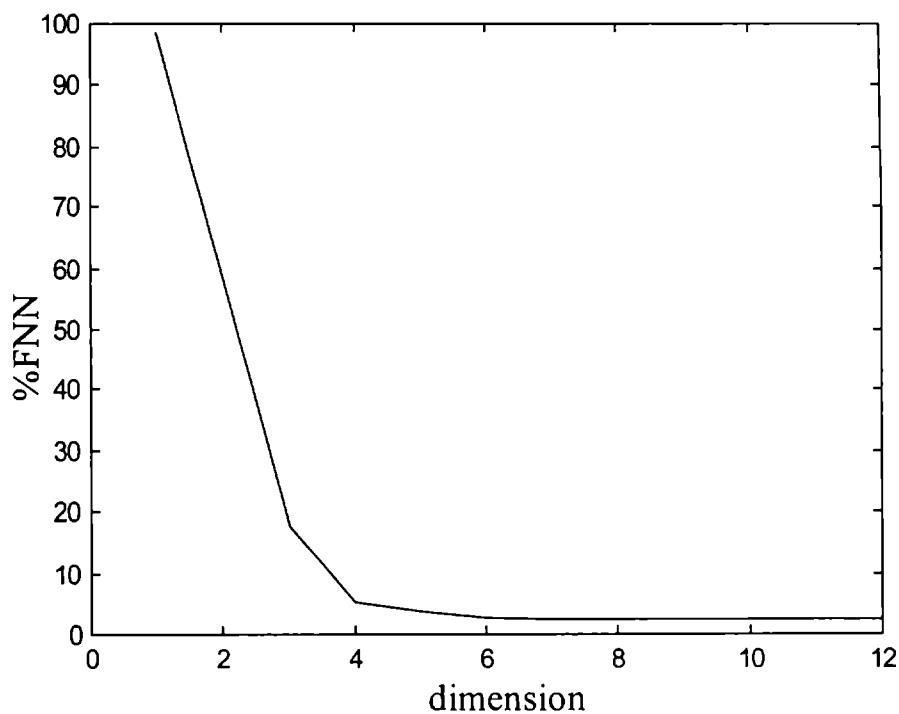
Fig. 10.2(b): Percentage of False Nearest Neighbor of Epileptic data at Fp1

Any nonlinear dynamical system can be characterized accurately only if all its invariant parameters are determined. This requires the identification of different time scales involved in the dynamical process. It should further be emphasized that ergodic parameters are indeed important the ultimate goal should be an understanding of the dynamics of the system. It is therefore important to propose a model that would generate these parameters and which has predictive capability. As a starting point an investigation of time scales in human brain dynamics is conducted in chapter 7. The significance of time scales especially on dynamical parameters has been discussed.

It has been previously noted that the values of invariant parameters are different at different locations of the brain. From a nonlinear dynamical point of view if the system were a simply connected one, extending over the entire brain, then the time series generated from different locations should give the same value of the invariant parameters. However in the case of human brain, the values of the invariant parameters are different at different locations. It can therefore be inferred that the system has several sub systems with different sets of dynamical equations. Since it has been theoretically established that human brain dynamics consist of a large number of time scales, a proper characterization of the dynamics is possible only if all its relevant time scales are identified. This indicates that there exist a large number of attractors of different characteristics distributed in the brain. These attractors interact to form different patterns depending upon the dynamics. A plot of ln C(r) Vs lnr of EEG at Fp1 of normal eyes closed data is given in Fig 10.3. The

graph indicates a scaling region and the value of the slope obtained is 4.63643, which

is the correlation dimension D2.
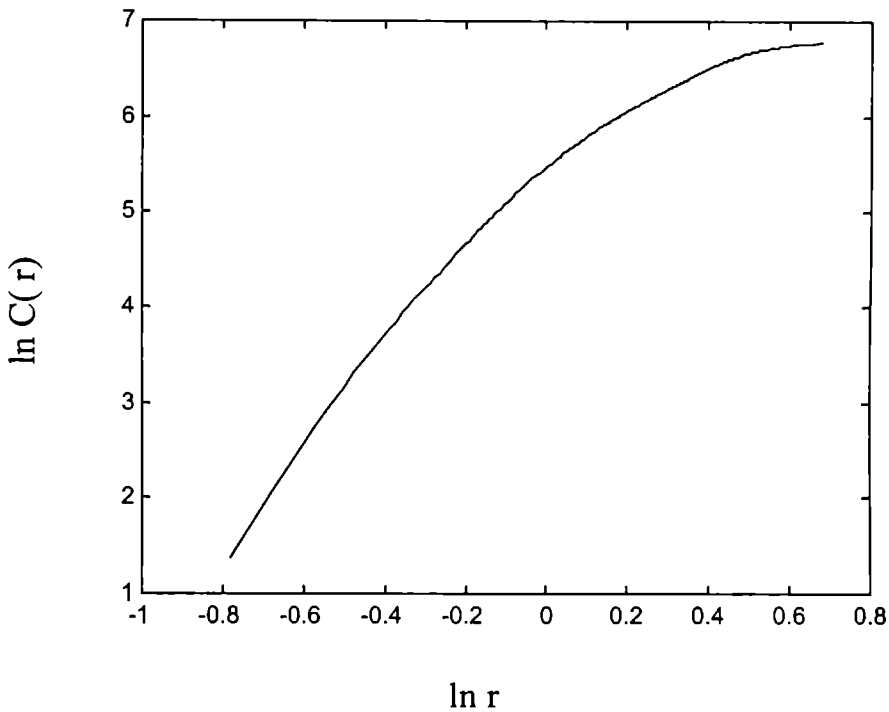
Fig. 10.3: ln C (r) Vs ln r plot of EEG at Fp1 of Normal eyes closed data.
[d_E =8, Td=14 Ts]

By calculating Td from AMI, it has been found that the values are distinctly

different for different windows as well as different for different channels (Fig 10.4).

This indicates nonstationarity. Since the time lag is a measure of time scale in the

system, the variation of this proves the existence of different time scales in the

dynamics. The average values of time lag Tav for five adjacent windows as well as

time lag, Tgr, grouping the same five windows together are evaluated for epileptic as well as for normal eyes closed case.
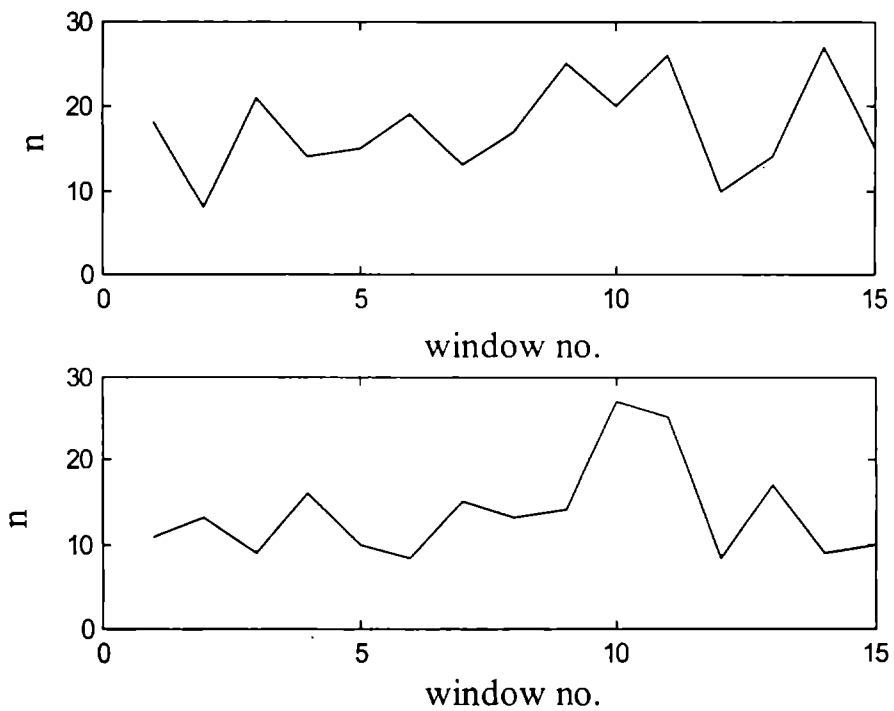
Fig.10.4: Variation of Td / Ts against window number for an epileptic data
(a) at Fp1 (b) at O2

For the epileptic condition, these windows are selected as one with predominant epileptic seizure condition and two on either side. In the case of normal subjects with eyes closed, Tav and Tgr are very close and very often coincides for most of the channels whereas for epileptic data the values are quite apart in many of the channels as given in Table 10.1.

Table 10.1: Tav and Tgr during normal eyes closed and epileptic conditions.

Channel No.	(Normal eyes closed)		(epileptic discharge)	
	Tav	Tgr	Tav	Tgr
1	7.0	7.0	13.4	20
2	7.1	8.0	20	28
3	7.0	7.0	15	15
4	7.7	8.0	13	13
5	8.0	8.0	11.6	23
6	8.0	8.0	11.6	20
7	6.8	7.0	15.4	22
8	7.0	8.0	17.2	20

Eventhough the variation of time lag is an indication of time scale in the system, the difference in Tgr and Tav, especially when Tgr greater than Tav indicates that during epileptic condition the time scales involved in the dynamics are more in number as compared to normal eyes closed condition. Further, it has been found that for those windows with predominant epileptic discharge the value of Td is comparatively larger than the other windows. This is because during epileptic condition many more time scales are introduced into the dynamics which are reflected in Td. Thus, nonstationarity is due to time scales of the system. In spite of these limitations, several attempts are made to study the dynamics of human brain from the nonlinear standpoint. One should realize that all the invariant parameters D2 and K2 are evaluated at the same value of time lag (Popivanov et al., 1998). The evaluation of the invariant parameters especially the dynamical parameters, for pathological conditions needs caution as they involve interaction of different time scales.
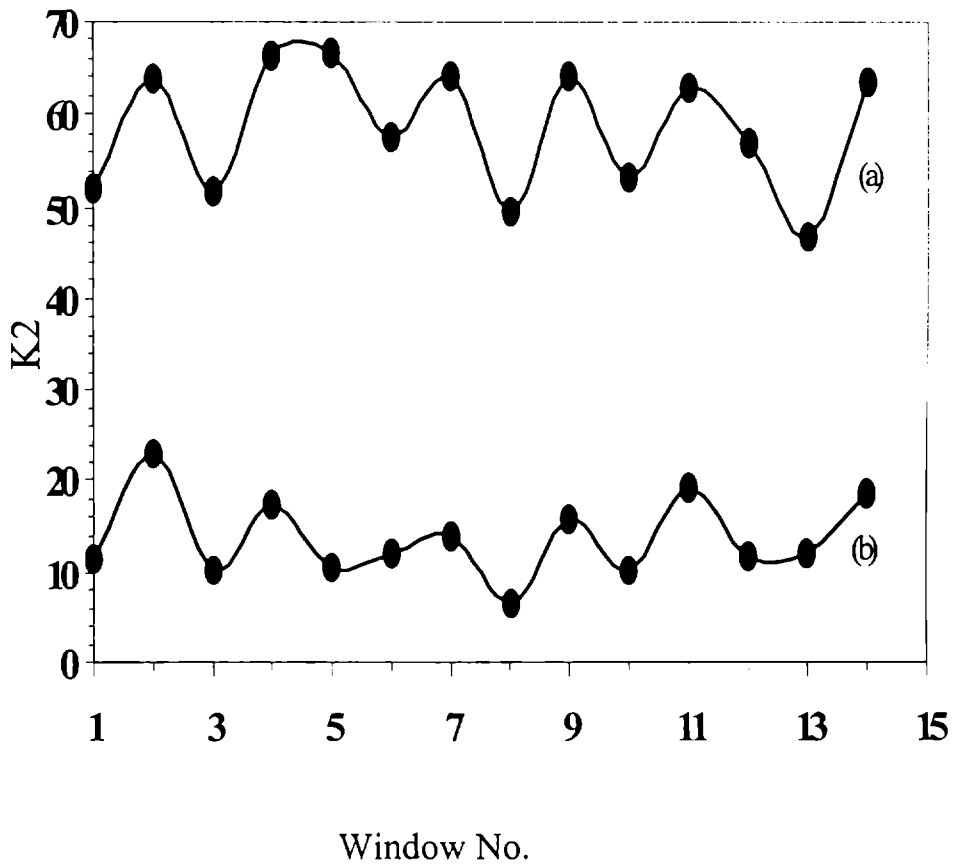
Window No.

Fig 10.5: K2 with respect to window number for normal eyes closed data at Fp1

(a) corresponding to T_s and (b) corresponding to T_d

It has been found that for normal eyes closed condition, K2 with Td as well as with Ts show a certain degree of parallelism in variation with respect to windows as shown in Fig 10.5. However K2 with Td and Ts bears no resemblance whatsoever for epileptic condition as in Fig 10.6.

162
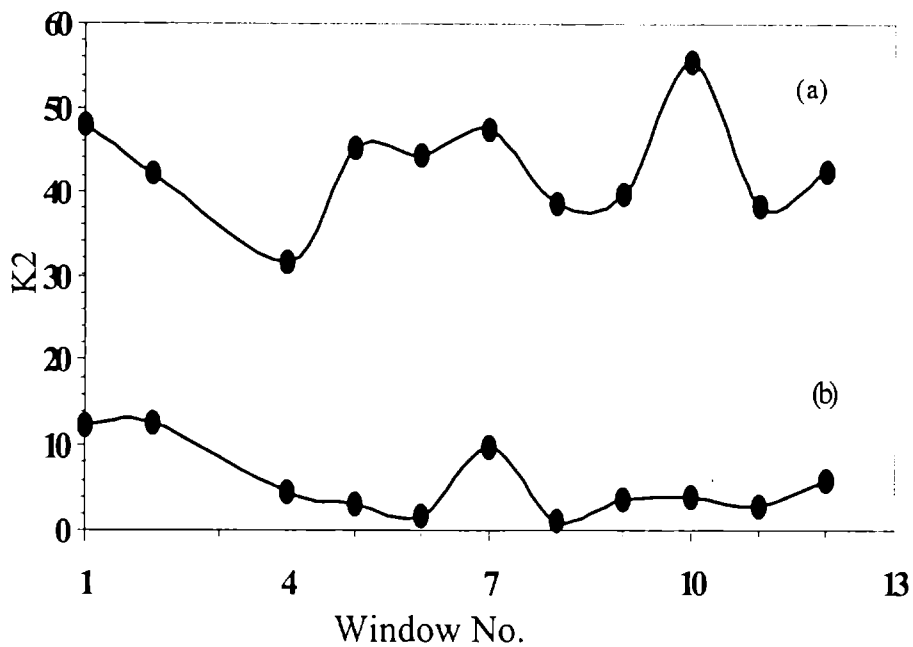
Fig 10.6: K2 with respect to window number at Fp1 for epileptic data

(a) corresponds to Ts and (b) corresponds to Td

Further, K2 with Ts has larger value and variation compared to K2 with Td. This is because during epileptic condition the time scales involved in the process are more, which in turn show a larger value of Td in AMI criteria. As time lag increases in the phase space reconstruction, many interactions are lost which in turn masks the dynamics corresponding to time scales within the time lag Td. This affects the evaluation of entropy. Hence, K2 with Ts shows more variation compared to K2 with Td in the case of epileptic data. However the variation of K2 with respect to different values of time lag for the case of epileptic as well as for normal eyes closed condition are identical as shown in Fig 10.7
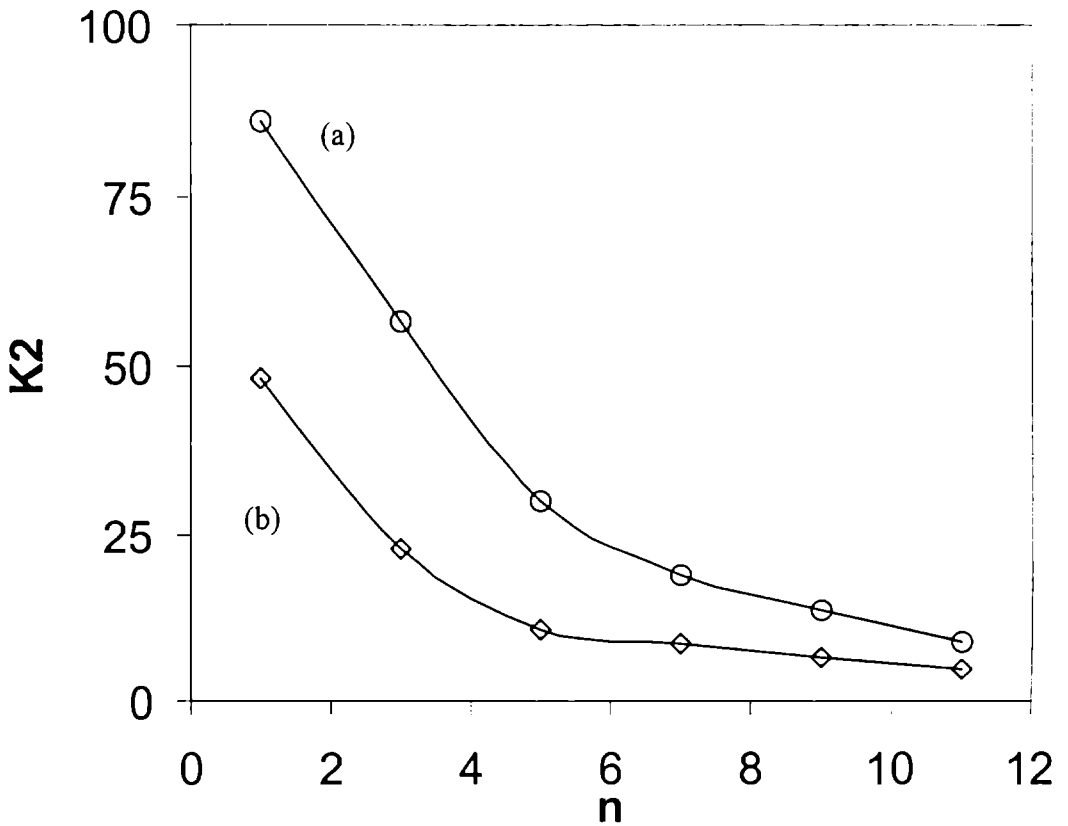
Fig 10.7: Variation of K2 for different values of n (Td/Ts)

(a) Normal eyes closed data (b) epileptic data

This indicates that the selection of time lag from AMI or any other similar criteria should be used only for D2. K2 being the dynamical parameter should be evaluated with a lag time as small as possible to incorporate as many time scales as possible. This conclusively proves that the selection of time scales for different pathological conditions are very crucial as the criterion differs for different conditions.

10.2 Inferring Dynamics of brain from EEG during meditation

The neural dynamics in meditative states are not well understood to date and an objective validation of such states is indeed necessary. Studies have shown that autonomic control, increased coherence and alpha pre-ponderance are dominant in experienced meditators. However, many of the findings need to be established and a search for realistic neurophysiological model that may explain such finding is essential for a scientific understanding of yoga and meditation. Further, the meditative practices are currently being viewed as an alternative mode for health promotion and better living. The recent developments in the physics of complex systems and nonlinear sciences provide a new opportunity for neuroscience to pursue the analysis of brain as a dynamic physical system. The problem of conscious autonomic control is associated with issues of chaotic feedback control of heart and brain. Here meditation as a tool to explore the brain mechanisms of higher cognitive states has been used. Nonlinear dynamics is fundamentally a different approach in the analysis of brain states, where one visualizes deterministic mathematical models of neural systems which give rise to complex dynamics in the presence of stochastic fluctuations.

There are reports giving different dynamical parameter of brain during various pathological and mental conditions of brain. Several studies have shown remarkable change in EEG, GSR, metabolic activity and heart rate during meditation (Mc Evoy et al, 1980). There are reports of changes in brain stem activities in processing evoked responses (Stigsby et al, 1981). Also, there are reports of EEG changes during meditation using spectral analysis (Benson et al 1990). It is quite

natural to assume that under mediation there may be a shift in brain dynamics because of focussed attention and other meditation related breathing control or psychomotor effects. The EEG record of volunteer during Vipassana meditation (data2) has been employed in some of the investigation. The data has been divided into different nonoverlapping windows. Data in each window is reconstructed in a phase space with time lag from AMI and the selection of embedding dimension from Global False nearest neighbors as described in the previous case.

It has been found that the average values of D2 and K2 are higher as compared to "premeditating state" in all the channels as shown in Table 10.2. This indicates that during meditation the degrees of freedom as well as information capacity increase. Further the complexity of the system also increases. To further clarify these points the Least upper bound (maximum), LUB and the Greatest lower Bound (minimum),GLB are determined for all the channels in both the conditions as shown in Fig. 10.8 and 10.9. Except for the Greatest lower bound of K2 all the values are distinctly different for all the channels. It may be realised that during meditation as there is no "external input", the only possibility for this behaviour is that during meditation the deterministic component shrinks and the background random firing becomes dominant. This manifests itself in a larger attractor and greater entropy. An alternate view could be that during meditation the lower dimensional attractors coalesce to make larger ones. Also noise introduces coherence by taking advantage of stochastic perturbation, which result in a high dimensional state.

Table 10.2: Average value of D2 and K2

Channels	Before Meditation		During meditation	
	D2	K2	D2	K2
Fp1	6.36	4.87	7.80	6.87
Fp2	6.17	4.86	8.14	7.00
F3	6.15	4.52	8.13	7.57
F4	6.30	5.30	8.37	6.81
F7	6.11	4.62	7.97	7.19
F8	6.45	3.98	8.77	7.53
C3	6.01	5.09	7.87	7.50
C4	6.23	4.89	7.88	8.46
T3	6.44	5.71	6.98	7.42
T4	6.51	6.46	6.92	6.60
P3	5.48	4.71	7.74	10.47
P4	5.47	5.11	8.14	8.52
T5	5.40	5.12	7.84	8.12
T6	5.55	5.87	8.12	6.92
O1	5.22	4.90	7.62	7.10
O2	5.67	5.19	8.18	9.40

No. of windows : 15, $d_E > 12$, No.of data points in each window = 1000
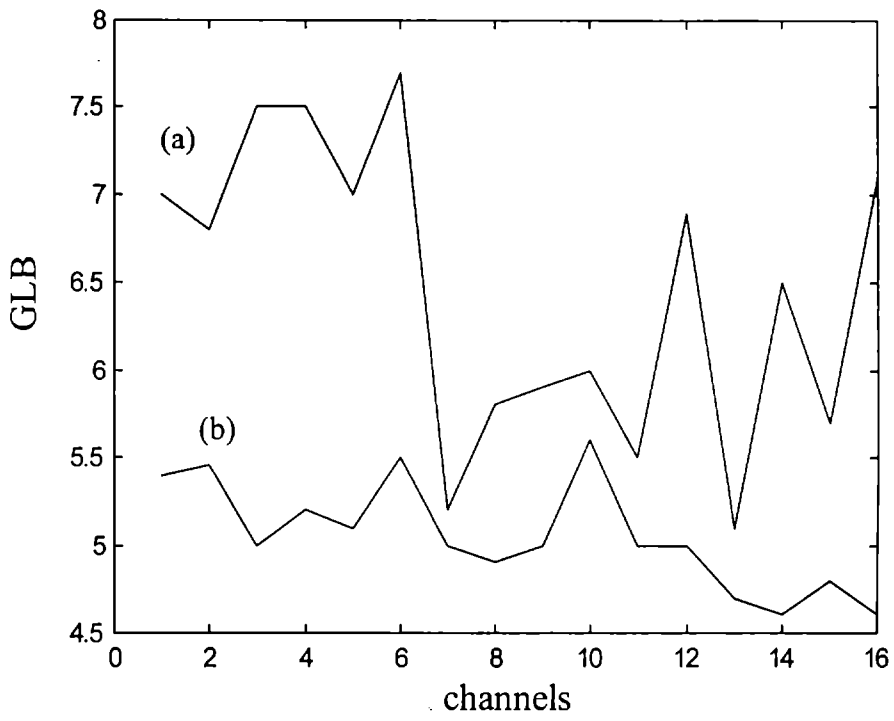
Fig 10.8(i): GLB value of D2 against channels (a) meditation (b) eyes closed
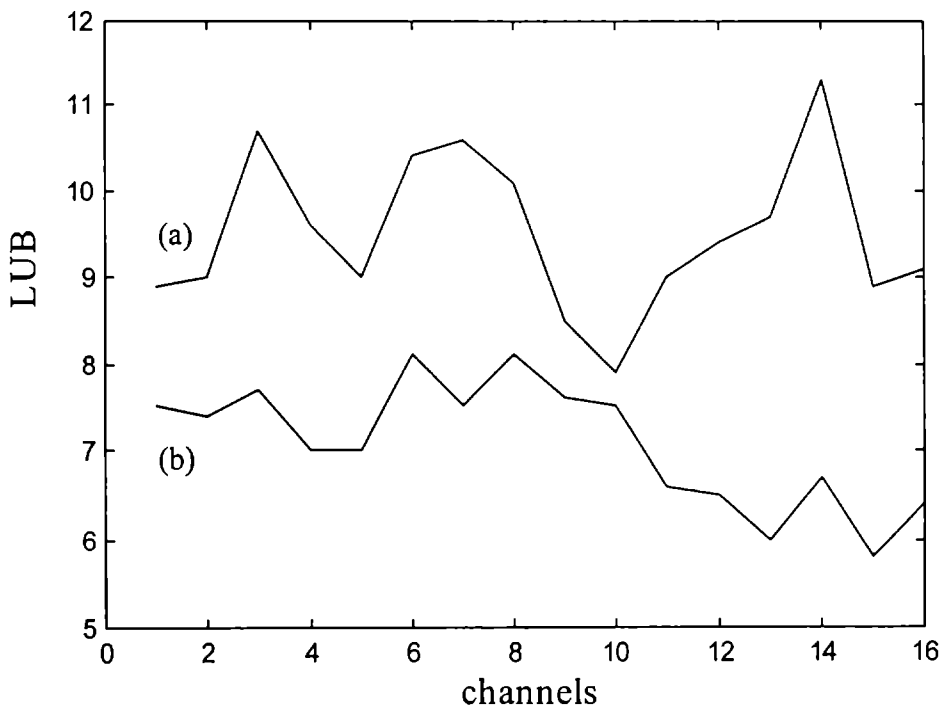
Fig 10.8(ii): LUB value of D2 against channels (a) meditation (b) eyes closed

168
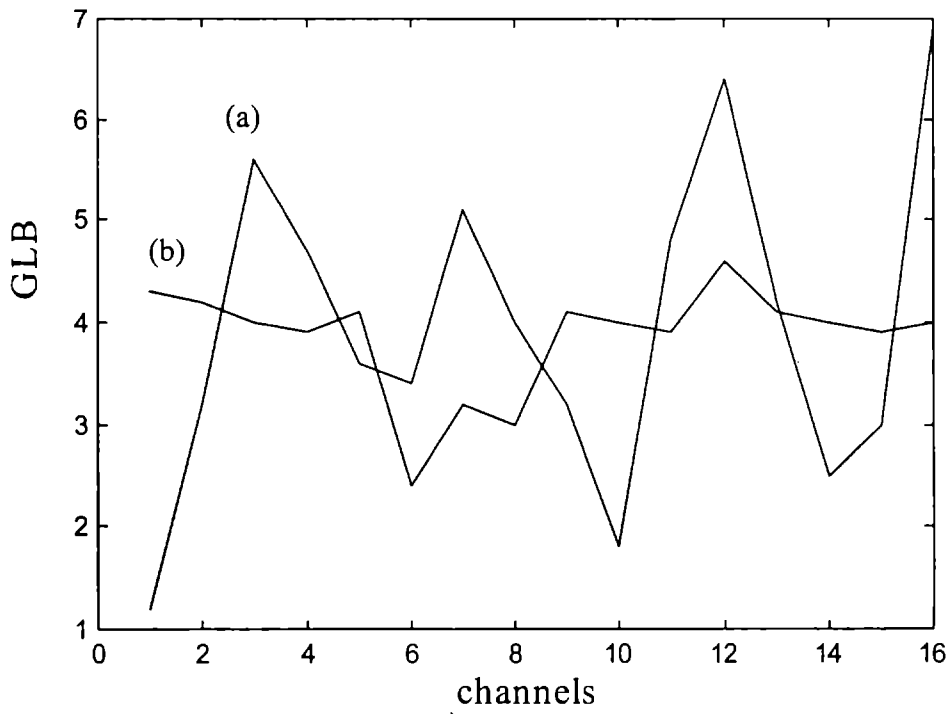
Fig 10.9(i): GLB value of K2 against channels (a) meditation (b) eyes closed
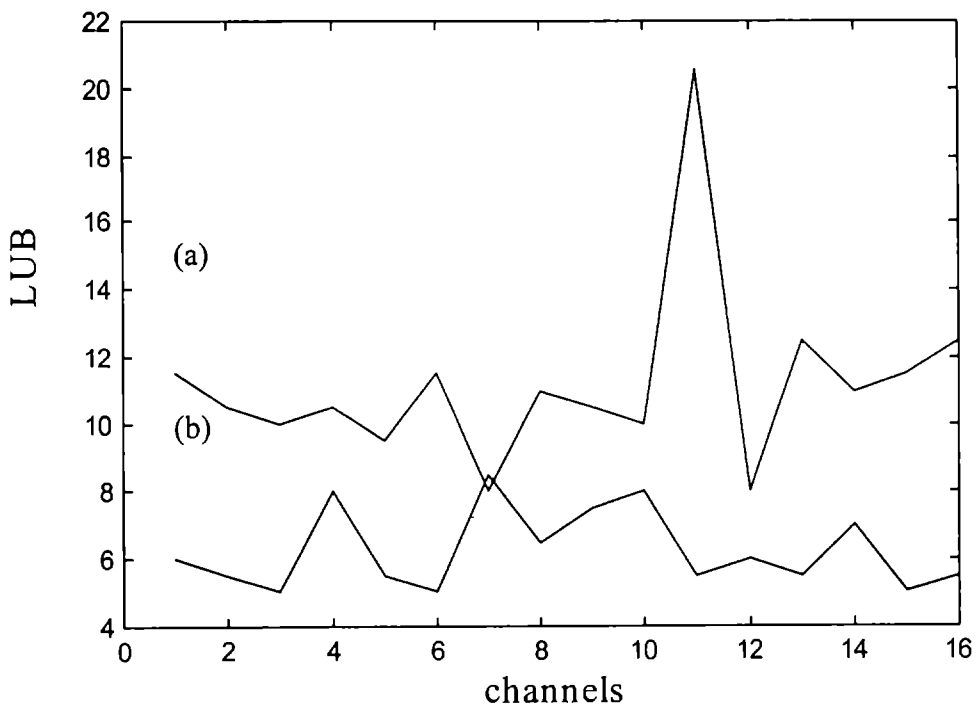
Fig 10.9(ii): LUB value of K2 against channels (a) meditation (b) eyes closed

169

PART II: CORTICAL COORDINATION

In the previous section it has been shown that human brain dynamics involve different time scales which in turn indicates that there are large class of attractors. This shows that the dynamics of brain during a process can be viewed as a result of coordination of different regions of brain. In this section the coordination of different regions of brain has been investigated with a view to study the collective dynamics.

10.3 Understanding coordination of brain regions – Analytical Signal approach

In the first section a method is introduced in which it has been shown that phase synchronization can be used to obtain an insight into the mutual interaction between sub systems in the neural system. It has then shown that these can be used to enhance an understanding of human brain as an action dynamic system. The data from a subject who practises meditation of the Vipassana scheme is recorded. In this as the subject starts the meditating state and in the initial state his thoughts go over to all kinds of uncorrelated domains. He allows this to happen in the beginning stages and slowly brings it back to a focussed state. This is a Buddhist mode and is different from either Transcendental or Vedic meditation. The final stage of Transcendental meditation is sleep while in Vedic schemes, the focussing effort is done right at the beginning. Data is collected from a subject who is a regular practitioner of this mode. The first part of the data is when the subject is before entering into the meditation process. It should be realised that this state from a regular practitioner is different from one who does not do meditation at al. However for the present study this gives the difference between a non meditating state and meditating state for the same

subject. It may be mentioned that the data from two different persons, one a practitioner and the other a novice will have different psychological make up and this adds to the existence of unknown parameters that would influence the performance. This disparity can be minimised if one collect the data from the same subject under different states of meditation.

Chaos is expected in nonlinear feedback systems possessing time delays from the periodic forcing of neural oscillators and as such, is expected to produce recurrent inhibition and other effects. Understanding the changes in dynamical invariants and phase entrainment are the preliminary steps in understanding the basic brain mechanisms during meditative practices. During meditation subjects have focused attention. An investigation is conducted to understand the co-ordination of brain regions before and during meditation.

To study the phase synchronization of different regions of the brain, instantaneous phase of the signal (data 2) from each channel is calculated by means of Hillbert transform. To search for ($\varphi_{(1,1)}$) locking, a histogram of relative phase distribution is drawn from the phase difference between two channels and a peak in the histogram ensures phase locking. To characterise the strength of interaction, deviation of actual distribution of relative phase from a uniform one is determined. Thus interaction between two cortical locations is determined by finding ρ, the synchronization index from a bivariate data set. The index ρ takes values between 0 and 1. $\rho = 0$ Corresponds to absence of synchronization while $\rho = 1$ corresponds to perfect synchronization. The present analysis is restricted to (1:1) synchronization.

The synchronization index during pre-meditation resting eye-closed state reveals strong interactions among various brains, whereas the synchronization index decreases during meditative state of the same subject. In resting pre-meditative state different brain regions have mutual interactions with varying degrees of synchronization. However during meditation, the synchronization index is reduced across many channels. This could possibly be explained that prior to meditation, the Brain State is manifestation of conscious interaction with the external world, the internal thought processes and perceptual mechanisms. The ongoing associative neural processes stimulate phase synchronization of oscillators in different locations of brain. These associative process of the brain result in the awareness of the external and internal world and brain is involved in the generation of a number of independent input / output commands in response to such awareness. Fig 10.10 (a&b) gives the histogram of relative phase distribution ρ between pre-frontal and frontal region in the left hemisphere of the brain.

Magnitude of relative phase
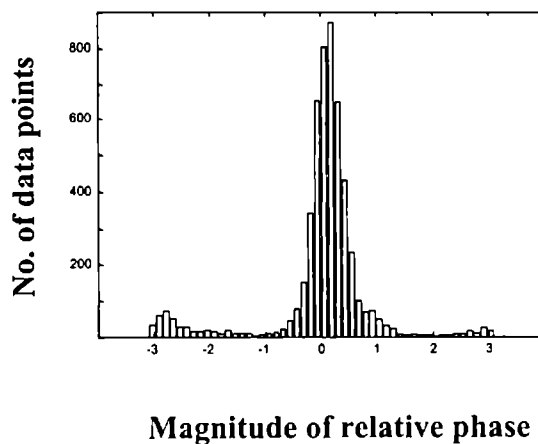
Fig 10.10 (a): Histogram of relative phase prior to meditation between Fp1 and F3 for a particular window (ρ = 0.308)

Magnitude of relative phase
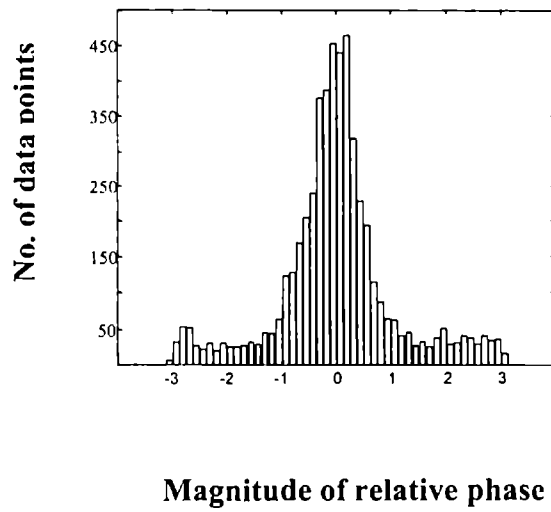
Fig10.10 (b): Histogram of relative phase during meditation between Fp1 and F3 for a particular window (ρ= 0.1454)

Magnitude of relative phase
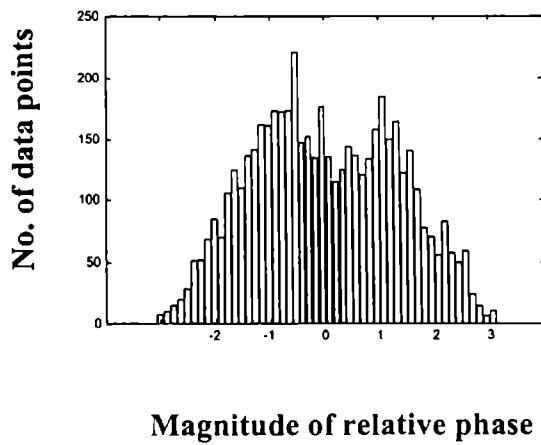
Fig 10.10 (c): Histogram of relative phase prior to meditation between Fp1 and T5 for a particular window (ρ = 0.048)

Before meditation, one can observe a peak in the relative phase distribution whereas during meditation, the distribution is broadened indicating that the co-ordination between the two regions is reduced. Fig 10.10(c) gives the histogram of relative phase distribution of pre-frontal and temporal region again in the left hemisphere before meditation. There is no sharp peak and the distribution is very much broadened indicating a very little interaction. Similar observation is also obtained during meditation in these regions. Fig 10.11 gives the strength of interaction calculated for running windows of duration 2 seconds between right prefrontal region and the left frontal region. The observed interaction between left and right hemisphere is an indication of information flow between the two lobes of brain.
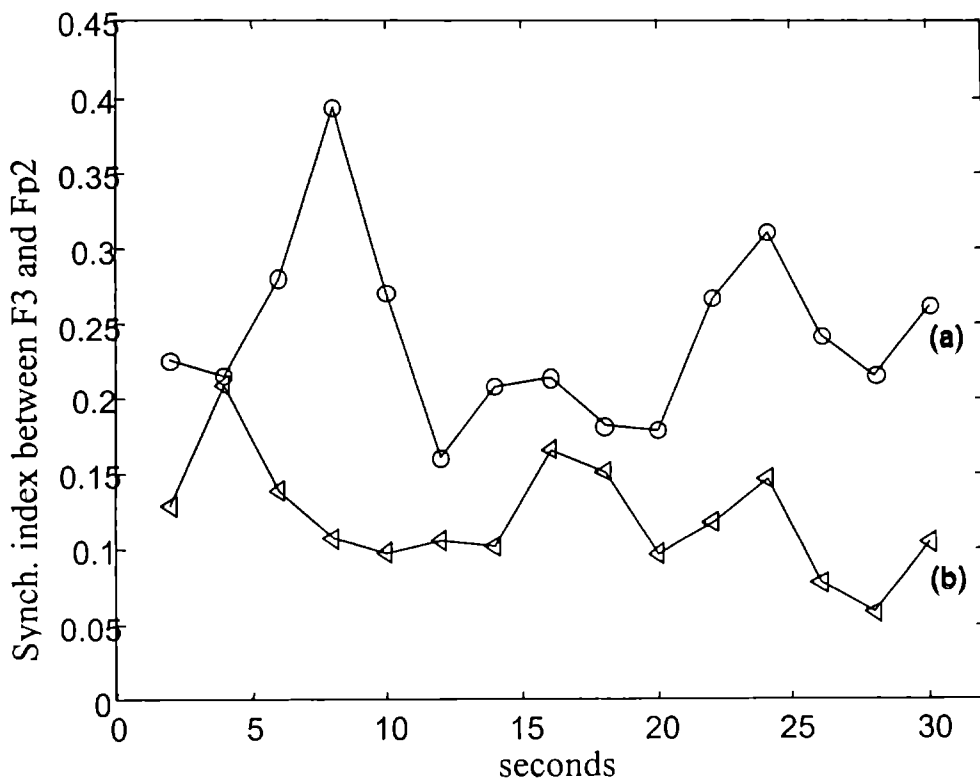
Fig 10.11: Synchronization index between F3 and Fp2. (a) Before meditation eyes closed (b) During meditation

The synchronization index during pre-mediation resting eye-closed state reveals strong interactions among various brains. Whereas the synchronization index decreases during meditative state of the same subject as shown in Fig 10.12.
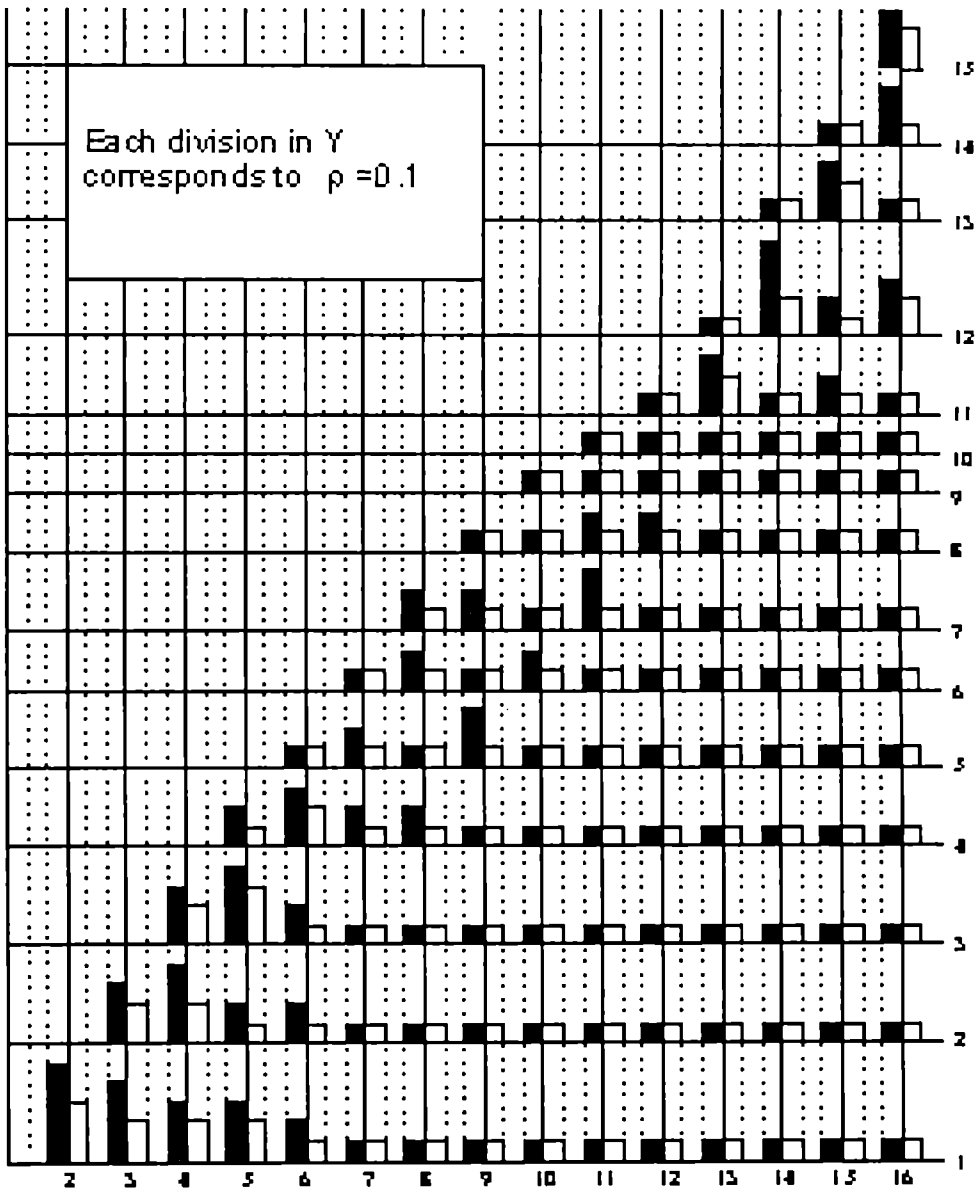
Fig 10.12: Average value of synchronization index. Dark shade corresponds to before meditation and white corresponds to during meditation.

The phase synchronization index is calculated using a single window of 4096 data points. This shows that the co-ordination is reduced as the distance between locations gets increased.

The above investigation on meditation strongly tempts one to consider the brain as a system of collection of different classes of attractors and before meditation, they interact to form structures with reduced complexity or degrees of freedom. This is an indication of the setting in of coherent state, which describes the functioning of brain as a single entity. During meditation many interactions are reduced, which are reflected in the values of synchronization index, the attractors have more degree of freedom, which results in a comparatively larger value of D2 and K2.These results presented here give an insight into the collective dynamics of brain in general.

This study shows that the different parts of the brain interact more strongly during non-meditating state as compared to meditating state. This can be explained based on the fundamental aspects of meditation. During eyes closed condition different regions of the brain interact with each other through thought process to get a coherent state. Interaction between different regions of brain, as stated earlier, generates associative memory. During meditation, one is trained to control thought processes, which will lead to de-coupling of different regions of the brain. This is clear from the lowering of values of synchronization index. This suggests that during meditation the brain is free from external and internal stimuli and moves to expansive state with greater degree of freedom. Neocortical synchronization is seen

as the necessary mechanism to thought process. The phase-synchronization index across various zones of the neocortex shows weak interactions during meditations. It may thus causing less stress to neural system and the mechanism may be helpful in studying the effect of meditation on mental stress and other related psychological problems. It may prove beneficial in the study of synchronization for different pathological conditions like seizure or epilepsy. From a statistical viewpoint, one can realize that brain system achieves greater coherence when it interacts with the external world. When the subject goes over to meditating state this coherence is lost. The transition may be viewed as emergence or structure / pattern formation in a nonlinear evolutionary system with on and off mechanisms. Further, the system is thermodynamically open which gives scope for unlimited state transitions. Further these results show the potential application of meditation for the treatment of neuropsychiatric disorders.

PART III: DYNAMICAL ASPECTS OF NEOCORTEX

A method to find the attractor potential is presented in this section. A new method to evaluate phase and amplitude of the time series from Poincare map is discussed. Using phase and amplitude coherence a new index called Coherence index is derived and this index along with other characterizing parameters used for studying the attractor interaction.

10.4 Determination of Phase from Poincare map

The widely used method to evaluate the phase of an arbitrary signal is using the concept of analytical signal theory proposed by Gabor. In this method phase of an arbitrary signal is evaluated by defining an analytic signal in which the real part of the analytic signal is the original signal whereas the imaginary part is the Hilbert transform of the signal. The basic notion in analytic concept is that the phase of an arbitrary signal changes linearly with time. Hence, phase can be evaluated by finding inverse tangent of the ratio of the imaginary part to real part of the analytic signal. However, this method of evaluation of phase is inaccurate in the case of data from nonlinear system, as in a nonlinear system the "phase changes linearly with time" need justification. Further Hilbert transform is a quadrature filter (Papoulis, 1984) that will nullify most of the nonlinear effects. Therefore, a new method has been introduced in which phase is defined using Poincare map. This section presents the inadequacy of phase definition from Hilbert transform that lead to the definition of phase from Poincare map. A comparative study has been conducted by evaluating the phase using Hilbert as well as Poincare map for Mixed sine waves, Rossler equation,

178

Nonlinear Langevin equation and EEG time series. The phase evaluated using Hilbert and Poincare for the time series generated for sets of sine waves (*standard data set d*), are presented in Fig 10.13 to Fig 10.15. The data simulated using a time step of inverse of ten times the maximum frequency content in the signal
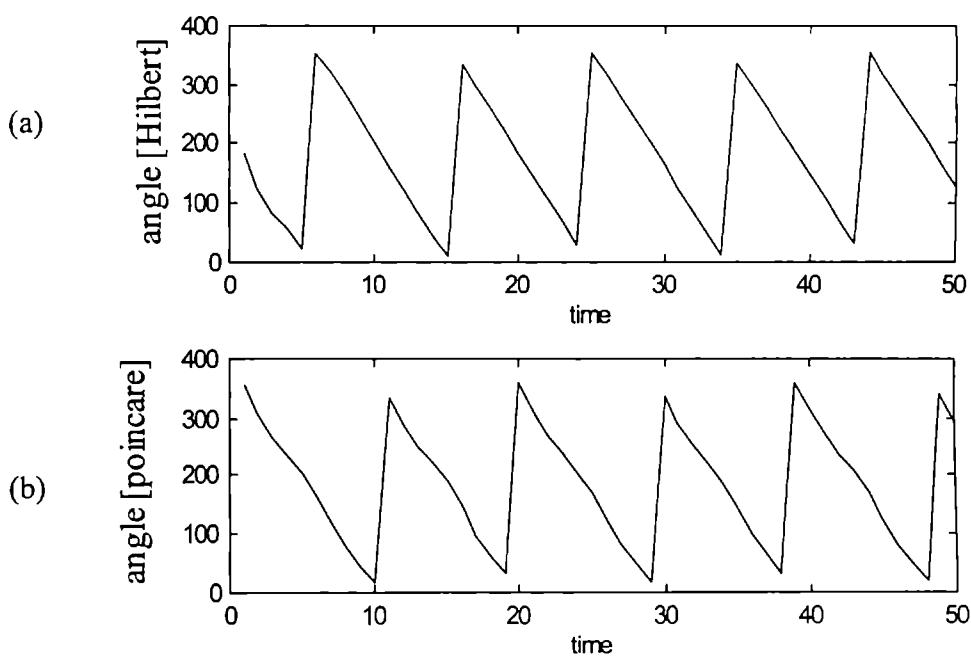

Fig 10.13: Phase evaluated for sine wave of frequency 7Hz using (a) Hilbert and (b) Poincare method.
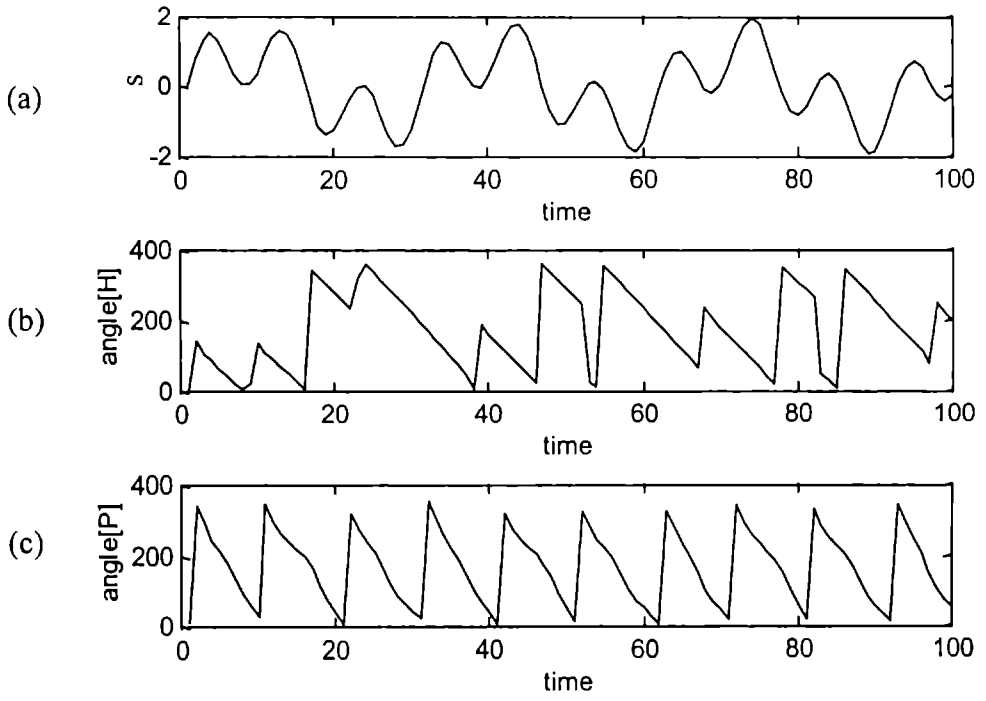
Fig 10.14: Phase evaluated for mixed sine waves of frequencies 7Hz and 22Hz

(a): Time series, s (b): angle evaluated using Hilbert method and

(c) angle from Poincare method

(a)

(b)

(c)
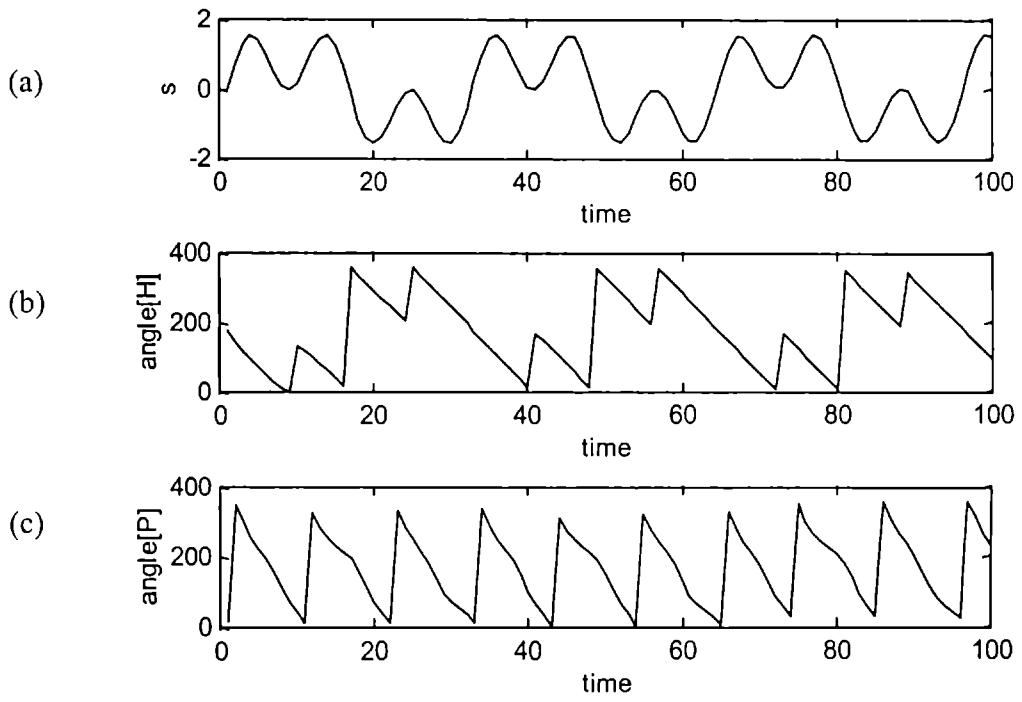
Fig 10.15: Phase evaluated for mixed sine waves of frequencies 7Hz and 21Hz

(a): Time series, s (b): angle evaluated using Hilbert method and

(c) angle from Poincare method

It has been found that the variation of phase for the case of sine wave with a single frequency is identical both in analytical and Poincare plane. The variation is in the 0 to 360^0 range and is true for a sine wave whose phase is well defined. However, in the case of mixed sine wave the variation is different as the Poincare map represents the close return of the trajectory as the evolution of one cycle. In Hilbert representation, the variation of phase is close to largest time scale in the signal in the case of mixed sine waves. This has great implication when the frequencies are incommensurate especially when the amplitude ratios are not unity.

The time series of Rossler equation (*standard data set c*) used for the evaluation of phase is presented in Fig. 10.16(a) while phase evaluated using Hilbert transform is presented in fig. 10.16(b) and Fig. 10.16(c) represents the phase from Poincare space. The notion that phase changes linearily with time fails in the Poincare representation, as the nonlinear structure is predominant in phase from Poincare map. This has to be accounted for as in the case of nonlinear system, since the nonlinearity inherent in the system can cause phase that is not linear with time. The Hilbert representation thus becomes only a qualitative variation of phase whereas Poincare representation takes into account the subtle aspect of the dynamics.
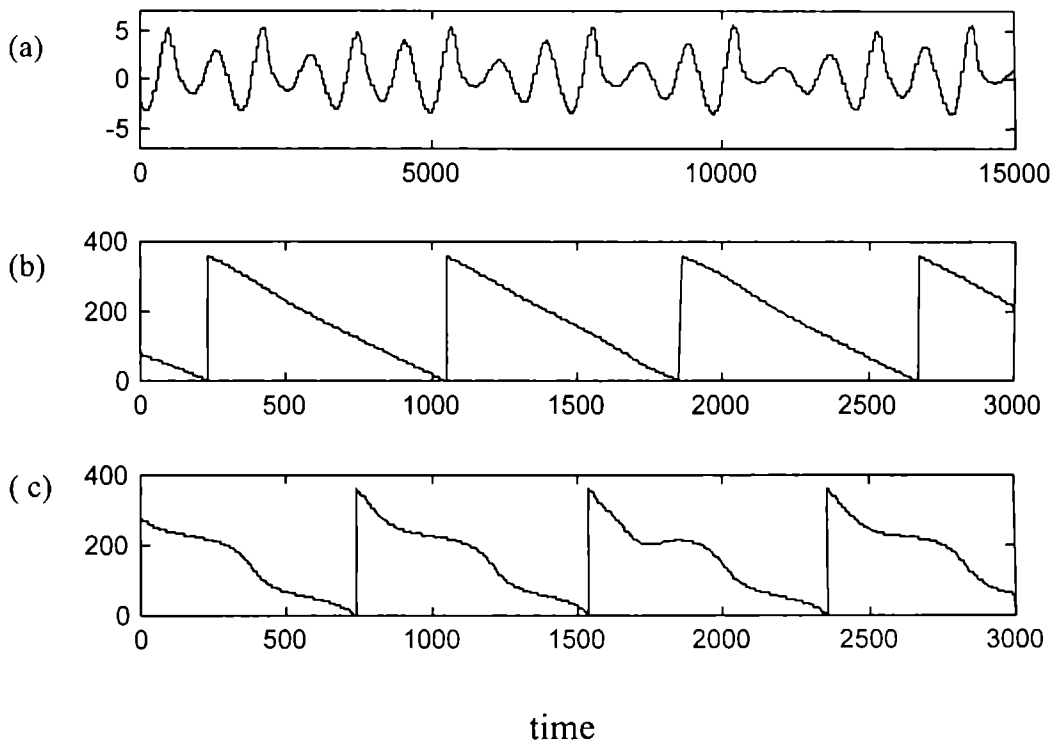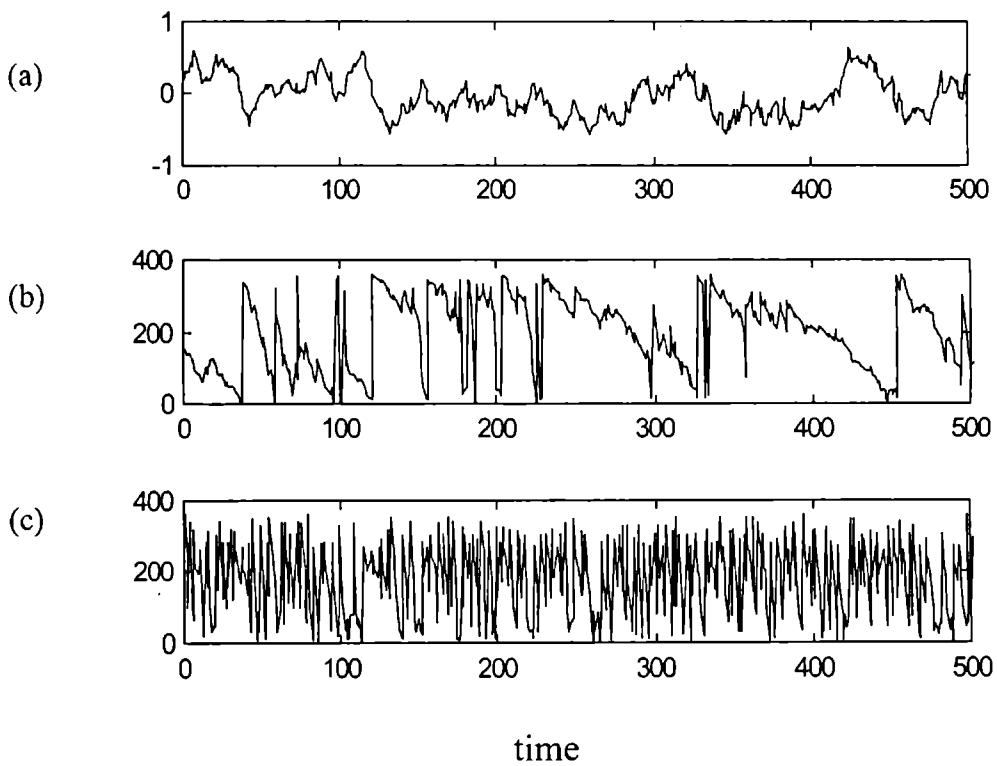
Fig 10.16: Phase evaluated for Rossler equation

(a): Time series s (b): angle evaluated using Hilbert method and

(c) angle from Poincare method

This method of investigation is extended to nonlinear Langevin equation

$$\frac{du}{dt} + \beta u^n = R(t) \qquad (10.1)$$

where u is the displacement, β is the diffusion coefficient and $R(t)$ is a normally distributed random number set with a mean zero and variance 1. In the present case, we took n=3. The equation (10.1) is integrated numerically for $\beta = -5$

(a)

(b)

(c)

time

Fig 10.17: Phase evaluated for nonlinear Langevin equation

(a): Time series s (b): angle evaluated using Hilbert method and

(c) angle from Poincare method

184

The time series is given in Fig.10.17 (a). The variation of phase is approximately linear in some of the regions as shown in Fig. 10.17 (b). While Fig.10.17(c) shows great deal of structure due to nonlinearity and stochasticity. Since the equation has, nonlinearity and stochasticity phase should oscillate according to this stochastic term. This feature is not seen in the phase from Hilbert transform. It should however be noted that the nonlinear interactions in the system might use the stochastic source function to modify its own frequency resulting in stochastic resonance (Gammaitoni et al, 1998) or synergism. The same procedure is repeated for EEG data from the left Occipetal region of a person in eyes closed condition and is presented in Fig. 10.18. Here also the nonlinearity is predominant in Poincare representation. This clearly indicates that the Hilbert space linearises the information and is not suitable for a highly nonlinear systems.
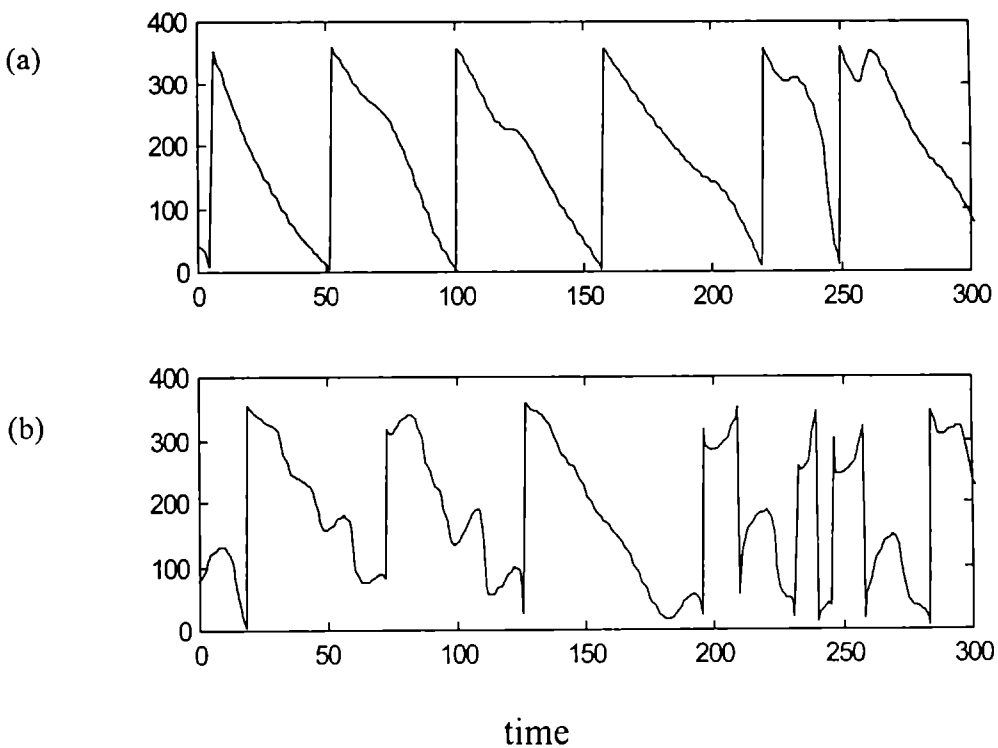

Fig 10.18: Phase (in degrees) of EEG (a) Hilbert (b) Poincare

10.5 Determination of Synchronization Indices

The method adopted for quantifying the degree of synchronization has been proposed by Tass et al. (1998). However, in this method they have defined an index based on Shanon entropy from the relative phase distribution. In the present work, an additional quantity has been defined considering relative amplitude distribution. Using phase and amplitude synchronization indices a third index has been defined. Thus, in general three indices such as *Phase Synchronization index, Amplitude Synchronization index and Synchronization Coherence index* have been defined. Here Phase and amplitude are derived from Poincare map and corresponding indices have been calculated from the bivariate data. Phase Synchronization index using the relative phase distribution is calculated with the phases from the Poinare map for a bivariate data set. In a similar manner amplitude synchronization index is defined. Here also the amplitude corresponds to the length of the vector in Poincare space. Synchronization Coherence index is defined as the harmonic mean of Phase synchronization index and Amplitude synchronization index. Phase Synchronization index, Amplitude Synchronization index and Synchronization coherence index are similar to the measures Phase coherence, amplitude Coherence and Coherence index respectively. However in the former the quantification is evaluated by considering relative phase / amplitude distribution and they are the measures of a bivariate data set. Whereas in the latter one considers simply the phase / amplitude distribution and they are for univariate data set.

The phase synchronization index has been evaluated using phase from Hilbert as well as Poincare space for Coupled Rossler equations of Rosenblum with different values of coupling. The variation is presented in Fig 10.19. This clearly indicates that the variations of synchronization index values with coupling parameter are consistent in both the cases.
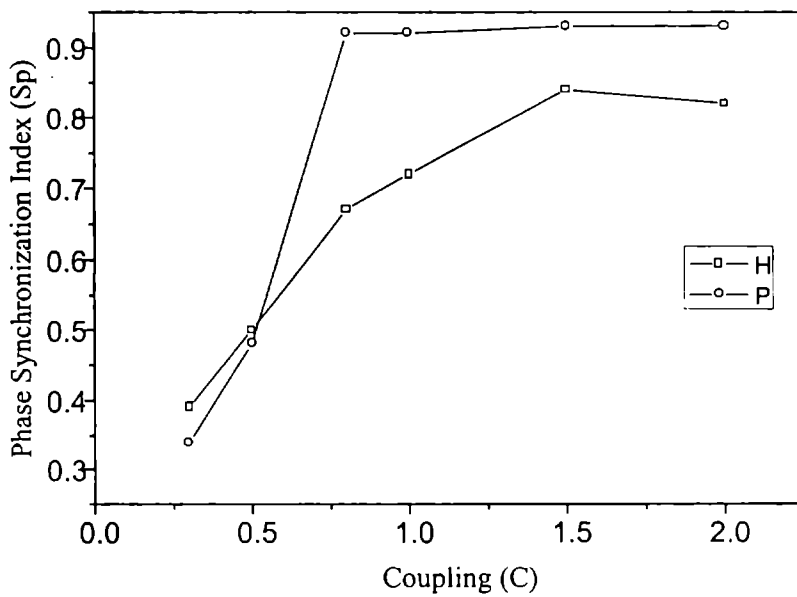

Fig 10.19 Phase synchronization index of Coupled Rossler equation

H-Hilbert

P-Poincare.

The phase synchronization index has been calculated for normal eyes closed data using both methods and they are presented in Fig10.20 (a). It has been found

that the variation of phase synchronization index using phase from Hilbert and Poincare is identical in eyes closed data.
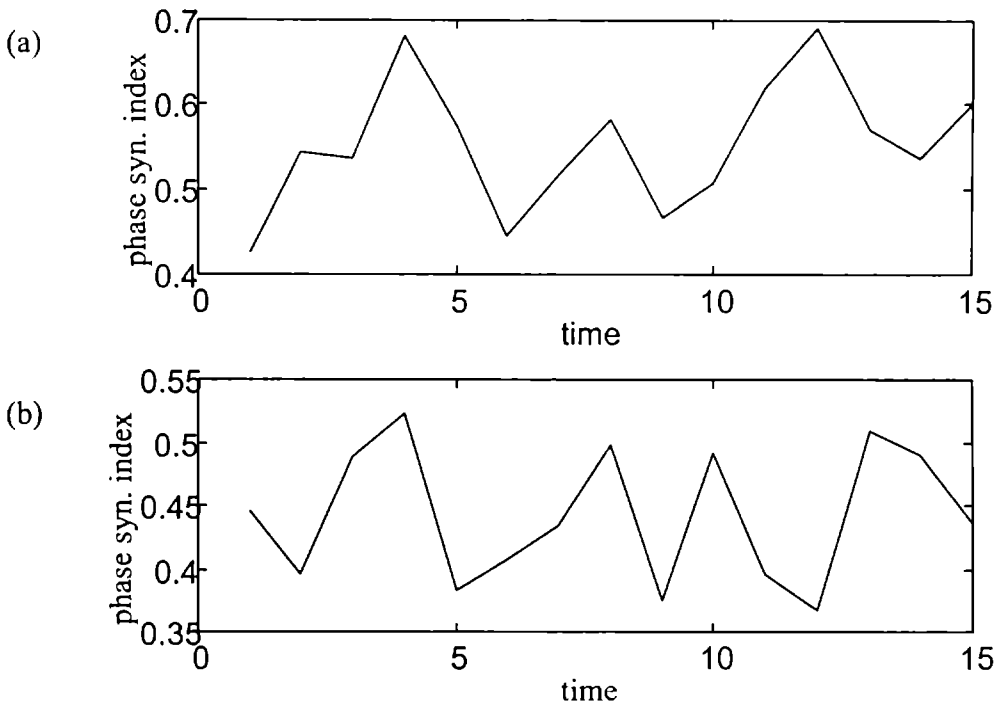

Fig 10.20(a) Phase synchronization index between Fp1 and Fp2 during eyes closed condition (a) Hilbert (b) Poincare

In the case of epileptic data phase synchronisation index calculated using Hilbert and Poincare method are different. However it has been found that in this case phase synchronisation index using Hilbert and Poincare method with a large time lag in reconstruction, are similar. The phase synchronization index has been calculated for normal eyes open data - using both methods and they are presented in Fig10.20 (b). Here also the variation of phase synchronisation index is identical.
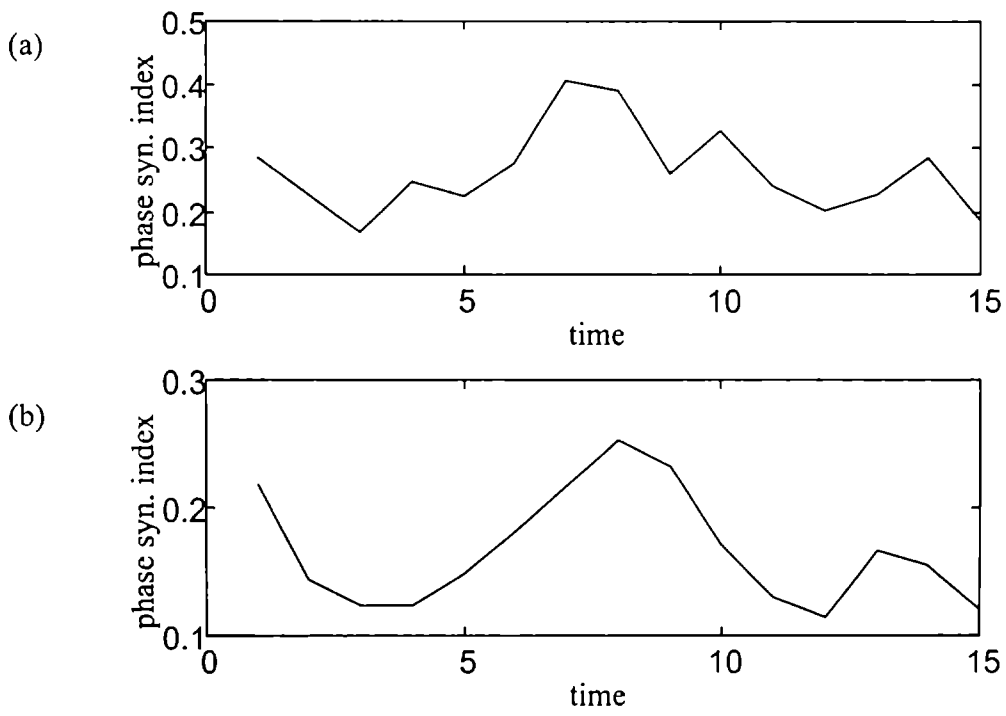
(a)

(b)

Fig 10.20(b) Phase synchronization index between Fp1 and Fp2 during eyes open condition (a) Hilbert (b) Poincare

Another parameter that is very important is the choice of time lag. If the time lag is very small the points will cluster around the diagonal of the Poincare plane, a property called redundancy, and the systems may appear to be synchronized even in the absence of synchronization. On the other hand if the time lag is very large it may not show the synchronization phenomenon even if it is present, a property called irrelevance. It has been found that the variation of phase synchronization index is less sensitive to large values of time lag. Thus, a proper choice of time lag can be

189

made by applying average mutual information criteria or any other similar criteria and studying the effect of time lag to a few values of lag near to the lag selected. To study the effect of time lag used in the reconstruction of Poincare map, Phase synchronization index is evaluated with different values of Time lag for eyes closed EEG data between Fp1 and F3 and given in Fig 10.18. The results indicate that there is no significant effect of time lag for wide range of lag.
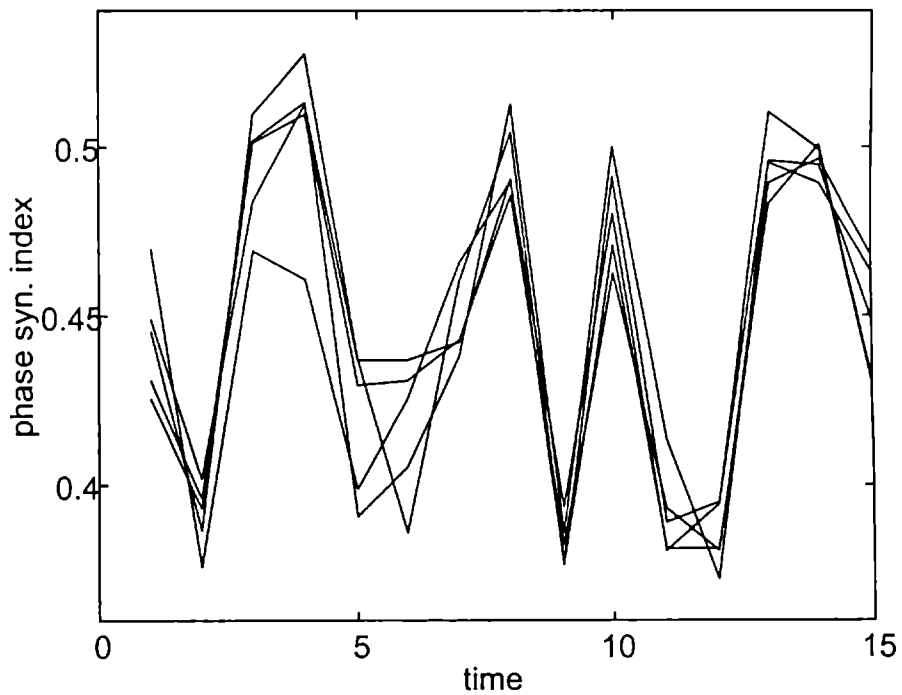

Fig. 10.21: Phase synchronization index using Poincare method at different Time lag. (n = 15, 18, 21, 22, 25)

This proves that the phase evaluation using poincare map forms an alternate method of finding the phase of a nonlinear system that incorporates to a larger measure nonlinearity and stochastic nature of the system. Further, the phase synchronization index obtained from the Poincare map is insensitive to the choice of

time lag. Thus it is very clear that the phase of a system can be effectively evaluated from a two dimensional reconstruction of the time series. The advantage of this method over analytical method is that Poincare method is simple. Further, the signal is not transferred through any kind of filter as most of the filters wipe out nonlinearity.

Another measure is the amplitude synchronization index that quantifies the degree of amplitude synchronization. This is effective over simple visual (x,y) representation as it gives a numeric value of depth of synchronization. The amplitude synchronization index has been evaluated for the coupled Rossler equation of Abarbanel. As the coupling value is increased the two systems are synchronized and the corresponding amplitude synchronization index increases. Fig 10.22 gives the amplitude synchronization index at various values of coupling.
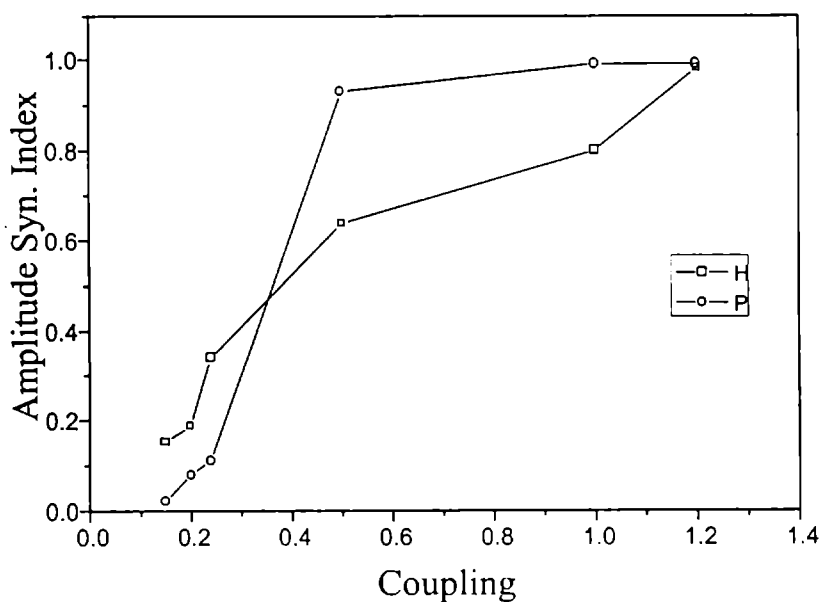

Fig 10.22: Amplitude synchronization index of Coupled Rossler system

H- Hilbert method P-Poincare method

The amplitude synchronization is also called global synchronization with reference to attractors in appropriate embedding space. The index however quantifies the degree of amplitude synchronization Eventhough the presence of phase synchronization also indicates the existence of global synchronization, the more realistic approach is to define an index that incorporates both the amplitude and phase synchronization. The Synchronization Coherence index gives the combine effects of both amplitude and phase synchronization between two systems. Phase synchronization index before meditation eyes closed condition and during meditation between Fp1 and Fp2 calculated for running windows of duration 2 seconds using Poincare map are presented in Fig10.23
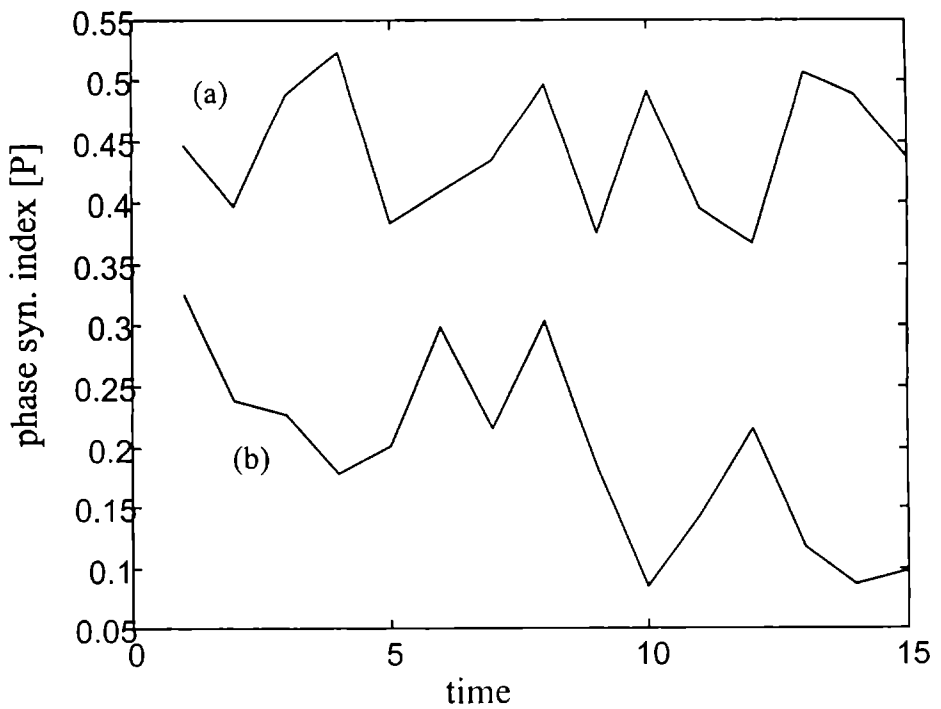

Fig. 10.23: Phase synchronization index between Fp1 and Fp2 (a) before meditation and (b) during meditation using Poincare method [P].

It clearly indicates that the synchronization index decreases during meditation. Further, it has been confirmed that the coordination between brain region decreases during meditation, the observation that has been made in the section 10.3. This is inferred from observing lowering of values of phase synchronization index between the channels. Similar observation is observed by evaluating synchronization index with phase from Poincare map. This suggests that a simple two-dimensional reconstruction is sufficient to study the subtle aspects of the dynamics. Further for the implementation of Hilbert transform one has to properly design a filter with amplitude response unity and phase response $\pi/2$ lag at all frequencies. On the other hand Poincare method is very easy to implement.

10.6 Phase Coherence, Amplitude Coherence and Coherence index.

The synchronization indices are found from the histogram of relative phase distribution from bivariate data. This index essentially gives the degree of coordination between two time series. However for characterizing a signal the indices must be derived from a univariate data. This is achieved by projecting the time series in a two dimensional phase space and deriving the parameters from this space. Three characterizing parameters, Phase coherence, amplitude Coherence and Coherence index, have been derived. This definition is similar to Synchronization indices definition. In this case a bivariate data is considered whereas for the definition of coherence index a univariate series is considered. Phase Coherence, Amplitude Coherence and Coherence index calculated for eyes closed and meditation data of nonoverlapping running windows length 1024 data points are presented in Fig 10.24
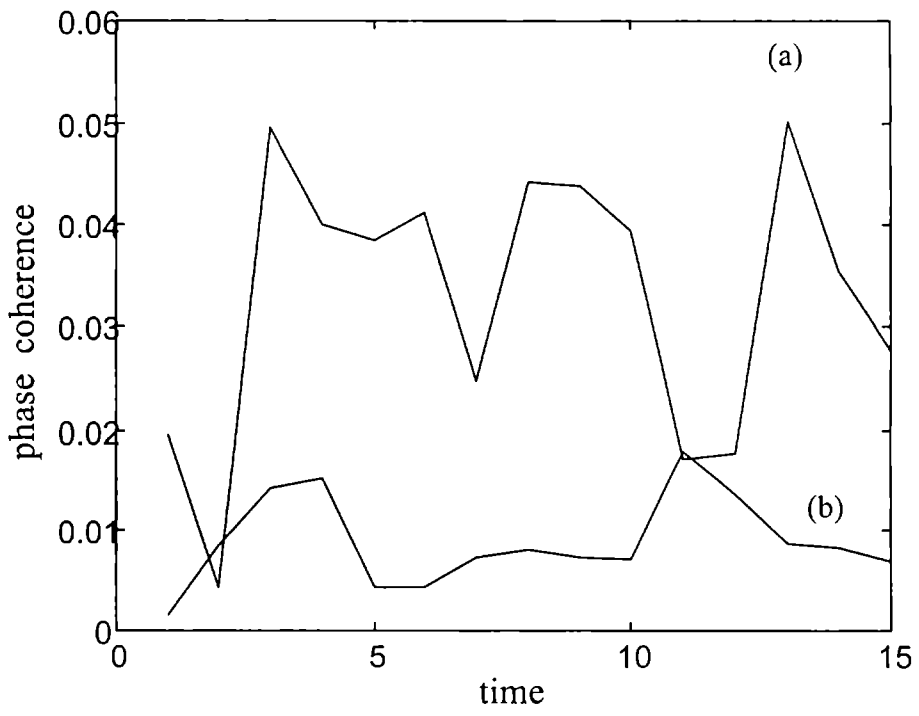
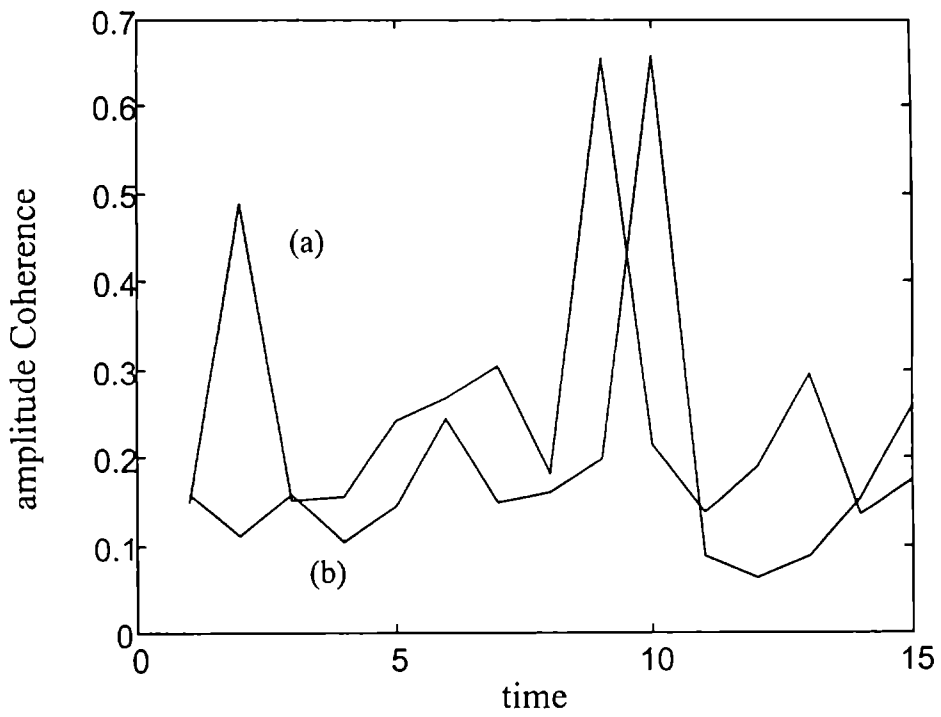Fig. 10.24 (i): Phase Coherence (a) meditation and (b) eyes closed

Fig. 10.24 (ii): Amplitude Coherence (a) meditation (b) eyes closed
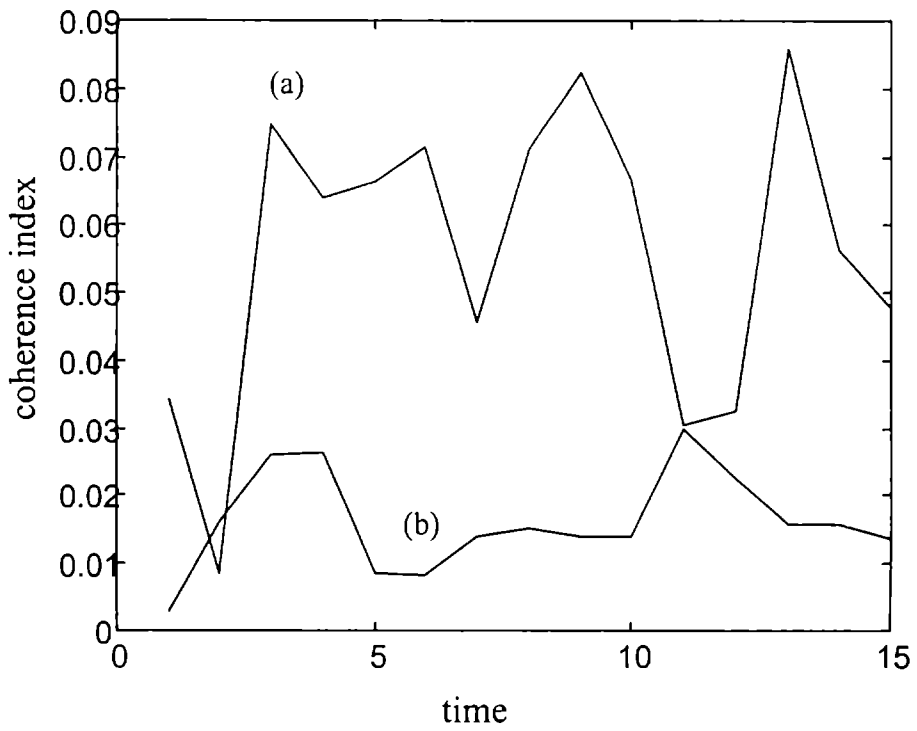
194

Fig. 10.24 (iii): Coherence index (a) meditation (b) eyes closed

It is very clear that Phase coherence, Amplitude coherence and Coherence index shows a clear variation in eyes closed and meditation. This implies that the parameter derived from the length and the orientation of the vectors in phase space can be used as another characterizing parameter along with Correlation dimension, Komogorov entropy, Lyapunov exponents etc. Further these new parameters can be viewed as temporal indices whereas synchronization indices are spatial indices.

10.7 Attractor Potential of EEG

In this last section an account of the evaluation of effective potential at various points (16 locations) distributed in the skull space is given. Evaluation of effective potential at any point in a dynamic system is a very difficult and involved process as could be seen from the various branches of physics such as gravitational and electronic systems. The process that is adopted has already been indicated in chapter 8. Effective potential is essentially a potential that a particle sees at an around its position in the system. In the case of electronic system it is a potential that an electron sees at a point due to interactions with all the particles in the Debye sphere. In the case of gravitational system there is no screening and hence the potential is due to its interactions with the rest of the universe. In both the above cases one knows that the potential between two particles is a function of the inverse of the distance between them. However to evaluate the effective potential, one has to invoke a distribution function and that depends upon the chosen time scale. In the electron problem the Debye's sphere concept is due to the interaction time scales which is the same as self consistent field approximation. In evaluating this, one has to evaluate a distribution function compatible with the chosen time scale and then evaluate the effective potential by averaging the two particle interaction potential with this distribution function as the weight function. However in the present approach the potential is evaluated from the Schrodinger equation as is usually done in dynamical system. (Toda, 1975).

This method is eminently suited for the present problem, since the exact form of Hamiltonian is not known. The problem is all the more difficult since the system is nonlinear, complex and stochastic and contains various organic constituents. The effective potential is evaluated for sixteen channels. The eigen values come out in a decreasing sequence and with the fifth eigen value it gets e folded and hence all further eigen values and corresponding eigen functions are neglected.

Since the wave functions are orthogonal among themselves, each of them can be constructed in a series of known set of orthogonal functions. The effective potential can now be expressed as

$$V(\phi) = \sum A_i \phi_i \qquad\qquad (10.2)$$

The obtained eigen functions are then fit in terms of Legendre function as

$$\phi_i = \sum_j a_{ij} P_j \qquad\qquad (10.3)$$

This further has to satisfy that ϕ_i ϕ_k are orthogonal. This implies

$$\int \phi_i \phi_k = \int a_{ij} b_{kl} P_j P_l = \delta_{ik} \qquad\qquad (10.4)$$

Now

$$\int P_j P_l \, d\mu \; = \; \delta_{jl} \qquad\qquad (10.5)$$

because of orthogonality of Legendre functions.

Therefore

$$V(\phi) \; = \; \sum A_i a_{ij} P_j \qquad\qquad (10.6)$$

The numbers bound on j or l has to be determined by the number of Legendre functions needed to fit the functions. However the harmonics upto the larger number should be retained. The exact values of the constituents a and b in the matrices will be functions of the parameters of the systems. This completes the evaluation of the effective potential. The attractor potential calculated for 16 channels for the eyes closed, eyes open and meditation is given in Fig 10.25.
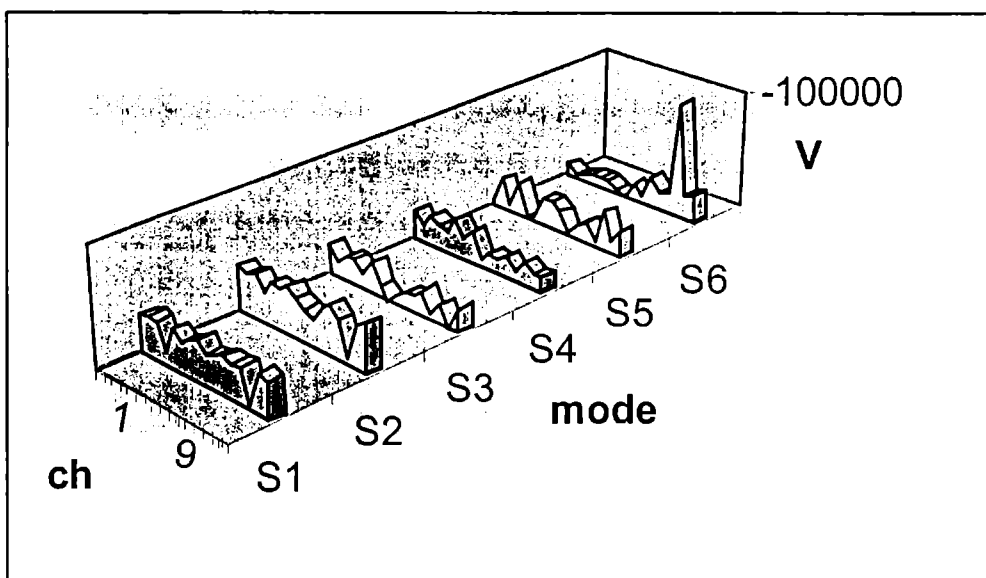

Fig. 10.25 (a): Attractor potential in eyes closed condition. S1-S6 represents modes corresponding to first six eigen values. Ch represents channel and V the potential
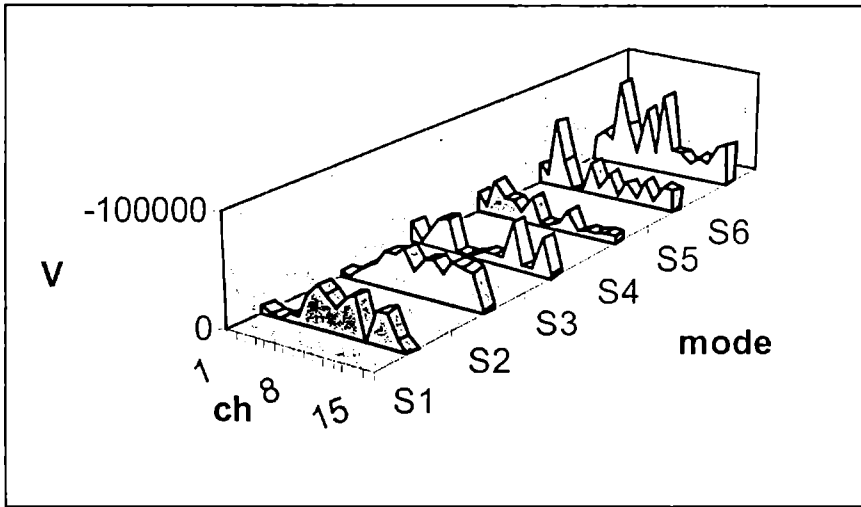
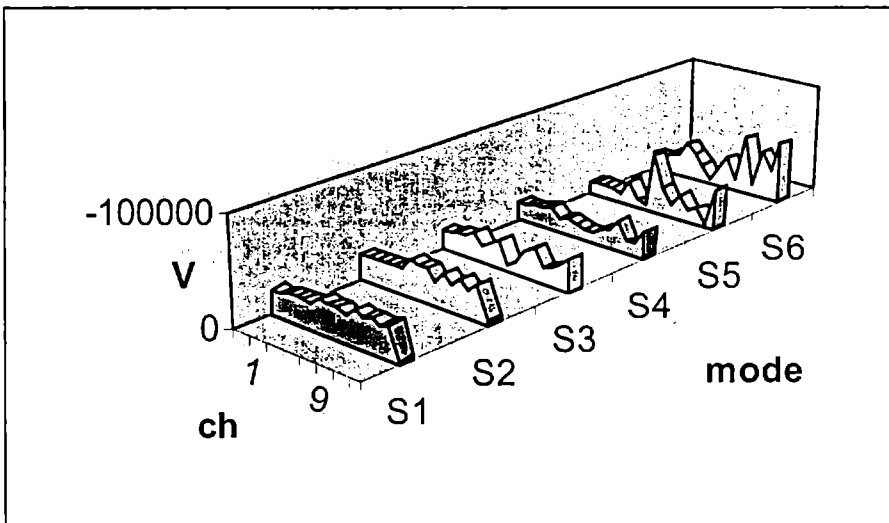Fig. 10.25 (b): Attractor potential in eyes open condition.

Fig. 10.25 (c): Attractor potential during meditation.

In these plots there are a few stable regions in the potential distribution as indicated by the potential wells and there are unstable regions also depicted by the peaks. This is what one would expect in a chaotic system, as there are stable and unstable modes. However more investigation is needed to study the relevance of attractor potential in chaotic dynamics. In the absence of any defining equation depicting the dynamics this is probably the most direct way of inferring the dynamics.

RESULTS AND DISCUSSION

A complex system like brain can be modeled only if its invariant parameters are accurately determined. The invariant parameters especially the dynamical parameters are sensitive to the choice of time scale and the values of the parameters are different for different window as well as different channels. This is generally referred as due to nonstationary property of the system. It has been shown that in neurodynamics nonstationarity is due to large class of time scales. In evaluating the characterizing parameters, the time series is embedded in an appropriate space with a proper choice of lag from autocorrelation function or average mutual information criteria or any other similar criteria. It has been found that such choice of time lag is suitable only for the evaluation of Correlation dimension. Kolmogorov entropy being a dynamical parameter is found very sensitive to the choice of time lag especially during epileptic conditions. In determining D2 and K2, the same time lag determined from AMI is generally used. While this time lag indeed gives a good measure of D2, any time scale shorter than this is being averaged out which in turn affects the evaluation of information capacity. Thus in the study of various dynamical conditions of brain one must choose time lag as small as possible to incorporate many time scales involved in the dynamical process. Nevertheless, this prescription is more useful to get a qualitative insight in the functioning of such a complex, nonlinear, nonequilibrium system such as human brain.

The real importance of time scales in the study of brain functioning has been presented, as choices of time scales are very crucial in understanding neurodynamics. It has also been shown how to obtain a relevant time scale pertaining to a particular state of the brain. In this work a global analysis is performed by taking eight / sixteen channel output, which indicates that these characteristics time scales vary with the different locations and during an experience, a large number of attractors are present in the brain and they obviously must be interacting amongst each other. These time scales are either a single scale or as a group of scales can be a set of **synergic** time scales and are not fundamental ones. Hence, each time scale is a consequence of combination of various fundamental scales that combine in a nonlinear manner. It is indeed difficult or rather impossible to break down this synergic time scale into fundamental components. Thus, human brain dynamics can be viewed as an "attractor gas" with large class of attractors some or many of them being strange ones with fractal dimension. It may also be realized that these attractors change their characteristic parameters, resulting in nonstationary nature in the time series. Hence, one has a system of grand canonical ensemble of strange attractors with its characteristics including its number ever changing. It is also true that the system is thermodynamically open.

Dynamics of human brain during meditation has been compared with that during non-meditating (eyes closed condition) state using the methods of nonlinear dynamics. Studies involving phase synchronization technique show that the different parts of the brain interact more strongly during non-meditating state as compared to

202

meditating state. This inference also indicates that the neural dynamics involving a large class of attractors.

Investigating the possibility of inferring the dynamics of human brain during a process human brain dynamics is considered as consisting of large class of attractors and their effective potential, attractor potential, is evaluated from EEG signal. Attractor potential is evaluated by finding the correlation wavefunctions using a singular value decomposition technique. These wave functions are then used to evaluate the interaction potential. In the absence of any defining equation depicting the dynamics, this is probably the most direct way of inferring the dynamics. The potential function for the various eigen functions at a given point generated for the different eigen values gives the nonlinearities in the system. The system is found highly complex with an ever-active neural system without number conservation. The Coherence property of the system is studied by evaluating an index derived from Poincare space. As the state changes in the parametric space the characteristic vector constructed in this space change both in its amplitude and orientation. As the Coherence index is evaluated from a single time series this index along with another characteristic parameters can be used for developing a model of Neurodynammics. A general model also has been proposed. However, more investigation is needed to study the feasibility of the model for clinical purposes. Further one can explore the possibility of using the newly developed parameters such as Phase coherence, amplitude coherence, Coherence index, attractor potential and different synchronization indices for clinical applications. These parameters along with the already known ones can be used to develop an on line brain imaging system.

REFERENCES

Abarbanel, H.D.I., Brown, R., Sidorowich, J.J. and Tsimiring, L.Sh. Analysis of Observed chaotic data in physical systems. Rev. Mod. Phys. 1993, vol. 65, 1331.

Aihara, K., Matsumoto, G. and Ikegaya, Y. Periodic and nonperiodic responses of a periodically forced Hodgkin-Huxley oscillator. J. Theor. Biol. 1984, vol. 109, 249.

Aihara, K., Matsumoto, G. and Ischiwaka, M. An alternating periodic chaotic sequence observed in neural oscillators. Phys. Lett. A, 1985, vol. 111, 251.

Anderson, J A and Cooper, L. N. Biological organization of memory. Pluriscience Encyclopedia Universals France S.A, 1978

Babloyantz, A., Salazar, J.M. and Nicolis, C. Evidence of chaotic dynamics of brain activity during the sleep cycle. Phys. Lett. A, 1985, vol. 3, 152.

Balescu, R. Equilibrium and Nonequilibrium statistical mechanics. Wiley Interscience, 1975.

Benson, H., Malhotara, M.S., Goldman, R.F., Jacobs, G.D. and Hopkins, P.J.Three case reports of the metabolic and electroencephalographic changes during advanced Buddhist meditation technique. Behavioural Medicine, 1990, vol. 90, 90-95.

Bressloff, P C, Physical Rev. E, 1995, vol. 51, 5064

Broomhead D and King G P. Extracting qualitative dynamics from experimental data, Physica D, 1986, vol. 20, 217

Cowan, J.D. and Sharp, D.H. Neural Nets. Quart. Rev. Biophys. 1988, vol. 21, 365.

Dunki, R. M. and Schmid, G.B. Unfolding dimension and the search for functional markers in human electroencephalogram. Phys. Rev. E 1998, vol. 57, 2115

Eckmann, J P., Kamphorst, S O and Ruelle, D. Recurrence plots of dynamical systems. Euro. Phys. Lett. , 1987, vol 4, 973

Elbert, T., Ray, W.J., Kowalik, Z. J., Skinner, J.E., Graf, K.E. and Birbaumer, N. Chaos and Physiology: Deterministic chaos in excitable cell assemblies. Physiol. Rev, 1994, vol. 74, 1

Epstein, M. J. Nonlinear Dynamics, Mathematical Biology and Social science. Lecture notes. Vol. IV, Santa Fe Institute. Studies in the sciences of complexity,1997

Farmer, J. D, Ott, E and Yorke, J. A. The dimension of chaotic attractors. Physica D, 1983, vol. 7, 153.

Fraser, A.M. and Swinney, H.L. Independent coordinates for strange attractors from mutual information. Phys. Rev. A., 1986, vol. 33, 1134.

Freeman, W. J. EEG analysis gives model of neuronal template matching mechanism for sensory search with olfactory bulb. Biol. Cybern. 1979, vol. 35, 221

Freeman, W. J. Simulation of chaotic EEG patterns with a dynamic model of the olfactory system. Biol. Cybern. 1987, vol. 56, 139

Gammaitoni, L., Hanggi, P., Jung, P., Marchesoni, M. Stochastic Resonance. Rev. Mod. Phys. 1998, vol. 70, 223

Gould E, Reeves A J, Graziano M S A, Gross, C G.Science 1999, vol.286, 548

Grassberger, P. and Procaccia, I. Characterisation of strange attractors. Phys. Rev. Lett., 1983a., vol. 50, 346.

Grassberger, P. and Procaccia, I. Estimation of Kolmogorov entropy from a chaotic signal. Phys. Rev. E., 1983b, vol. 28, 2591.

Grassberger, P. and Procaccia, I. Measuring the strangeness of strange attractors. PhysicaD, 1983, vol. 9, 189.

Havstad, J. and Ehlers, C. L. Attractor dimension of nonstationary dynamical system from small data sets. Phys. Rev. A., 1989, vol. 15, 845.

Hayashi, H. and Ishiyaka, S. Chaos in Molluscan Neuron. Chaos in Biological systems. Degn, H, Holden, A. V and Oslsen, L. F (Eds), Plenum, NY, 1987, 157

Hayashi, H., Ishiyaka, S and Hirakawa, K. Transition to chaos via intermittencyin Onchidun pacemaker neuron. Phys. Lett A, 1983, vol. 98, 474.

Hayashi. H, Nakaom and Hirakawa, K. Chaos in self sustained oscillation of an excitable biological membrane under sinusoidal stimulation. Phys. Lett A, 1982, vol.88, 265

Hebb, D.O. The organization of behaviour. Wiley NY, 1964.

Hodgkin, A.L. and Huxley, A.F. Quantitative description of membrane current and its application to conduction and excitation in nerve. J. Physiol. 1952, vol. 117, 500.

Holden, A.V and Ramadan, S.M. Response of a Molluscan neuron to a cyclic input: entrainment and phase locking. Biol. Cybern. 1981, vol. 41, 157

Isliker, H. and Kurths. J. A test for stationarity : finding parts in a time series apt for correlation dimension estimates. Int. J. Bif. Chaos, 1993, vol. 3, 1573.

Jansen, B. H and Brandt, M.E. Proceedings of the second annual conference on Nonlinear Dynamical analysis of the EEG, World Scientific, Singapore, 1993

Kantz, H. and Schreiber, T. Nonlinear Time Series Analysis, Cambridge Univ. Press, 1997

Kennel, M.B, Brown, R. and Abarbanel, H.D.I. Determining the embedding dimension for phase space reconstruction using a geometrical construction. Phys. Rev. A, 1992, vol. 15, 3403.

Kostelich., E.J. and Schreiber, T. Noise reduction in chaotic time series data: a survey of common methods. Phys. Rev. E, 1993, vol. 48, 1752.

Lalaja, V, Nampoori, V. P. N and Pratap, R. Nonlinear analysis of an EEG during epileptic seizure. Current Sci. 1987, vol. 56, 1039

Lalaja, V. Studies in Nonlinear Dynamical Systems in Neurophysics and Astrophysics. Phd thesis, Cochin University of Science and Technology, 1990

Lanczos, C. and Gellai, B. Fourier analysis of random sequences. Comp. & Math. Appl. 1975, vol 1, 269.

Mitra, N. and Skinner, J.E. Low dimensional chaos maps learning in a model neuropil (rabbit olfactory bulb). Integrat. Physiol. Behav. Sci., 1993, vol. 27, 304.

Mpitsos, G.J., Burton, R. M Jr. Cruch, H.C. and Soinila, S.O. Evidence for chaos in spike train of neurons that generate rhythmic motor patterns. Brain Res. Bull., 1985, vol. 21, 529

Novak P., Buddhist Meditation and Consciousness of time. Journal of Consciousness Studies, 1996, vol. 3, 267-277

Ott, E. Chaos in dynamical systems, Cambridge univ. press, 1993

Papoulis, A. Signal Analysis. McGraw. Hill Int. Edition, Electrical and Electronics Engg. Series, 1984

Parikh, J C and Pratap, R. A map describing the EEG activity of brain. Pramana J Phys., 1991, vol. 36, 347

Parikh, J.C and Pratap, R. An evolutionary model of a neural network. J. Theor. Biol, 1984, vol. 108, 31.

Parlitz, U, Junge, L., Lauterborn, W. and Kocareb, L. Experimental observation of phase synchronisation. Phys. Rev. E, 1996, vol. 54, 2115.

Pikovsky, A.S, Rosenblum, M.G., Osipov, G.B. and Kurths, J. Phase synchronisation of chaotic oscillators by external driving, Physica D, 1997, vol. 104, 219.

Popivanov, D., Mineva, A. and Dushanova, J. Tracking EEG signal dynamics during mental tasks. IEEE Engg. Med. Biol. 1998, vol 17, 89.

Pradhan, N and Dutt, N.D. Use of running fractal dimension for the analysis of chaging patterns in electroencephalogram. IEEE Comp. Biol. Med. 1993, vol. 23, 281

Pradhan, N. and Sadasivan, P. K. Validity of complexity measure to EEG. Int. J. Bif. Chaos. 1997, vol. 17, 173.

Pradhan, N. Nonlinear dynamics of brain activity in different behavioural states. Nonlinear dynamics and Computational physics. Sheorey, V.B (Ed.), Narosa publishing house, 1999.

Pratap, R. An analytic theory of sensory transduction. Proc. of Int. Conf. on Nonlinear Dynamics and Brain function. Sreenivasan, R., Pradhan, N. and Rapp, P. E. (Eds), Nova, 2000.

Pribram K H . Brain and Reception-Holonomy ans structure in Figural Processing, Lawrence Erlbaum Assoc., 1991

Prichard, W.S. and Duke, D.W. Measuring chaos in the brain: a tutorial review of nonlinear dynamical EEG analysis. Int. J. Neurosci. 1992, vol. 67, 31.

Prigogine I. Nonequilibrium statistical mechanics. Interscience NY 1962.

Provenzale, A., Smith, L. A, Vio, R. and Murante, G. Distinguishing between low dimensional dynamics and randomness in measured time series, Physica D, 1992, vol.58, 51

Rapp, P. E. Chaos in the neurosciences - Cautionary tales from the frontier, Biologist, 1993, vol. 40, 89.

Rapp, P. E., Albano, A.M, Schmah, T. and Farwell, L. A causally filtered noise can mimic low dimensional chaotic attractors. Phys. Rev. A., 1991, vol. 47, 2289.

Rapp, P. E., Bashore, T. Martinerie, J., Albano, A., Deguzman, C., Zimmerman, I. D. and Mees, A. Dynamics of brain electrical activity. Brain. Topogr. 1990, vol. 2, 99

Rapp, P. E., Zimmermann, I.D., Albano, A. M., Deguzman, C. and Greenbaum, N.N. Dynamics of spontaneous neural activities in the simian motor cortex: the dimension of chaotic neuron. Phys. Lett. A, 1985, vol. 6, 335.

Rapp, P.E. A Guide to dynamical analysis, 1990. (personal communication).

Rapp, P.E. Nonlinear Dynamical analysis and the investigation of the human central nervous system. Proc. of Int. Conf. on Nonlinear Dynamics and Brain function. Sreenivasan, R., Pradhan, N. and Rapp, P. E. (Eds), Nova, 2000.

Rashevsky, N. Mathematical biophysics. University of Chicago press. 1938.

Rosenblum, M.G, Kurths, J. Pikovsky, A, Schafer, C., Tass P. and Abel, H.H. synchronzation in noisy systems and cardiorespiratory interaction. IEEE Engg. Med. Biol., 1998, 46.

Rosenblum, M.G., Pikovsky, A.S. and Kurths, J. Phase synchronisation of chaotic oscillators. Phys. Rev. Lett., 1996, vol. 76, 1804.

Rossler, O.E. An equation for continous chaos. Phys. Lett. A, 1976, vol. 57, 397.

Rulkov, N.F., Sushchik, M. M., Tsimring, L S. and Abarbanel, H. D. I. Generalized synchronization of chaos in directionally coupled chaotic systems., Phys. Rev. E., 1995, vol. 51, 930.

Schuster, H.G. Deterministic chaos. Third augmented edition. 1995, pp28.

Skarda, C.A. and Freeman, W.J. How brain makes chaos in order to make sense of the world. Behav. Brain. Sci. 1987, vol. 10, 161.

Skinner, J. E, Carpeggiani, C., Candesman, C.E. and Fulton, K.W. The correlation dimension of the heart beat is reduced by biocardial ischemia in conscious pig. Circ. Res. 1991, vol. 68, 966

Spehlmann, R. EEG primer. Elsevier Biomedical press, NY, 1986